Development of Porous Rubber Pavement for the Canadian Climate

by

Tamanna Kabir

A thesis
presented to the University of Waterloo
in fulfillment of the
thesis requirement for the degree of
Doctor of Philosophy
in
Civil Engineering

Waterloo, Ontario, Canada, 2023

Examining Committee Membership

The following served on the Examining Committee for this thesis. The decision of the Examining Committee is held by majority vote.

External Examiner	**Dr. Jennifer Drake** Civil and Environmental Engineering, Carleton University, Ottawa, Canada
Supervisor	**Dr. Susan Tighe** Civil and Environmental Engineering, University of Waterloo, Waterloo, Canada
Co-Supervisor	**Dr. Shunde Yin** Civil and Environmental Engineering, University of Waterloo, Waterloo, Canada
Internal Member	**Dr. Hassan Baaj** Civil and Environmental Engineering, University of Waterloo, Waterloo, Canada
Internal Member	**Dr. Vimy Henderson** Civil and Environmental Engineering, University of Waterloo, Waterloo, Canada
Internal-External Member	**Dr. Kaan Inal** Mechanical and Mechatronics Engineering, University of Waterloo, Waterloo, Canada

Author's Declaration

This thesis consists of material all of which I authored or co-authored: see Statement of Contributions included in the thesis. This is a true copy of the thesis, including any required final revisions, as accepted by my examiners.

I understand that my thesis may be made electronically available to the public.

Statement of Contributions

This thesis comprises research outcomes and publications that are partially co-authored as follows: Chapter 4 consists of two conference papers; the first one is titled "Porous Rubber Pavement – In Situ Performance Evaluation of Stiffness and Friction in Canada," is co-authored by me, my colleague Dr. Abimbola G. Oyeyi, Dr. Hanaa Al-Bayati, Dr. Daniel Pickel and my supervisor Professor Susan Tighe. Dr. Abimbola G. Oyeyi helped me with analysis and field testing, and Dr. Hanaa Al-Bayati and Dr. Daniel Pickel assisted me in field testing. The second one is titled "Performance evaluation of Porous Rubber Pavement (PRP) in the Canadian climate" and is co-authored by me, my colleague Dr. Abimbola G. Oyeyi, Dr. Hanaa Al-Bayati and my supervisor Professor Susan Tighe. Dr. Abimbola G. Oyeyi accompanied me in the field testing, guided me in the analysis, and got support from Dr. Hanaa Al-Bayati during the field testing. Chapter 5, Chapter 6 and Chapter 7 comprise three independent journal papers. Chapter 5, titled "Laboratory mix preparation and investigation of mechanical behaviour of polyurethane-bound Porous Rubber Pavement," is co-authored by me, my colleague Dr. Hanaa Al-Bayati and my supervisor Professor Susan Tighe. Dr. Hanaa Al-Bayati contributed to setting up laboratory testing and reviewed the paper. Chapter 6, titled "Durability Evaluation of Porous Rubber Pavement," is co-authored by my supervisor and me. Chapter 7, titled "Construction and performance evaluation of polyurethane-bound Porous Rubber Pavement (PRP) trial section in the cold climate," is co-authored by my supervisor and me. I did the test plans, analyses, and discussions throughout the research work under my supervisor's direct supervision and guidance. In addition, I prepared detailed experimental plans together with my supervisor.

Chapter 4

- **Kabir, T.**, Oyeyi, A.G., Al-Bayati, H., Pickel, D., Tighe, S. (2023). Porous Rubber Pavement—In Situ Performance Evaluation of Stiffness and Friction in Canada. In: , *et al*. Proceedings of the Canadian Society of Civil Engineering Annual Conference 2021. CSCE 2021. Lecture Notes in Civil Engineering, vol 248. Springer, Singapore. https://doi.org/10.1007/978-981-19-1004-3_7

  This paper was awarded 1st Place - Best Student Paper Award in the Engineering Materials Specialty session.

- **Kabir, T.**, Oyeyi, A. G., Al-Bayati, H., & Tighe, S. (2020). Performance Evaluation of Porous Rubber Pavement (PRP) in the Canadian Climate. Paper presented at the TAC Conference & Exhibition, Canada.

Chapter 5

- **Kabir, T.**, Al-Bayati, H. & Tighe, S. (2023). Laboratory mix preparation and investigation of mechanical behaviour of Polyurethane-bound Porous Rubber Pavement. Under review in Cleaner Materials (Revised Manuscript Submitted).

Chapter 6

- **Kabir, T.** & Tighe, S. (2023). Durability evaluation of Porous Rubber Pavement. The paper outlined in Chapter 6 has not yet been published.

Chapter 7

- **Kabir, T.** & Tighe, S. (2023). Construction and Performance Evaluation of Polyurethane-Bound Porous Rubber Pavement (PRP) Trial Section in the Cold Climate. Sustainability 2023, 15, 2413. https://doi.org/10.3390/su15032413

Abstract

Permeable pavement usage in North America has increased over the last decade as a viable stormwater management system. Porous Rubber Pavement (PRP) is a new material in this category which has been currently utilized as a pavement surface material for low-traffic areas and pedestrian walkways. This material consists of recycled crumb rubber aggregates, granite aggregates and polyurethane as a binder and is proportioned to attain a very high percentage of interconnected air voids (up to 45%). As a new pavement material in North America, the properties and performance of PRP are not thoroughly understood for cold climate conditions. This research aimed to understand the properties and performance of PRP and improve its performance as a pavement surface material for the Canadian climate. This objective is achieved through an evaluation of existing sites and mixes, developing new mixes through an experimental design process, and evaluating new mixes in the laboratory facilities. Some of the mixes were selected to apply in the trial section to assess field performance. Finally, recommendations and guidelines are developed for this climatic zone. Through the experimental design, four new mixes were developed using different proportions of stone aggregates, rubber aggregates and polyurethane binder. Also, using the proportion of the Control Mix, four polyurethane binders were used to make four different mixes to determine the different binder effects in PRPs. In the next stage of research, two trial sections were constructed using selected mixes along with the Control Mix. In addition, samples were also prepared from the field mixes to test their properties in the laboratory. Then the field performance of the various mixes was evaluated over a series of months. They were initially tested immediately following construction before fully opening for traffic. Then three weeks after construction and after seven months when the sections had experienced their first winter. Preliminary field investigations showed that with the current commercial mix, the achieved elastic modulus of PRP surfaces ranged between 37 MPa and 33 MPa. Besides, frictional values ranged between 57 BPN and 74 BPN. Higher IRI values were calculated for both sites, ranging between 7.56 m/km to 15.77 m/km. The average infiltration rate for the pavement surface areas was found to be 30836 mm/hr.

The mechanical properties and durability of the Control Mix and newly developed mixes were investigated. The tensile and compressive strength of the mixes were found to be higher when the percentages of stone aggregates and binders were increased in the mixes. Additionally, an increase in air voids in the samples reduced the materials' tensile and compressive strength. Concerning the types

of binder and sources, the obtained results showed no considerable influence of different types of binder in compressive strength test results, whereas binder sources influenced the tensile strength of the PRP materials. PRP samples with varying compositions retained more than 70% of their tensile strength after conditioning with five freeze-thaw cycles. However, due to the variety of binders used, retained tensile strength for PRP samples varied, and some showed retained tensile strength below 70%.

The durability study showed that the granite stones that were used for all the sample preparation were not strong enough to withstand higher abrasion loss. However, PRPs with different compositions showed good rutting resistance, ranging from 0.3mm to 2.8mm in different mixes. Moisture-induced damage, stripping related abrasion was also found to be very small in PRP mixes, ranging from 2.6% to 0.1%. Also, the use of different binders from different sources showed that the B2—aliphatic binder could withstand more rutting than other binders. A Los Angeles abrasion tester tested unconditioned and conditioned samples to determine the materials' ravelling resistance. The result showed that abrasion loss increased in the samples after conditioning with five freeze-thaw cycles. However, it was consistent with the mix types. On the other hand, abrasion loss of samples with different binders occurred differently in the conditioned and unconditioned situations and was inconsistent in the mixes.

Subgrade samples were collected from sites A and B during the trial section construction. The bearing capacity of subgrade soil for Site B was found to be higher than that of Site A. Subsequently, the performance of the mixes in the sections was evaluated through a series of field testing. The LWD results showed that the stiffness modulus differed for the same mixes at Site A and Site B. Besides, all the mixes showed higher stiffness in the 2nd field test than the 1st since compaction occurred on the pavement after opening for traffic. Nevertheless, after experiencing their first winter, a reduction in stiffness was observed for all mixes in the 3rd test. The BPT test revealed that a higher frictional value of PRP mixes was associated with a higher percentage of rubber aggregates and a lower percentage of binder in the mixes. At the same time, a reduction in BPN values was observed in the 2nd test than in the 1st since the sections were further compacted and polished after opening for traffic. In addition, the surface ravelling and transported loose particles affected the frictional values in the 3rd test, increasing the BPN numbers. Initial rut depths on Site A for different mixes ranged from -7.0 mm to -8.7mm, and the range was -5.8 mm to -10.7mm for Site B. However, after fully opening for traffic, greater rut depths were observed on each section due to the additional compaction under the wheel paths. The permeability of the PRP sections ranged from 28368 mm/h to 45605 mm/h, which is higher than the highest rainfall rate in Canada (298.8 mm/h). However, most of the sections showed higher

permeability in the 2nd test. After the first winter, the permeability of some of the sections was found to be further increased, whereas others were found to be decreased due to the influence of site surroundings. In the 1st and 2nd field tests, no visible surface distress was observed at Site A and Site B. A small amount of surface distress was observed after the first winter (seven months after the construction), which included a slight loss of coarse aggregate, minor ravelling, small cracking, and rutting. Throughout the trial section construction process, it was also observed that by improving the construction methods and making slight modifications during the construction process (like increased compaction), the performance of PRPs could be further enhanced.

Finally, a set of recommendations and guidelines were developed for using the PRP in the Canadian climate.

Acknowledgements

I am deeply indebted to many people for helping me throughout this research. First, I would like to express my most profound appreciation to my supervisor, Prof. Susan Tighe, for giving me this opportunity and believing in me through thick and thin. It would not have been possible without her extraordinary leadership and guidance. Furthermore, not only in my academic life, she is always caring and considerate of my personal life. Moreover, I want to express my deep appreciation to my co-supervisor, Prof. Shunde Yin; my committee members, Prof. Hassan Baaj, Prof. Vimy Henderson and Prof. Kaan Inal from the University of Waterloo, and Prof. Jennifer Drake from Carleton University, Canada.

Stormflow Surfacing funded this research with the big hope of creating an environment-friendly solution for stormwater in Canada. I am incredibly grateful to the ambitious and visionary people of Stormflow Surfacing, Jim Roth, Julie Roth and Becky Shaw. The Mitacs Accelerate program also provided funding for this research. I want to extend my sincere thanks to Mitacs.

My sincere gratitude goes to the Civil and Environmental Engineering Department staff, Richard Morrison, Peter Volcic, Douglas Hirst, Robert Kaptein, and Victor Lewis, for their professional advice and support during this research. Special appreciation to PSI Technologies for allowing me to run testing in their facility throughout the pandemic.

A special thanks to my colleague Dr. Hanaa Al-Bayati for helping me with laboratory testing, field testing and reviewing my writings throughout the research. I am also very grateful to my friend Dr. Haya Al Mutairi and Dr. Abimbola Grace Oyeyi, for always being here for me. Thanks should also go to my colleague and friends who never missed a chance to help me during my work, Dr. Dan Pickel, Dr. Eskedil Melese, Dr. Frank Mi-Way Ni, Dr. Frank (Yang) Liu, Dr. Taha Younes, Ali Qabur, Dandi Zhao, Roberto Aurilio, Dr. Saeid Salehiashani, Dr. Taher Baghaee Moghaddam, Adam Schneider and all other colleagues in CPATT. Also, I'd like to recognize those who supported me by any means but are not mentioned here by their names.

I want to extend my sincere thanks and respect to my beloved family, my husband and son, for their patience and understanding throughout my research.

Almighty Allah, thank you so much for this life and countless blessings. Also, for the strength, you give me to keep going and make each day meaningful in a righteous way.

Dedication

To my wonderful mother, who gave me the spark to begin this journey.

To my beloved father, who instilled in me the strong will to persist through this challenging journey.

To my dear only brother, who showed me the limitless power I have.

Even though you are no longer physically with me, your love and guidance continue to guide me through every step of my life. I cherish the memories and love we shared, and I know that you are now in a place of peace and happiness in heaven.

Table of Contents

List of Figures

List of Tables

List of Equations

Chapter 1
Introduction

1.1 Background

This thesis starts with a general introduction, literature review and methodology. Then it consists of two conference papers and three journal articles that are submitted for review in journals. Two conference papers contain the result and analysis from preliminary fieldwork. The first conference paper was presented at the CSCE 2021 Annual Conference. This paper evaluates the field performance of existing PRP in terms of its strength and frictional property. The second conference paper was presented at the Innovations in Pavement Management, Engineering and Technologies Session at the 2020 TAC Conference & Exhibition. This paper presents results obtained from preliminary field testing focusing on surface roughness, permeability, and surface distress. The findings from these two conference papers create the initial knowledge base for the PRPs. That also helped identify the PRP materials' aspects that need more improvement. One journal article (Chapter 5) has been submitted to Cleaner Materials and is under review. This paper investigates the mechanical behaviour of Porous Rubber Pavement materials using different compositions and binders. The result obtained from it could be used to evaluate the change in mechanical properties with the change in its composition and identify the better mix for pavement surface. The paper outlined in Chapter 6 has not yet been published. This paper evaluates the durability of different mix compositions and the effect of different binders on durability. The outcome of this paper and the previous one could be used to characterize the PRP material. However, in this research, the outcome has been utilized to select the better-performing mixes which were used in the trial sections. In Chapter 7, another paper is outlined and submitted to the Sustainability journal. This paper explains the details of trial section construction and compares the newly developed mixes' performance with the Control mix in the real environment. Also, evaluate the samples prepared from field mixes in the laboratory to identify the changes in the properties during actual construction. At the end of those chapters, a chapter is included that gives a general conclusion and recommendations.

The research presented in this thesis is conducted under the supervision of Professor Susan Tighe. Stormflow Surfacing and Mitacs Accelerated Program funded this study. The primary investigator is listed as the first author for all the published and submitted papers. All the papers listed in this dissertation are original works and the sole production of the primary investigator.

This study used the Centre for Pavement and Transportation Technology (CPATT) and Civil and Environmental Engineering facilities for conducting laboratory testing at the University of Waterloo. A few tests were run in PSI Technologies' testing facilities.

1.2 Motivation

Cities are growing very fast in terms of population, and this is accompanied by various types of development. As a result, building new infrastructure is necessary to accommodate and support this growth. With the building of roads, parking lots, driveways and other similar kinds of structures, impermeable surfaces are expanding as well. This leads to increased volumes and rates of stormwater runoffs along with accumulation and wash-off from a variety of contaminants. Permeable pavements are introduced in contemporary development practices to regenerate the predevelopment hydrological regime. These permeable pavements could be useful for dense existing developments where the stormwater management system is limited and in new development by eliminating sewer infrastructure (Drake; Bradford, et al., 2012). While conventional impermeable paving materials interrupt the natural hydrological system by replacing natural soil surface, permeable pavement can reduce surface runoff, maintain the underground water table and improve water quality through its filtering capability. Along with the beneficial attributes of permeable pavements for best stormwater management practice, they have widespread environmental and safety benefits (Schaus, 2007).

Permeable pavements have become more common in North America over the last decade. The most common permeable types of pavements in the North American cold climatic region are pervious concrete, porous asphalt and permeable interlocking concrete pavers (Drake; Bradford, et al., 2012, Hein, 2014). Porous Rubber Pavement (PRP) is a comparatively new addition to these types of pavements. This material consists of rubber aggregates, granite aggregates and polyurethane as a binder and is proportioned to attain a very high content of interconnected air voids. PRPs can have a large percentage of interconnected air voids, which is up to 40% (Wang; Schacht, et al., 2017). In addition, the use of a substantial amount of crumb rubber makes PRPs highly elastic material. Because of their very permeable nature, PRP pavements could be remarkably beneficial for preventing hydroplaning, glare, spray and splash on the road surface during surface runoff. Additionally, permeability and elasticity contribute to better tire-road noise reduction performance than conventional pavements (Kalman; Biligiri, et al., , 2011, Persuade, 2015).

PRPs are not only advantageous for their technical benefits related to stormwater management and pavement safety but also can pertain extra benefits for the environment by using crumb rubber from recycled tires. Statistics related to waste tires show that every year, Canadians discard more than 30 million rubber tires, and each waste tire consists of approximately 70% to 80% of rubber (Micor, 2020, Kritsonis, T., 2018). PRPs could divert a significant percentage of rubber tires from landfilling by creating alternative use of recycled tire rubber.

In North America, PRPs are used on low-traffic roads and pedestrian walkways as a surface material. It should be noted that this application is in limited areas only. However, as a pavement material, its performance is still unexplored in the North American climate.

As a low-impact design material and beneficial tool for the stormwater management system, porous or permeable pavements have been used in North America for a couple of decades. In Canada, permeable pavements are usually asphalt, concrete or interlocking concrete pavers (Hein, 2014, Hein and Smith, 2016). The primary concern about permeable pavements is their lower strength and durability, which limit their use to light trafficked pavements only (Drake; Bradford, et al., 2012, Schaus, 2007, EPA, 1999). Despite their beneficial impacts on light-trafficked pavements, the lower strength and durability of permeable pavements are hindering their large-scale use even on light trafficked areas. Different permeable pavements are encountering these issues mentioned earlier in different ways. For example, porous asphalt mixtures are susceptible to binder drain-down, which leads to the ravelling of the pavement surface or reduction in porosity (Bindu, 2012, Schaus, 2007). The lower freeze-thaw resistance of pervious concrete constrains its use in a cold climatic region (Henderson, 2012, NRMCA, 2004). Interlocking permeable concrete pavement shows a better performance only for the filtered surface run-off and when the construction detail is adequate (Smith, 2006). It is expected that the performance of permeable pavement could be enhanced in terms of stormwater management, freeze-thaw resistance and reduction in snow accumulations by using PRPs in the Canadian climate. Pavement performance for freeze-thaw resistance and stormwater management is critical in the Canadian climate since this climate experiences an extended period of low temperature in winter and relatively high temperatures in summer, along with moderate rainfall. Besides, PRPs can contribute to environmental sustainability by reusing recycled tire crumbs and redirecting them from landfilling. Therefore, PRPs could be a potential alternative to the prevalent permeable pavement materials.

1.3 Problem Statement

In the North American context, PRP is a new material. Although there is limited research and development, some information on these systems is available from European countries like Sweden, The Netherlands, Germany, and Norway. Japan and China are also in the very initial stages of examining these materials. In European and Asian countries, PRPs have been used as surface-wearing courses on highways or high-trafficked pavement, focusing mainly on traffic noise reduction (Kalman; Biligiri, et al., , 2011, Wang; Liu, et al., 2017, Sandberg, August 24, 2015). The PRPs in Europe appear to be designed using different materials enabling for usage on the high-trafficked pavement. On the other hand, example cases in North America show that PRPs have been used in this region as a surface material only on light-trafficked pavements and for pedestrian paths. Due to its recent inception, consistent construction methods have not been established, leading to varying pavement performance. No research has been found in the literature that investigates PRPs for North America. Thus, the properties of PRPs and their performance as pavement materials are still not fully quantified and understood.

1.4 Research Hypotheses

The hypotheses of this research are:

1. **PRP can preserve a greater level of permeability in different mixes without compromising its strength.** Permeability is assumed to be impacted primarily by the materials' interconnected air voids and internal structures. Given that a narrow range of stone and rubber aggregates from the same sources are utilized across all PRP mixes and that a significant degree of interconnected voids is anticipated to be generated. Thus, all the mixes are expected to sustain higher permeability.
2. **The percentage of stone aggregates impacts the performance of the PRP mix.** The increase of stone aggregates increases the modulus (stiffness) along with the increase of wet friction and hydraulic conductivity. On the other hand, the increase in stone aggregates could also increase abrasion and strain under stress by reducing the overall cohesion among the constituent materials.
3. **The percentage of polyurethane binder content influences the strength and durability of the PRP.** The increase of polyurethane binders increases the overall cohesion of the mix,

which reduces ravelling. It also increases the strength at the expense of void content in the material. However, the increase in binder content also decreases aggregate-to-aggregate contact, which could ultimately impact the tensile strength and micro-cracking of the material.

4. **The rate of compaction is critical for the strength and durability of PRP**. Due to its open-graded nature, minimal compaction is applied to achieve target air voids (up to 40%) to maintain hydraulic conductivity, which impacts its performance in terms of reduction in stiffness, strength, durability etc.
5. **PRP can perform well as an alternative permeable pavement material.** From anecdotal evidence, it is found that this material has already been used for low-traffic areas. However, no performance test was conducted to evaluate PRP as a pavement material.

1.5 Research Objective

The aim of this study was to improve the performance of PRP in the Canadian climate as a pavement surface material for a low-trafficked area by achieving the following objectives:

- Evaluation of the existing Permeable Rubber Pavement (PRP) in terms of its design, construction and field performance.
- Evaluation of the material's properties/performance by laboratory testing to determine its strength and durability.
- Investigation of the performance of different new PRP mixes in the laboratory and field.
- Development of the guideline through recommendation for using PRPs in the Canadian climate as pavement surface material.

Chapter 2
Literature Review

2.1 State of the Art of Permeable Pavement

2.1.1 Permeable Pavement

The fundamental difference between traditional and permeable pavement is how they behave and drain the surface water. Conventional dense graded pavements are designed and constructed with a road crown which allows water or fluids to flow along the pavement surface. In this case, water drains towards catch basins and or ditches along the side of the pavements. On the other hand, permeable pavements are designed to allow for water infiltration through the surface material to the underlying layers (Schaus, 2007). The permeable pavement was first developed in the late 1960s at the Franklin Institute of Research Laboratories in the United States with the support of the United States Environmental Protection Agency (EPA). The earliest permeable pavements were installed and scientifically monitored at the Woodland parking lot near Houston, Texas, in 1975 (Thelen and Howe, 1978, Schaus, 2007, Hansen, 2008).

From the time of its first development, the permeable pavement has been considered one of the significant contributors to sustainability by reducing the environmental impact in a useful way. Allowing precipitation and run-off to flow through the permeable structure significantly reduces stormwater run-off and avoids overloading the stormwater drainage system. It has become one of the best management practices for capturing, infiltrating, storing and flowing water into the natural surroundings. This type of pavement can contribute to the improvement of water quality in the groundwater table by filtering the pollutants during infiltration (EPA, 1999, Hein, 2014, Schaus, 2007, Schwartz, C., 2020).

Careful structural design and hydrological construction of permeable pavements can ensure they are efficient and cost-effective over the design life of low-trafficked pavements (Hein, 2014). The typical permeable pavement structure is shown in Figure 1.

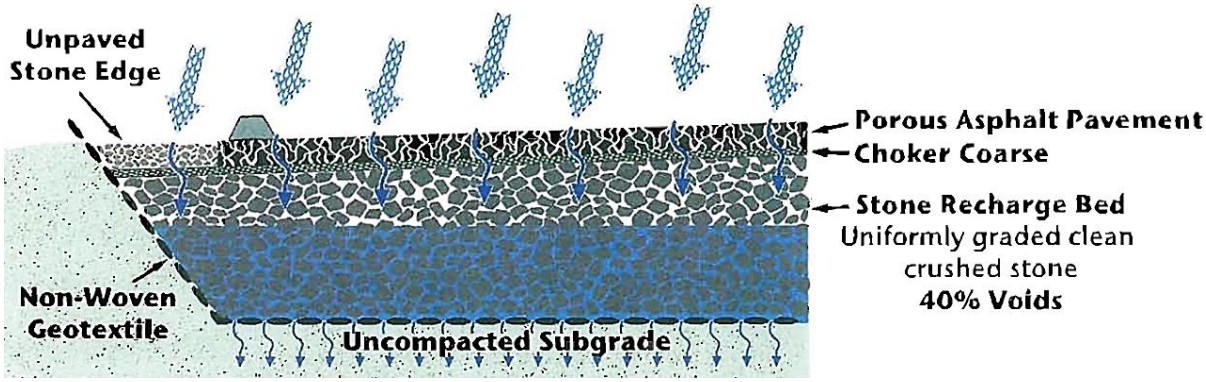

Figure 1 Typical permeable pavement cross-section

Source: (Hansen, 2008)

The sufficient structural design of permeable pavement is critical for attaining strength, which accommodates the loading on the pavement without failure. Besides the structural design, the hydrological design is vital for effective stormwater management by infiltrating, storing and releasing water. Three design approaches are considered for hydrological design.

First, permeable pavement can fully infiltrate the water into the subgrade.

Second, water can be infiltrated into the subgrade partially. It is the case for those permeable pavements where subgrades have lower infiltration capability. Thus, water partially exits the pavement structure by underdrains.

Third, no water infiltrates into the subgrade. In that case, the pavement system can be enveloped with geomembranes or other mechanisms that prevent water from entering into the subgrade; and stored water exits the pavement structure by underdrain (Hein, 2014).

Figure 2 shows the different approaches that are typically adopted for permeable pavement construction.

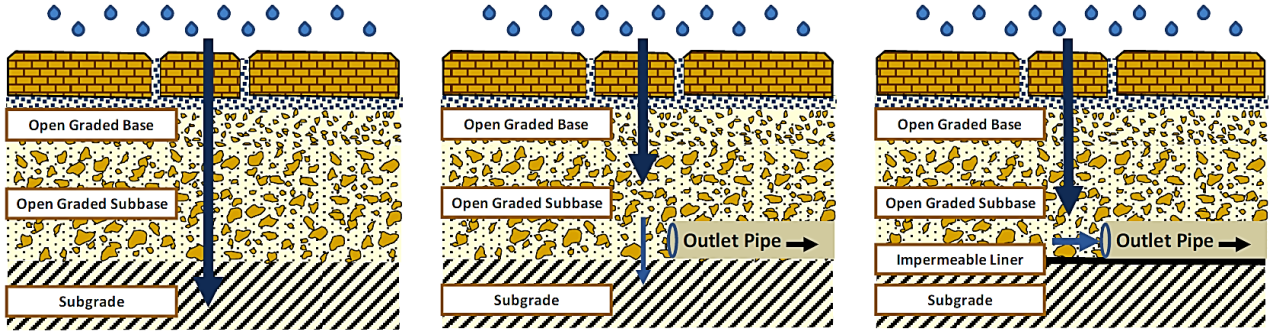

(a) Full infiltration (b) Partial infiltration (c) No infiltration

Figure 2 Approaches for permeable pavement design

Source: (Hein, 2014)

A few design considerations are taken into account for designing permeable pavements. It starts with evaluating the site drainage, which includes the overall drainage capability of the site and its surroundings. It is because the potential contamination around the site may pollute water and reduce water infiltration in the long term. Another important consideration for this type of pavement is studying traffic loading in terms of loading conditions. Typically, permeable pavements are not used for high and concentrated traffic areas with heavy vehicles.

The selection of suitable permeable pavement types depends on different factors. For instance, porous asphalt or pervious concrete could be a better option for some specific slope conditions, whereas, for the areas where the vehicle takes turns, permeable interlocking concrete or grid pavement could be more beneficial. Pavement types also need to be selected based on how steep the slope is. Usually, most permeable pavements should have slopes of less than 5 percent (Hein, 2014).

Permeable pavement surface must have sufficient permeability to infiltrate stormwater into the subbase. Stone recharge bed and storage reservoir must have an adequate void volume to store all infiltrated water. The thickness of the stone recharge bed typically is 305 mm (12”) to 914 mm (36”), which allows water to drain in 12 to 72 hours (Schwartz, C., 2020). The soil type, compaction or consolidation rate determine the permeability of the subgrade. The subgrade infiltration rate usually ranges between 2.5 mm/h to 254 mm/h for these types of pavements. In most areas of North America, full infiltration design is possible if the subgrade infiltration rate is at least 12 mm/h. The depth of the groundwater level is another important consideration for permeable pavement. The top surface of the

subgrade under a permeable pavement should be no less than 0.6 m from the seasonal groundwater table. (Hein, 2014, Schwartz, C., 2020).

From the surface course to subgrade, permeable pavements differ from conventional pavements, as shown in Figure 3. While conventional pavements provide a wearing surface to reduce traffic-related stress-strain to the next layers, maintain riding comfort, and prevent water infiltration through the pavement surface, the permeable pavement provides a stable wearing surface with a significantly higher rate of interconnected air voids of a minimum 15% to infiltrate water into the next layers. Base layers of conventional pavement are compacted to achieve the structural capacity of the pavement system and to reduce traffic-induced stress and strain on the subgrade. Several layers of base and subbase can be designed for conventional pavement in between surface layers and subgrade. On the other hand, layers under the permeable surface give limited strength to the pavement structure. Under the permeable surface layer, a single-sized clean crushed stone is used for preparing a stable choker course. After that, a single-sized large crushed stone is used with high void ratios, typically 40%, for preparing a recharge bed to store stormwater for a period. In this layer, geotextile could be used for separating the layer to prevent the migration of fine subgrade materials to the recharge bed. In conventional pavement, the subgrade is compacted to a higher percentage to create a strong and stable platform for the pavement structure. However, the subgrade under the permeable pavement is uncompacted or lightly compacted based on the supplementary water drainage system (Schwartz, C., 2020).

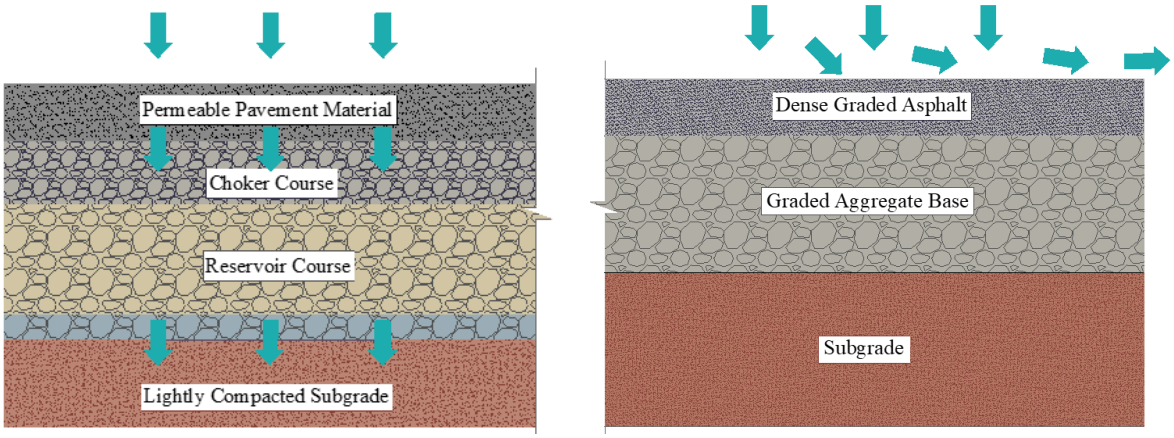

Figure 3 Difference in water drainage between permeable and impermeable pavement

2.1.2 Permeable Pavement in North America

2.1.2.1 Challenges

Permeable pavement is not a new concept in the North American climate, as it has been used since its early development in the late 1960s. Despite the significant number of benefits, this low-impact pavement has not been used widely because of its lower strength and durability. In a cold climate, other complexities can also be added to the pavement performance, such as freeze-thaw resistance, ravelling and coarse aggregate loss related to winter maintenance (in contact with snowplow) and potential clogging associated with the need to sand and salt the materials as part of typical winter maintenance activities. Permeable pavements are usually designed with a higher air void percentage. Water is expected to infiltrate freely through the void system and into the subgrade completely, leaving no water to freeze. However, areas, where the average daily temperature stays below the freezing point for a long time may saturate the system by clogging and preventing drainage. Additional water trying to pass the system remains on the surface and eventually freezes, which causes notable damage to the pavement (Schaus, 2007, NRMCA, 2004). Through different research investigations, it was found that freeze-thaw resistance can be achievable for permeable pavement since larger air voids allow water to expand sufficiently (Thelen and Howe, 1978). The Franklin Institute conducted research in the late 1970s on freeze-thaw damage on permeable pavement. They found that permeable pavement can avoid freeze-thaw if it is designed, installed and maintained correctly. Their testing showed no damage or stresses even after several hundred freeze-thaw cycles (Schaus, 2007).

2.1.2.2 Types and Application

As mentioned earlier, common types of permeable pavement used in North America are porous asphalt, pervious concrete and permeable interlocking pavers (Hein and Smith, 2016).

Porous asphalt pavements, like other permeable pavements, as shown in Figure 4, are used to introduce more sustainability and to ensure less environmental impact on the project. To promote adequate infiltration, porous asphalt has a higher percentage of air voids ranging from 15% to 20% (or higher) (Hall and Schwartz, 2018). This type of material shows great potential for reducing nighttime temperature compared to another similar kind of material, which can positively influence the urban heat island effect (Hall and Schwartz, 2018, Schaus, 2007, Carbone; Mancuso, et al., , 2014, Stempihar; Pourshams-Manzouri, et al., 2012). However, durability is one of the major concerns for porous asphalt

pavement. Since asphalt retains more heat than concrete materials, porous asphalt is more susceptible to ravelling or material breakdown. Another concern related to porous asphalt is the draining down of the asphalt binder, which leads to the irregular distribution of asphalt binder in the mix. As a result, the areas with lower binder content show ravelling and areas with higher binder content show a reduction in porosity. The possible reason for this binder drains down phenomenon could be summarized as construction practice, gravitational force or transportation of mix. Fibres are recommended in some of these cases since they help to stabilize asphalt during production and placement (Cooley; Brown, et al., 2000, Schaus, 2007, Bindu, 2012). However, porous asphalt is a cost-effective material compared to its counterpart pervious concrete since the thickness of the surface material is comparatively lower. Usually, the thickness of the porous asphalt surface is 63.5mm (2.5") to 152mm (6") (Hansen, 2008).

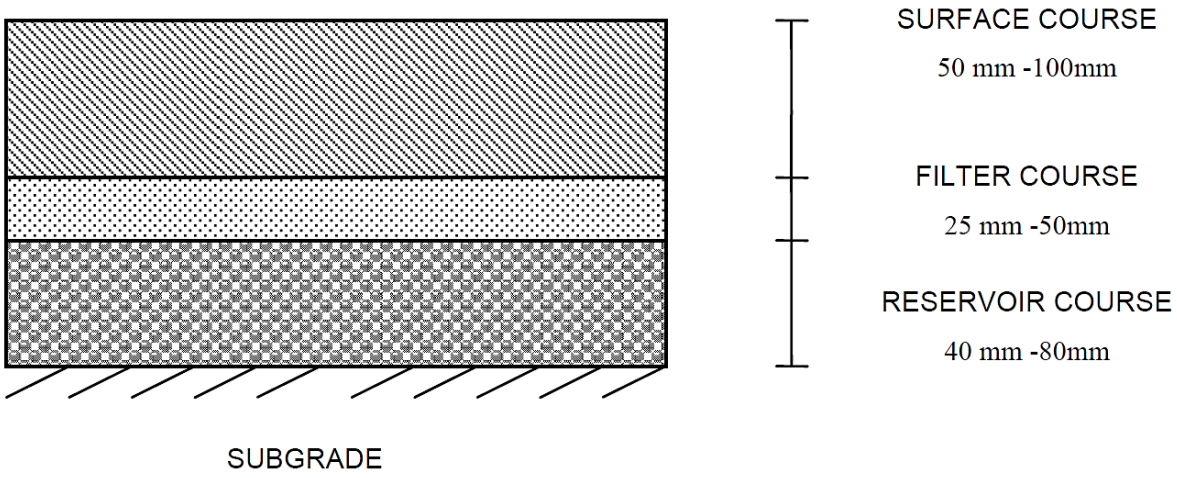

Figure 4 Recommended Porous Asphalt Pavement Section

Source: (Schaus, 2007)

Pervious concrete is becoming popular as a pavement material considering its durability compared to porous asphalt. However, freeze-thaw damages threaten the use of pervious concrete in the cold climate. Moreover, pervious concrete structures can be saturated due to clogging and/or other reasons and remain frozen in areas where the average daily temperature stays below the freezing point for a long time (NRMCA, 2004). In that scenario, additional water can create pressure on the thin layer of the cement that coats the aggregates leading to distresses like spalling, cracking and ravelling. However, several studies show that adding air-entraining admixtures to the pervious concrete pavement can

protect the cement paste from freeze-thaw damage (NRMCA, 2004, Henderson, 2012). Also, changing the way of maintenance activity and increasing the frequency of maintenance related to deicing can improve this situation (Schaus, 2007). Generally, pervious concrete can be slightly more expensive since the surface thickness is greater than porous asphalt.

Permeable interlocking concrete pavements are another option for the conservation of space and reduction of impervious cover on project sites. The structure below can be the same as other permeable pavements. This type of pavement is visually pleasing; different colours and patterns can create harmony with the surrounding areas. Furthermore, tree plantation is easier within this type of pavement. This pavement can be immediately ready without waiting for the curing time and can control crack locations with lots of joints. Recent experience shows that this pavement performs better when surface runoff is filtered before infiltrating through the pavement surface. It also requires good construction skills as well as regular inspection and attention. According to the Interlocking Concrete Pavement Institute (ICPI), mainly four types of permeable interlocking concrete pavers as shown in Figure 5 -are used in North America; interlocking shapes with openings, enlarged permeable joints, pervious concrete units and pervious concrete grid pavers (Drake; Bradford, et al., 2012, Smith, 2006, Hein and Smith, 2016). Interlocking shapes with openings create the opening for entering the water by creating patterns. It maintains good side-to-side contact to withstand the load. Enlarged permeable joint pavers have wide joints up to 35mm (1 3/8”) to accommodate spacers, open-graded crushed stones, grass or topsoil for accommodating joints. Pervious concrete pavers are used for low-loading areas like pedestrian paths, bicycle routes and so on. They are closely placed, and water can directly infiltrate through them since they do not have fines. Concrete grid pavers can be placed on both the open-graded and dense-graded base. Mostly they are used for light traffic areas, like parking lots, industrial yards etc.

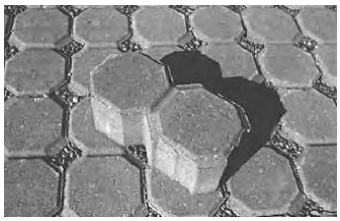
(a) Interlocking shapes with openings


(b) Pervious concrete unit

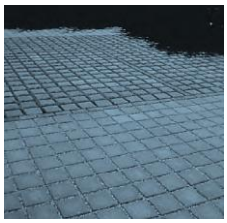
(c) Enlarged permeable joint


(d) Pervious concrete grid pavers

Figure 5 Different types of permeable interlocking concrete pavers

Source: (Smith, 2006)

2.1.3 The Invention of PoroElastic Road Surface (PERS)

PoroElastic Road Surface (PERS) is a flexible and permeable pavement material, mainly composed of rubber granules mostly from scrapped tires, polyurethane and other supplementary materials such as sand, rocks or other friction-increasing additives (Wang; Liu, et al., 2017, Sandberg; Goubert, et al., 2010). Sandberg, U. and Ejsmont, J. A. defined PERS as,

> *"a wearing course for roads with a very high content of interconnecting voids so as to facilitate the passage of air and water through it, while at the same time the surface is elastic due to the use of rubber (or other elastic products) as a main aggregate. The design air void content is at least 20 % by volume and the design rubber content is at least 20 % by weight"* (Sandberg and Ejsmont, 2002).

This material was invented and patented by Mr. Nils-Åke Nilsson in Stockholm, Sweden, at the end of the 1970s. In the original patented mix, only rubber granules from scrap tires and polyurethane were used. Since the wet friction of this kind of material could be below the regulatory limit, friction-enhancing materials like stone aggregates, sand etc., were added to the later mixes. However, mixing a third major component of the stone aggregate in the PERS mix makes the material more complicated (Kalman; Biligiri, et al., , 2011).

2.1.4 Research and Development of PERS

Invention and investigation in Sweden during 1975-1989: After invention in Sweden, the first acoustic test was performed on PERS along with very simplified wear, rolling resistance and durability test. The material was rubber granules bonded with a polyurethane binder. Three trial sections were constructed, and it was found that without exposure to traffic, it could last as long as ten years. It also

showed good winter durability. However, after exposure to local streets vehicle, it was loosened from the base course just after a few weeks (Sandberg; Goubert, et al., 2010). Figure 6 shows the test and trial section in Sweden.

(a) Road wear simulator at VTI in the mid-1980s

(b) Strips of PERS laid on closed down Torslanda Airport in 1984

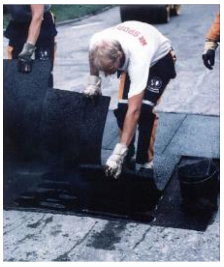

(c) Panels of PERS on the street in Sweden were laid in 1987 for winter durability testing

Figure 6 Invention and investigation in Sweden during 1975-1989

Source: (Sandberg, August 24, 2015, Sandberg; Goubert, et al., 2010)

The trial section in Norway in 1989: In 1989, the first Norwegian trial section of PERS was constructed. It was a 130 m long urban street of two-lane. 19mm thick wearing course of PERS was placed. The mix contained 4-8 mm rubber granules, 13% polyurethane binder with 35% air voids. The road showed a noise reduction of 7-9 dB(A) for a car. The friction coefficient measured by 'Mu-meter' was found to be 0.36, which was not an acceptable value. After a few months of construction, during early winter, a large part of the surface was ripped off by snowplough, as shown in Figure 7. The probable cause mentioned was that the surface did not get enough time for hardening after construction, which was usually five days (Sandberg, August 24, 2015, Sandberg; Goubert, et al., 2010).

Figure 7 After the first snowplough Norwegian trial section near the joint with the hard asphalt surface

Source: (Sandberg; Goubert, et al., 2010)

Test from 1995 – 2000 by adding sands with the previous mix: The original inventor of PERS, Nils-Åke Nilsson, ran the new test for a company called Acoustic control AB. The mixture contained rubber granules, sand and bituminous binder though the proportion was not disclosed to the public. The trial section laid during 1996-1997 in Sweden showed 7-10dB(A) noise reduction with improved durability and ravelling resistance. It also improved the initial condition where surface depression used to occur due to the long time standing of cars (disappeared after some time of vehicle leaving) (Sandberg; Goubert, et al., 2010).

Development of PERS in Japan during 1994 - 2009: In the mid-1990s Public Work Research Institute (PWRI) became interested in PERS and its construction. Extensive tests were done in Japan during 1994-2009. A few tests are discussed in the report of Sandberg et al. (2010). Most of the research was conducted on the material's adhesion to the base course; and durability in terms of wearing resistance, wet friction and fire resistance. The first trial track was an oval track, and 1x1 m^2 plates of PERS were laid over 20 m of the track. The material was elongated rubber granules and 15% polyurethane binder. The PERS materials were found deboned with the base course very soon, and also, wet friction became low after some time. A fire test was conducted to see the impact of spillage of petrol and spark igniting fire after accidents. This material showed better performance than regular concrete or asphalt pavement that was because of the petrol instead of spreading contained on PERS for its porosity. After a number of trials, it was found that durability and wet friction were concerning issues for the PERS pavements. So, from 2006 to 2009, Yokohama Rubber Co. and Nippon Road Co. constructed some new trial sections, as shown in Figure 8. Most of those mixes contained 30% air voids

and silica sand. In the mix, the maximum aggregate size was 5 mm, rubber granules of 1mm, the rubber granules to aggregates ratio were 40:60 by volume, and polyurethane was used as a binder. With the semi-flexible base course, polyurethane was used both for primer and tac coat. They found that this mix design gave considerable structural strength with good wet friction and significant noise reduction. The sound absorption coefficient was found to be 35 %, and the elastic modulus was found to be 25 MPa for PERS and 250 MPa for dense asphalt concrete. The Nippon Road company measured the skid resistance using Dynamic Friction Tester (DFT), and the friction was found to be over 0.5 at 60 km/h. Ravelling problems were observed along the joints between screeds (Sandberg; Goubert, et al., 2010). There is still research going on PERS in Japan for further investigations.

(a) The first field test of PERS at PWRI in 1996

(b) Fire tests at PWRI

(c) Hiratsuka PERS section made by Yokohama and Nippon Road in 2009

Figure 8 Development of PERS in Japan

Source: (Sandberg; Goubert, et al., 2010)

Development of PERS at VTI 2000-2005: The project was a collaboration of the Swedish Agency for Innovation Systems (VINNOVA), EU project SILVIA and VTI, Sweden. The project's main aim was to develop PERS as a durable road noise-reducing material. In that project, the mix design components varied according to the following: rubber granules 60-90% by weight, rubber fines 0-5%, sand 0-10%, melamine 0-10%, polyurethane as binder 10-15%. They concluded that friction property increased with the increase of sand and rubber fines; on the other hand, this addition decreased the void content. The strength of the specimen increased with the increase of binder. In addition, surface polishing due to vehicle tires were found to be less than ordinary asphalt. Tensile strength was found at room temperature 0.5-0.7 MPa. Since asphalt concrete is temperature dependent, it could have less tensile strength than the value mentioned above. It has a lower tensile strength at a higher temperature.

To increase the adhesion with the base layer, the minimum tensile strength was required to be 0.5 MPa, along with adequate exposed aggregates from the base layer (Sandberg; Goubert, et al., 2010). Figure 9 shows the trial section construction and testing by VTI.

(a) Laying of PERS material, manual adjustment of uneven parts

(b) One of the test sections completed in 2004 with different PERS panels

(c) Friction tester performing measurement

Figure 9 The trial section construction and testing by VTI

Source: (Sandberg; Goubert, et al., 2010)

Development of PERS in The Netherlands during 2002-2011: The Noise Innovation Programme (2002-2008) started in the Netherlands in 2002, intending to develop a source-related measure to reduce noise from the rail and road at an affordable price. Forty-one trial sections were constructed with varying properties with respect to macro and mega texture, micro texture, porosity, elasticity and thickness. The overall result was not very satisfactory. After that, the Super Silent Road traffic (SSW) project was started in 2008 and continued till 2011. In that project, the noise reduction for car tires was 7.9 dB(A) compared to dense asphalt concrete, though the targeted value was 8 dB(A) (Sandberg; Goubert, et al., 2010).

Project PERSUADE during 2009-2015: Project PERSUADE (PoroElastic Road SUrface: an innovation to Avoid Damages to the Environment) is the first large-scale project for testing the poroelastic road surface (PERS) on trafficked roads in several European countries. Twelve universities and research institutes from different European Union (EU) countries partnered in this project. It was a 6-year long project started in September 2009 and funded by the European Union. The objective of this project was to develop PERS as a suitable noise abatement measure from its experimental concept with acceptable durability (Goubert, 24th August, 2015). As part of this project, PERS was used on different test sections as a wearing course shown in Figure 10.

(a) Test track in Kalvehave, Denmark, built in June 2014 (length 75 m)

(b) Test track in Herzele, Belgium, built in September 2014 (length 40 m)

(c) Test tracks in Linköping, Sweden, were laid in August-September 2014, with prefabricated panels (front, 30 m) and on-site construction (rear, 24 m)

(d) Test track in Krakow, Poland, built in September 2014 (length 70 m). For unknown reasons, the Polish test section has been damaged recently and will be replaced with regular asphalt, but not until as many measurements as possible have been done

(e) Test track in Nova Gorica, Slovenia, built-in December 2014 (length 20m). This poroelastic block pavement is made of PERS tiles glued onto cement concrete blocks.

Figure 10 Test sections of project PERSUADE

Source: (Persuade, 2015)

A good number of laboratory tests were also conducted during this project. A few of them are mentioned here. The PERS mix with approximately 50% of hard aggregates showed modulus values in the range of 30-50 MPa at load frequencies of 0.1 to 25 Hz at 210C, which is around 200 times lower than the asphalt pavement material in the same frequency and temperature. Besides, with the increase

of hard aggregates, friction values are also increased, and mix with 50 % hard aggregates shows similar friction values as conventional French dense asphalt concrete. On the other hand, ravelling resistance increased with the smaller aggregate size and reduced content of hard aggregates. The effect of fuel on PERS was found to be limited when compared to the porous asphalt. Regardless of the composition after the first loading cycles, PERS mixes showed higher deformation or non-elastic behaviour, but for the following consecutive loading, they were stable against higher hysteresis losses (Pierard; Kalman, et al., 2013). Test results also showed that on wearing resistance, the percentage of hard aggregates and air void in the material has a more significant influence. A lower percentage of both can enhance the wearing resistance of PERS (Goubert and Sandberg, 2016).

Research in China: A recent research was conducted for China, which aimed to explore the suitability of PERS as low-noise pavement for urban roads in cold regions in China. Few laboratory tests and numerical simulations were done to characterize the mechanical and functional performances of PERS, where conventional porous asphalt (PA) was used as a reference. The constituent materials for test samples were coarse rubber granules, fine rubber granules and polyurethane binders. Initially, the effects of various composition factors on ravelling resistance were investigated for PERS. After various stages of polishing applied by the Aachener-Ravelling-Tester (ARTe), ravelling resistance was measured by material loss. Acoustic performance and rutting resistance were also measured for validation purposes. In this research, binder content and degree of compaction were identified as critical factors for ravelling resistance. Almost no rutting was found in the material during this test. For sufficient durability, a minimum of 15% binder content and 98% compaction were recommended in that research (Wang; Schacht, et al., 2017). These factors later took into account for the next steps of research. The selected PERS sample had 35% void content, fine rubber granules and coarse rubber granules were 0.2 - 0.8 mm and 3.1- 6.0 mm, respectively. This stage of research aimed to identify the suitability of PERS for urban roads in the cold region of China. The result shows that the difference between the average tensile strength and the cooling-related tensile stress at a specific temperature, which is termed as tensile strength reserve, is higher than porous asphalt. However, at a low-temperature tensile strain of PERS is larger than porous asphalt. The research also identified that PERS shows better noise absorption performance and fewer surface cracks compared to porous asphalt. As a result of its flexible nature, it has the de-icing capability through the deformation of ice on its surface layers, as shown in Figure 11. The maximum horizontal strain in PERS is larger than in porous asphalt. The overall findings indicate its suitability for urban roads in cold regions. The research outcome also

encourages further investigations to move forward for significant economic and social benefits (Wang; Liu, et al., 2017).

(a) Impact setup and graphical representation of ice layer deformation

(b) Deformation of an ice layer on the PA surface under the impact of the drop hammer after one- and two-time, respectively

(c) Deformation of an ice layer on the PERS surface under the impact of the drop hammer after one- and two-time, respectively

Figure 11 Impact test setup and representation of ice deformation

Source: (Wang; Liu, et al., 2017)

2.2 Porous Rubber Pavement (PRP)

Porous Rubber Pavement (PRP) is a novel type of pavement material in North America, which is similar to PERS. The use of this material in this context is found only in very limited areas. The application of this material is also very different from the European context. In North America, a thin surface course of PRPs is used on different types of thin subbases for pathways, driveways, patios or light vehicle traffic, as shown in Figure 12.

(a) Google Campus Rubber Flooring, Playa Vista

(b) Rubber Blacktop at Elementary School

(c) Washington DC Tree Wells

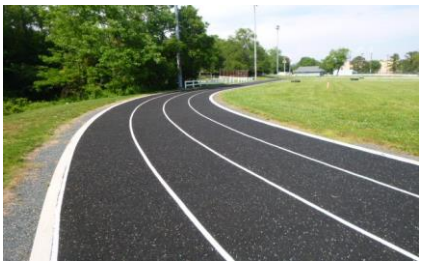

(d) U.S. Navy Rubber Running Track

(e) United Nations International School Rooftop Recreation, New York, NY

(f) Pattern and colour by PRP

Figure 12 Different applications of PRPs

Source: (Rubberway, 2020, Porous Pave Inc., 2017)

Constituents of PRP for this kind of application include tire-rubber granules, stone aggregates and polyurethane binders. In some PRPs, stone aggregates are not included to achieve more flexible and softer pavement. This combination is used for the areas where the impact-absorbing surface is required, but wheeled vehicles are restricted. It is commonly used in pool surroundings and playgrounds (Porous Pave Inc., 2017). However, no research has been found to date for developing this material in the North American context.

2.2.1.1 Constituent material

In most of the current practices in North America, PRP consists of 45.25% of recycled tires, 45.25% of stone aggregates and 9.5% of polyurethane binder by weight. Typically, it contains 27% to 29% interconnected voids by volume. For some applications, the composition of constituents is different, where instead of stone aggregates, only recycled tire rubber crumbs are used with a softer polyurethane binder. This composition is softer and more flexible than the typical one (Porous Pave Inc, 2019, Porous Pave Inc., 2017). In this research, PRPs containing both stone aggregates and recycled crumb rubber has been considered for further investigation. The constituents are discussed below briefly:

- **Recycled crumb rubber** – Crumb rubber chips of the consistent size of approximately 6.35mm (1/4”) to 9.5mm (3/8”) are usually used for PRPs. The grinding process ensures that more than 99.5% of the steel fragments are removed from the tires, and after cleaning the chips, colours are infused instead of applying a thin outer coating (Porous Pave Inc., 2017).

- **Stone aggregates** – Cleaned and kiln-dried stone aggregates of the consistent size of 9.5 mm (3/8”) to 19 mm (3/4”) are used for the PRPs. Usually, granite is used to avoid water absorption by aggregates, which are detrimental to bonding with polyurethane binder (Porous Pave Inc., 2017).

- **Polyurethane binder** – Polyurethane binder is a polymer where carbamate (urethane) links join organic units. The typical formation of polyurethane polymers can be achieved by the reaction of a di or poly-isocyanate with a polyol. Moist-cured polyurethane binder is solid at room temperature. After applying in the form of a melt, polyurethane sets not only physically by cooling but also chemically. The isocyanate groups react with the moisture of the environment at ambient temperature. After the chemical curing, the size of the molecules increases, and the adhesive acquires its final properties. The curing or setting starts within one hour of application and takes 24 hours to 48 hours to be fully cured. Most polyurethane binders are thermosetting, which means they do not melt when heated. However, there are thermoplastic polyurethanes also available that become soft when heated (Szycher, 2013, Akindoyo; Beg, et al., 2016, Krebs; Heider, et al., 1999, Soft-Surfaces, 2020).

2.2.1.2 Material Properties and Performance of PRP

Some laboratory tests were conducted for the PRP mix that is used as a control mix for this study, by Porous Pave, Grant, MI. Those results are summarized here.

Void content - Typical void content ranges between 27% to 29% for allowing fines to pass through easily.

Permeability – Permeability tested in the laboratory is found to be 5800 GPH.

Slip resistance – The static coefficient of friction, when tested in accordance with ASTM D 2047, is an average of 0.66.

Chemical leaching – EPA tested for metals, mercury, semi volatiles. The analyte was not detected at or above the threshold limit.

Flame resistance – Flame Spread Index 90, Smoke Developed Index 600, when tested following ASTM E 84.

Weathering durability - Accelerated Weathering in accordance with ASTM D 4798. Cycle A, ASTM G 155. Xenon UV exposure, 120 hours.

Freeze-thaw durability – ASTM C 666, Method B, 300 cycles of freeze-thaw; panel 1 Mass change minus 1.2%, Panel 2 mass change minus 0.5%, Panel 3 mass change plus 5.6%. No change in visual appearance from all panels.

Compressive strength – 4536 kg (10,000 lb) test – Average reading after 4 hours after release 0.0609.

9072 kg (20,000 lbs) test - Average reading after 3 hours after release 0.0350

Slough – Small amounts of rubber granules and rock aggregates slough routinely off or become loose on the surface of the installed product.

Source: (Porous Pave Inc., 2017)

2.2.1.3 Construction

In this section, the current practice of constructing the PRP surface in North America is discussed. First of all, the favourable weather condition is required for the construction of PRP pavement. Pavement can be installed if the temperature is between 7.2ºC (45ºF) to 35ºC (95ºF). It is better not to have any other construction work going on during the PRP installation. Adjacent material needs to be protected from exposure to binder material since binders can stain other materials. Figure 13 shows the typical structure of Porous Rubber Pavement. Usually, the thickness required for the PRP surface is 25 mm (1") to 50 mm (2"), based on the type of application. Since it is a novel application, a consistent method for the application of PRPs are not developed yet. However, the most used construction method is discussed below.

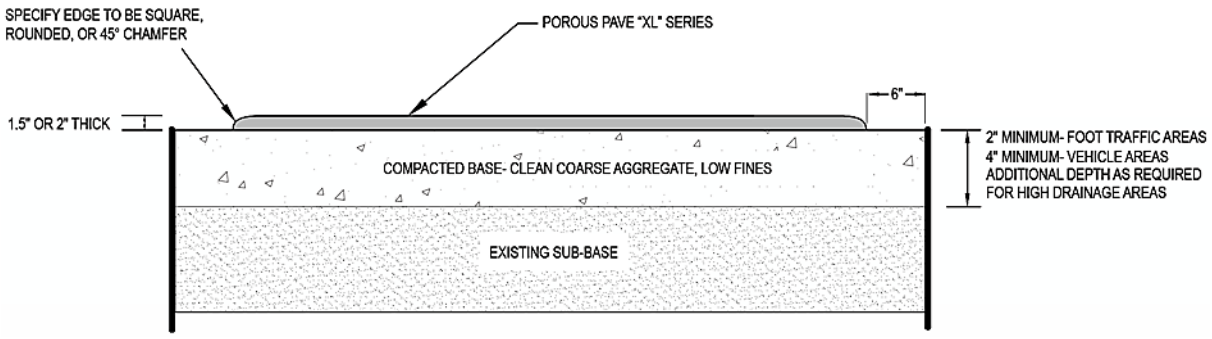

Figure 13 Typical structure of Porous Rubber Pavement

Source: (Porous Pave Inc., 2017)

- **Base preparation -** If the PRP is to be placed on an existing pavement surface, it requires 152 mm (6") of excavation. Then the area is filled with a single type of material as a base. This material should be graded and clean washed aggregates, which are low in fines and angular in shape, in order to ensure better locking during compaction. The size of the aggregates ranges from 9.5 mm (3/8") to 19 mm (¾") and needs to be uniform in quality, free from vegetable matter, shale, lumps, clay balls etc. In addition to that, different thicknesses of the crushed stone bed are required for different types of applications. For example, 50 mm (2") for non-vehicular applications, 101 mm (4") for light traffic applications and 152 mm (6") for comparatively heavy traffic applications. Base material should be compacted not less than 95% of the maximum density as determined by AASHTO T-180, Method D, and it contains approximately 18% of void space. Proper base construction is also an essential part of effective infiltration. Moreover, if the base material contains excessive moisture, it is difficult to maintain the required density. Thus, the material needs to be dried to achieve the required compaction uniformly. The base is installed and compacted to a minimum of 152 mm (6") beyond the PRP application area, as shown in Figure 13. Besides, soil condition is also an important factor to consider for base thickness. If the subgrade soil is very impermeable, the thicker base is required to hold the water and drain it later on. (Porous Pave Inc., 2017).

- **Mixing process -** The crumb rubber, stone aggregates and polyurethane binder are mixed in a mortar mixer for 45-60 seconds (maximum 90 seconds) until the rubber and aggregates are evenly coated with the binder and the stone aggregate looks dark or wet. Concurrently, over-mixing draws more moisture and will cause a slight but noticeable colour change. For different colours of PRPS, mixtures need to be prepared separately (Porous Pave Inc., 2017).

- **Placement and compaction -** The mixture can be pour-in-place on the application site using shovels, wheelbarrows, trowels, or screeds. For small sites, surfaces are made even by using trowels or bull floats, whereas, for larger sites, rollers are used. Vegetable oils are sprayed over the instrument to prevent the material from sticking. In current practice, dish soap and water mixer wipe on trowels or bull floats while shaping the surface. The soapy water acts as a release agent preventing the binder from adhering to floats. Even though the water is minimal, it will speed up the curing process.

- **Curing -** For curing, a favourable temperature is required, as mentioned in section 2.2.1.3. After installation, the temperature must not fall below 7.2ºC (45ºF) for about 6 hours, and the binder should not freeze until it is fully cured. The mist of water needs to be sprayed over the surface to get the best results. The curing process starts after one hour of the placement and can take up to 24 to 48 hours. The polyurethane binder is moisture-cured, but excess moisture can foam up the binder before curing, which cannot be repaired. After installation of material in full sunlight, the colour changes almost immediately, while installation in the shade or on a cloudy day takes a longer time to darken. Within the first month, it is darkening to its fullest extent. However, over time it gets back to its initial colour. Also, a special binder that is 100% UV stable is available to prevent colour change, but it is not a cost-effective option. For thicker applications, sometimes 2/3 of the application is made with the standard binder, and the top rest 1/3 is done with UV stable binder to protect the colour. Binders amber is nearly the same in all colours and typically not noticeable for darker colours, as shown in Figure 14 (Porous Pave Inc., 2017).

Figure 14 Ambering in PRP after curing

Source: (Porous Pave Inc., 2017)

2.2.1.4 Maintenance

Regular cleaning, repair and maintenance work can ensure a longer life of PRP surfaces, which is also true for other types of pavement materials. Regular cleaning by vacuum or force water is critical for maintaining infiltration through the material.

- **Cleaning -** To maintain the porosity and permeability of the PRP materials, proper cleaning is mandatory. For cleaning, either a large amount of water can be applied at low pressure or a shop vacuum or street sweeper can be used. However, a combination of both is recommended for current practice since the vacuum can remove fines from the sub-base along with sediments from the porous pave surface. So, the build-up of sediments in a subbase could be prevented. For winter maintenance, it is found that PRP surfaces can be snow plowed if shoes are used on plow blades. Salt does not damage the surface, but it can contaminate the underground water table. In fact, vacuum sweeping should be taken place immediately after any biomass loading on the surface (Porous Pave Inc., 2017, Hein, 2014)
- **Repair/replace/resurfacing -** Damaged or worn part of the PRP surface can be cut out, and new surface material can be placed on that spot in a similar method of first-time placement. Resurfacing yearly or bi-yearly can ensure the longevity of the surface. Resurfacing can be done by a mixture of binder, thinner and colourant, and their usual ratio is 5:1:1 by weight. It can be applied either by spraying or by using a roller. However, spraying is efficient since it can resurface almost double the area with the same amount of mixture. Direct binder application is not recommended in current practice since it can make the surface blocked and make the surface foamy, and impermeable (Porous Pave Inc., 2017).

2.2.2 Advantages

The use of PRPs can bring large-scale benefits in a single design, which may include a sustainable environment, safety, cost and urban design. With its development and proper application, it can be a potential permeable pavement material for solving several issues that are currently experiencing in the field.

- **Stormwater management -** While conventional pavement produces impermeable surface layers, the PRP surfaces can contribute to stormwater management. This porous surface can reduce surface runoff from the surrounding impermeable area through its infiltration capability, which undoubtedly reduces the need for additional stormwater management systems, like curbing and storm sewers. It can also improve the underground water quality by the removal of pollutants and recharge of local aquifers with clean water (EPA, 1999, Hansen, 2008, Schaus, 2007).

- **Safety issues -** PRP surfaces can also improve the safety of drivers and pedestrians. Since it can percolate rainwater quickly, it reduces the danger of hydroplaning. Reduction in stagnant water can also reduce spray, splash and glare, therefore improving the driver's visibility, specifically during wet night conditions (Thelen and Howe, 1978, Hansen, 2008, Schaus, 2007). Due to its flexible nature, ice deforms quickly on this surface, which can reduce the potential for black ice in cold climates (Wang; Liu, et al., 2017).

- **Noise reduction -** PRPs contain a high amount of crumb rubber aggregates, as well as a higher percentage of void contents (27% to 29%). Both properties of PRPs work together for road noise reduction. Studies showed that this type of material could reduce noise 10 dB(A) to12 dB(A), while low noise porous asphalt can only reduce about 7 dB(A) (Kalman; Biligiri, et al., , 2011, Sandberg and Ejsmont, 2002, Sandberg; Goubert, et al., 2010). The high amount of rubber aggregates makes the material highly elastic, which can enhance the road-tire contact to reduce noise (Wang; Liu, et al., 2017).

- **Use of recycled material -** This material can be beneficial for the environment since one of the main components is recycled tires. Worldwide, approximately 5 million tonnes of rubber tire is produced yearly. The main content of these tires is rubber, and we need to find a way to reuse this rubber. Otherwise, it goes to landfills, where it takes approximately 600 years for its complete decomposition (Almeida Júnior, A. F. D.; Battistelle, et al., 2012, Singh; Nimmo, et al., 2009, Wang; Liu, et al., 2017). Using recycled rubber tire crumbs can divert these tires from landfills and provides environmental benefits. In general, every 1000 sqft of PRP surface can save about 4100 pounds of tires from landfill (Porous Pave Inc., 2017)

- **Cost-effective material -** PRP surfaces can be economically advantageous since there is less need for new raw materials. Part of the materials come from recycled tires, which are not as expensive as any virgin component. Besides, in areas with some local regulatory restriction for surface coverage by impermeable surface or by structures, using a porous surface can increase the usable space while maintaining the required pervious surface area. Increasing usable space can also offset part of the construction cost of permeable pavement (Smith, 2006, Wang; Liu, et al., 2017).

- **Promotes urban vegetation and innovative material for urban design solutions** - Porous surfaces are suitable for allowing air and water to the tree roots. It can promote urban

vegetation, which is sometimes very challenging. PRP surfaces can be used on the tree well and replace metal tree grates. It can save the soil while supplying necessary air and water to the roots. It can be cut as the tree grows. Besides increasing permeable built-up usable area, this material can be used for maintenance strips, features like signs, lamp posts, patios etc. (Porous Pave Inc., 2017). Figure 15 shows the section on to use this material in tree surroundings and other examples of different uses.

Figure 15 Construction of PRP surface in a tree well and for other uses

Source: (Porous Pave Inc., 2017)

2.2.3 Disadvantages

Along with the list of advantages, PRP also has some drawbacks, which prevent its wider commercial prospects.

- **Durability and strength** – Although PRPs can bring lots of benefits to a project, the lower strength and durability significantly reduce their potential use. On one side, the use of rubber crumb and a large percentage of air voids make it a low-impact material; on the other hand, this combination impacts its durability and strength. Moreover, freeze-thaw resistance and winter maintenance in a cold climate can also impact the performance of PRPs. An optimum composition for PRPs' adequate strength is yet unidentified.
- **Functionality** - The functionality of the PRP surfaces is dependent on their permeability over time. Due to its porous nature, silt or other fine debris can deposit inside the pores and can clog the system. This can inhibit water infiltration capability and trap water inside the system, which is very detrimental to the material itself.
- **Anaerobic soil condition** - Anaerobic conditions can be developed in underlying soils if the water is unable to dry out before another rain or storm event. In the case of anaerobic conditions, limited oxygen in soil can be supplied to respiring organisms in soil (Inglett;

Reddy, et al., 2005). Although gradual clogging can create this anaerobic condition, it can also help remove that debris from the surface before it reaches the sub-base. Otherwise, they can be accumulated in the subbase or the underdrains, which is not easy to remove.

- **Groundwater contamination** - There is a great potential for groundwater contamination through PRP surfaces, as any of the de-icing salt or sand that is used for snow removal may penetrate through the voids to the groundwater. Moreover, any other toxic chemicals leak into the system may reach up to the groundwater table and contaminate the water. Thus, it is sometimes challenging to maintain underground water quality (Hansen, 2008, Schaus, 2007, EPA, 1999).
- **Lack of technical knowledge** – Since PRP is a new pavement material in North America, only limited applications can be found. As a result, the behaviour of the material, as well as its performance as a pavement material, is not established yet. Even no consistent technique for application is developed. Thus, another disadvantage can be the lack of technical expertise in the North American context, which may cause early construction failure (Hansen, 2008, Schaus, 2007, Hein, 2014, EPA, 1999, Porous Pave Inc, 2019).

Chapter 3
Research Methodology

3.1 Introduction

To accomplish the objective of this research, a series of three primary tasks were executed, comprising a preliminary field performance assessment, laboratory testing, and the construction, monitoring and evaluation of trial sections. As depicted in Figure 16, a comprehensive methodology was employed in this study. A preliminary field examination was carried out on two existing parking lots featuring PRP to gauge PRP's initial performance as a pavement surface material within the Canadian climate. Essential field performance evaluations were conducted during the examination, including assessments of stiffness, friction, roughness, permeability, and surface distress. The laboratory evaluations were also carried out on existing mix that is utilized in current practice, as well as newly developed mixes that were developed in the laboratory, with varying percentages of components and different binders. The aim of these laboratory tests was to evaluate the strength and durability of the mixes. In the course of these laboratory evaluations, a consistent method for sample preparation and the calculation of air voids for PRP was developed, which had not been previously available in current practice. After the laboratory evaluations of the mixes were completed, two trial sections were constructed utilizing the selected mixes. Post-construction evaluations were conducted immediately following construction, as well as three weeks and seven months after construction, and monitoring will be continued to evaluate the long-term performance of the trial sections. Finally, recommendations for the use of PRP as a surface material within the Canadian climate were outlined based on the results of this study.

3.2 Preliminary Field Evaluation

During the preliminary field performance evaluations, a Light Weight Deflectometer (LWD) was employed to assess the Modulus of Elasticity and deflection of the pavement. In addition, the British Pendulum Tester (BPT) and T2GO friction analyzer were employed to evaluate the frictional properties, while the SurPRO walking profiler and Dipstick were used to measure pavement roughness. The NCAT field permeameter was also utilized for permeability testing. Furthermore, a visual inspection was conducted to evaluate surface distress. These field tests were performed on pre-existing parking lots featuring PRP surfaces. Detailed methodology for the field testing is explained in Chapter 4 and Chapter 7.

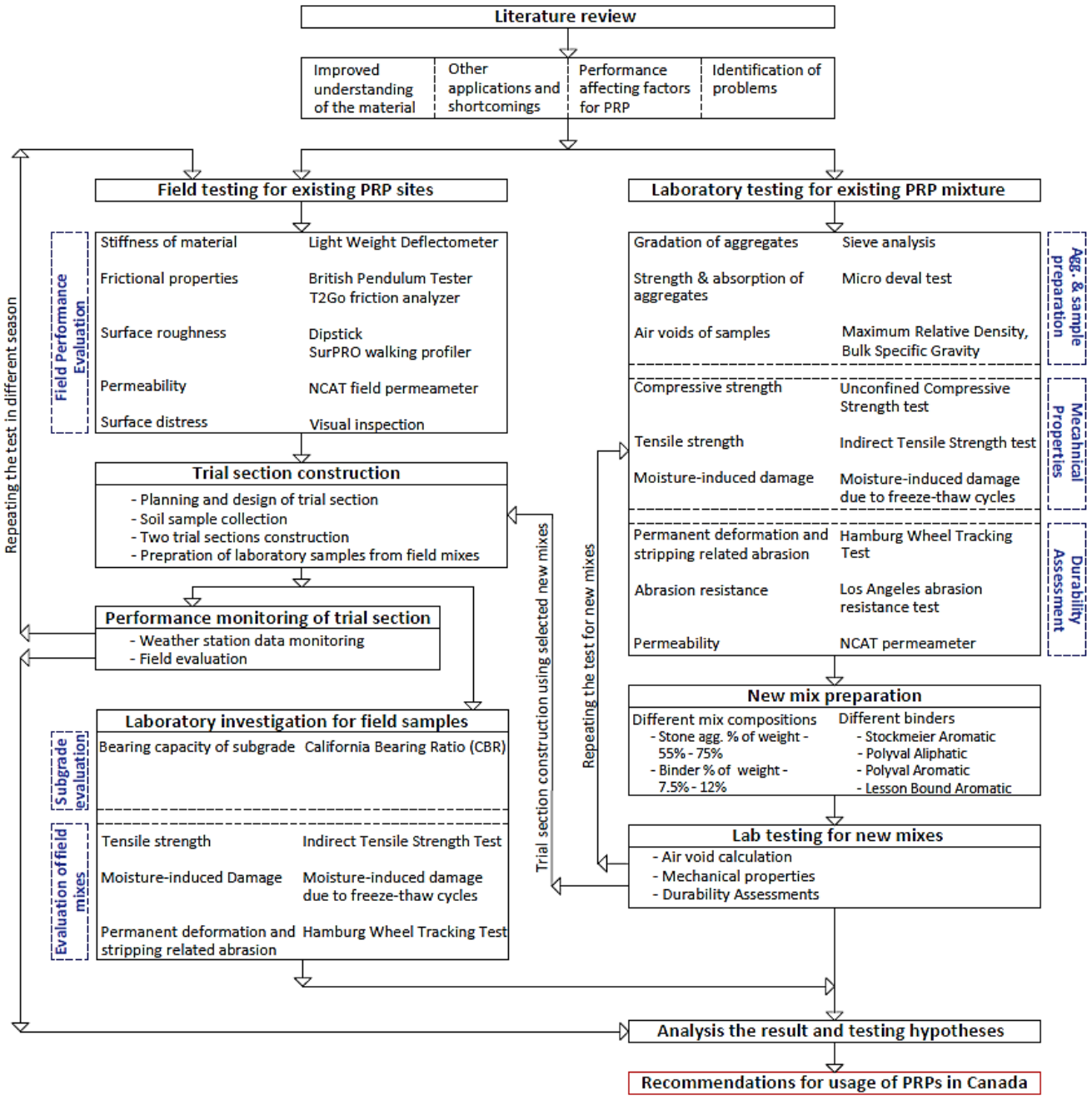

Figure 16 Research methodology

3.3 Laboratory Tests

There is no established standard for laboratory testing of PRP materials. Due to its elastic behaviour, PRP is closer to permeable asphalt or conventional asphalt pavements. Even for permeable asphalt pavement, only a few published standards are available. Nevertheless, the majority of tests required to evaluate the mechanical properties and durability of permeable pavements were similar to those used for conventional pavements, with variations in compliance targets and permissible minimum and maximum values (Hein, 2014). In this research, testing was conducted in accordance with standards for permeable or conventional pavement materials, with adjustments made following initial results. Additionally, a consistent method for sample preparation in the laboratory was developed, as well as a new method for calculating the air voids of PRP samples. To assess primary mechanical behaviour, compressive strength, indirect tensile strength, and moisture-induced damage due to freeze-thaw cycles were evaluated. For durability assessment, permanent deformation or rutting, abrasion resistance, and permeability were tested. Detailed laboratory test methods are in Chapter 5, Chapter 6 and Chapter 7.

3.4 Trial Section Construction, Monitoring and Evaluation

Following laboratory testing, two trial sections were constructed using selected mixes in addition to a Control Mix, with the objective of assessing and comparing the field performance of the laboratory mixtures to that of the Control Mix. Upon construction completion, the trial sections' performance was evaluated immediately, three weeks after construction, and seven months after construction. To evaluate the field performance, the pavement's stiffness, frictional properties, roughness, and permeability were analyzed using a Light Weight Deflectometer (LWD), British Pendulum Tester (BPT), Dipstick, and NCAT Permeameter, respectively. In addition, samples prepared from the field mixtures were also examined in the laboratory to determine any deviation from the laboratory mixtures.

Eventually, all data collected from preliminary field testing, laboratory testing, and trial sections were analyzed and integrated to comprehensively understand PRP materials. Based on this understanding, recommendations were formulated for the application of PRP materials as pavement surface material in the Canadian climate.

Chapter 4

Preliminary Study of Porous Rubber Pavement

4.1 Porous Rubber Pavement – In Situ Performance Evaluation of Stiffness and Friction in Canada

This paper was presented at the CSCE 2021 Annual Conference in Canada. It was also awarded 1st Place - Best Student Paper Award in the Engineering Materials Specialty session.

4.1.1 Abstract

Porous Rubber Pavement (PRP) is a relatively new material for low-trafficked pavements. This material consists of rubber aggregates, granite aggregates and polyurethane as a binder and is proportioned to attain a very high content of interconnected air voids. PRP has widespread environmental and safety benefits. While conventional impermeable paving materials interrupt our natural hydrological system by replacing natural soil surface, porous rubber pavement could reduce surface runoff, maintain the underground water table and improve water quality through its filtering capability. However, this low-impact design material is not currently widely used on pavements. Specifically, in Canada, its use is only limited to low-volume traffic and low-driving speed areas like parking lots and driveways. As a pavement material, its performance is still unexplored in the Canadian climate. Exhaustive research has been designed to investigate this material in this climate. This paper presents a part of the initial investigation of this material, which evaluates the performance of existing PRP in terms of its strength and friction on the field. To examine the stiffness of this material, Lightweight Deflectometer was used. Friction is examined and compared using British Pendulum Tester and T2GO friction analyzer. The average Modulus of Elasticity of PRP is noted to be between 33 MPa and 37 MPa, which is significantly lower than conventional asphalt pavement. Average BPN was found to be between 57 - 74, and frictional values significantly reduced (almost 22%) under the wheel path. T2GO results also show a lower coefficient of friction value below 0.4 under the wheel path. Although both of the friction analyzing equipment show a similar trend, the T2GO produced more consistent results. The overall result shows that the stiffness of PRPs is considerably low as a pavement material. However, it exceeds the frictional threshold value for pavements. This study provides insight into the existing performance of PRP and the basis for future studies to improve its performance for broader pavement applications.

4.1.2 Introduction

With the growing needs and requirements for more development, building new infrastructures becomes unavoidable. Thus, impermeable surfaces are increasing with new construction as well. Conventional impervious pavement surfaces are adding additional load to the storm-water management system with increasing surface runoff, which is triggering other problems like washing off contaminants, damaging pavements, and making roads unsafe for drivers and pedestrians (Drake; Bradford, et al., 2012, Schaus, 2007). In these circumstances, permeable pavements can be a part of the best management practices. These types of pavements are not a very new concept in North America. They have been used since research on it commenced at The Franklin Institute Research Laboratories in the United States with the support of the United States Environmental Protection Agency (EPA) in the late 1960s (EPA, 1999, Thelen and Howe, 1978). Different types of permeable pavement have been explored for the last couple of decades. They are mostly permeable asphalt, pervious concrete and permeable interlocking concrete pavers (Hein, 2014). Porous Rubber Pavement (PRP) is a novel type of permeable pavement material that has been incepted in North America only in recent years.

4.1.3 Background

PRP is a highly permeable pavement material consisting of stone aggregates, crumb rubber aggregates and polyurethane binders. PRPs can have a large percentage of interconnected air voids, which is up to 40% (Wang; Schacht, et al., 2017). This material was first introduced and used in Sweden in the late 1970s. In the later years, it gained interest in other European countries like Belgium, Norway, and The Netherlands and a few Asian countries like Japan, and China, where this material is mostly known as PoroElastic Road Surface or PERS (Sandberg; Goubert, et al., 2010, Wang; Liu, et al., 2017). In European and Asian countries, PRPs have been used as surface-wearing courses on highways or high-trafficked pavement, focusing primarily on traffic noise reduction. PRPs show high elasticity because of the use of a large amount of crumb rubber in the composition. The permeability and elasticity of PRPs contribute significantly to reducing tire-road noise than other types of pavements (Persuade, 2015).

As part of the early Norwegian research on this material, a trial section was constructed in 1989. The mix contained 4-8mm rubber granules, 13% polyurethane binder with 35% air voids, and the wearing course was 19mm thick. Along with the noise reduction of 7-9 dB(A) for a car, the friction coefficient measured by ‘Mu-meter’ was found to be 0.36, which was below the regulatory value (Sandberg;

Goubert, et al., 2010). From 2006 to 2009, in Japan, a few trial sections were constructed with mixes containing 30% air voids and silica sand. In their mix, they used the maximum aggregate size of 5mm, rubber granules of 1mm, rubber granules to aggregates ratio were 40:60 by volume and polyurethane as a binder. From these trial sections, the sound absorption coefficient was found to be 35% and the elastic modulus 25 MPa, whereas 250 MPa for conventional dense asphalt concrete (Kalman; Biligiri, et al., , 2011, Sandberg; Goubert, et al., 2010).

However, North American examples show that PRPs have been used in this region only on low-trafficked roads, pedestrian paths or playgrounds. Because of its highly permeable nature, it could show better performance for preventing hydroplaning, glare, spray, and splash on the road surface during surface runoff. This material can pertain extra benefit to the environment since it uses recycled tires. Worldwide approximately 5 million tonnes of rubber tire are produced yearly. The main content of these tires is rubber, and we need to find a way to make reuse of this rubber. Otherwise, it goes to a landfill, and it takes approximately 600 years for its complete decomposition (Almeida Júnior, A. F. D.; Battistelle, et al., 2012, Singh; Nimmo, et al., 2009, Wang; Schacht, et al., 2017). Using recycled rubber tire crumbs can divert these tires from landfills. According to one of the producers of PRP, every 1000 sqft of PRP surface can save about 4100 pounds of tires from landfills (Porous Pave Inc., 2017). Despite its use for different purposes, the properties of the material and its performance as a pavement material are still unexplored in the North American climate due to a lack of research.

4.1.4 Scope

Extensive research has been planned for investigating and improving the performance of PRPs in the Canadian climate with research facilities in the Center for Pavement and Transportation Technology (CPATT) of the University of Waterloo. A part of the initial field investigation is presented in this paper. Thus, the paper presents and analyzes the stiffness and friction performance of already existing PRPs in the field.

4.1.5 Methodology

4.1.5.1 Test Equipment

Light Weight Deflectometer was used to measure the stiffness of PRPs to determine their strength from the existing field. Light Weight Deflectometer (LWD) is a hand portable falling weight device used to determine the deflection due to a falling weight. From the output of the deflection bearing capacity

modulus of the pavement is determined. So, the stiffness of the upper layer of the pavement can be estimated from this device (Elhakim; Elbaz, et al., 2014, Mallick, R. B. and El-Korchi, T., 2018). The elastic modulus of PRPs was measured at the two test locations.

The British Pendulum Tester and T2GO friction analyzer were used for analyzing the friction of PRPs. Friction was tested only at Location 2 (Figure 17).

The T2GO allows continuous measuring of the skid resistance at low speeds (Iwanowski; Blacha, et al., 2018). T2GO can measure friction on both dry and contaminated surfaces. It is ideal for measuring in areas where it might be challenging to get access by a more substantial trailer or vehicle-type friction tester (Sarsys-ASFT, 2019). The device has two rubber tires that are used in measuring the skid resistance. Based on a known mass and braking force, the coefficient of static surface friction is measured at approximately 0.5 m intervals (Pickel, 2018). Since other tests were being performed concurrently, the entire pavement could not be made wet; hence, the results reflect the static coefficient of friction in dry conditions.

British Pendulum Tester or British Pendulum Skid Resistance Tester is a dynamic pendulum impact type tester. It has a rubber slider at its end, and the slider edge is propelled over a pavement surface, and the tester measures the energy loss. A higher BPN is related to a more significant loss of energy. So, a higher BPN number gives higher friction value (Pickel, 2018). From that result, the frictional property of the pavement surface is measured, which is associated with the microtexture of the pavement surface (ASTM E303−93, 2018). However, it measures the frictional property at a low speed (Saito and et al, 1996). The test point at Location 2 (Figure 17) was wetted before the test to get the frictional properties in wet conditions.

4.1.5.2 Material Properties

The PRP used for this study consists of recycled crumb rubber, cleaned and kiln-dried granite aggregates and moist-cured polyurethane binder. The proportions of the constituents are reported in Table 1. The grinding process of crumb rubber aggregates ensures that more than 99.5% of the steel fragments are removed from the tires, and after cleaning the chips, colours are infused instead of a thin outer coating. The polyurethane binder was B5HN Binder, provided by Porous Pave Inc.

Table 1 Material Composition

	Crumb rubber	Granite aggregates	Polyurethane binder
% by weight	45.25	45.25	9.5
Size of aggregates	1.18 to 2.36 mm	4.75 to 6.75 mm.	

4.1.5.3 Test Sites

Field tests were conducted on two (2) sites. The first field test was conducted on a residential driveway at Stratford, Ontario, otherwise referred to as "Location 1," and the second field test was conducted on the driveway of Lot 42, in Kitchener, Ontario, otherwise referred to as "Location 2". Figure 17 and Figure 18 show the test sites and their mapping for conducting tests.

Figure 19 also presents the pavement structure in both locations. Location 1 has been in existence for over six years, with no form of repairs or maintenance work performed on the pavement. The durisol blocks utilized beneath the PRP at this location are made from a proprietary cement-bonded wood fibre material and placed directly over the existing soil. Location 2 was constructed in July 2017 with the PRP material over a clean crushed stone subbase. After one year, repair work was needed due to deformation caused by extra heavy traffic producing corrugations on the pavement surface. The damaged part was cut and replaced by new PRP material of similar characteristics as the original. At this location, railroad tracks cut across part of the site, and in others, there was crumbled asphalt and concrete pavement. Figure 18a shows the detailed plan of Location 1, and Figure 18b detailed plan of Location 2 with surrounding structures and heavy traffic areas on the PRP pavement highlighted by the hatched areas.

a. Location 1 b. Location 2

Figure 17 Field test locations

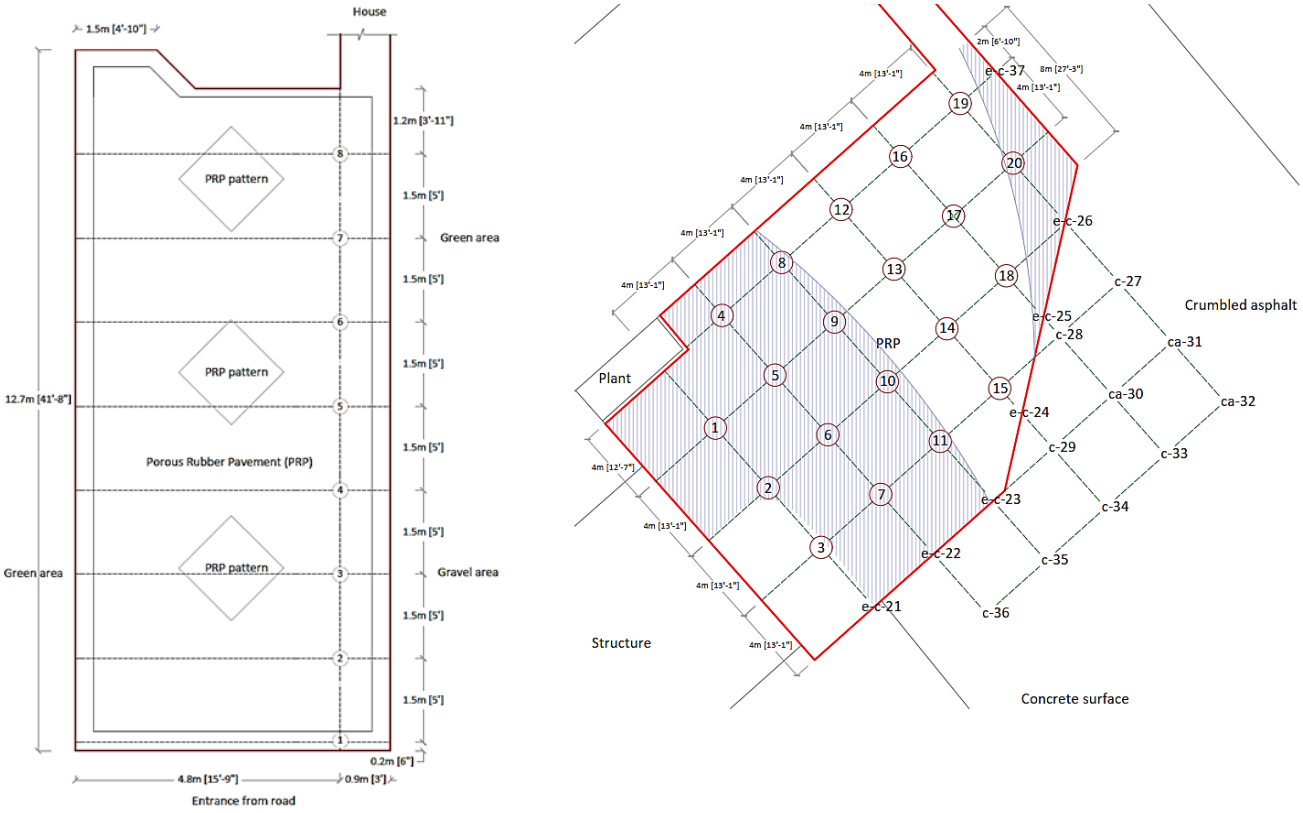

a. Location 1 b. Location 2

Figure 18 Test Sites Layout

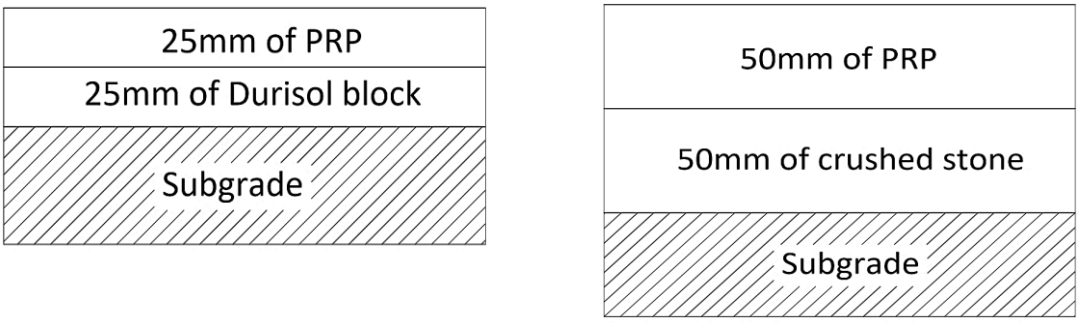

a. Location 1 b. Location 2

Figure 19 Pavement structure

4.1.6 Findings

4.1.6.1 LWD Result for Location 2

Twenty-three points were tested with the LWD. Among them, fourteen points (indicated by the suffix 'P') were on the PRP pavement area (Figure 20, indicated by the blue bars). Five Points were on the edge area, where outside of the edge was either concrete or crumbled asphalt (indicated by the green bars). Outside the PRP pavement area, four points on the concrete surface were tested to see the different responses of the pavement due to the difference in material.

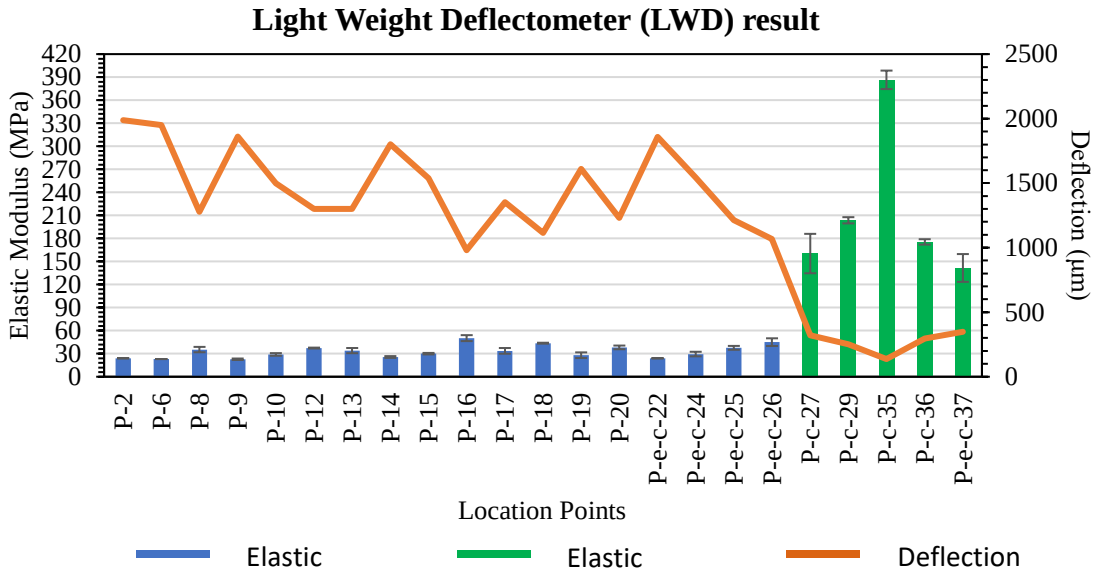

Figure 20 Lightweight Deflectometer Test result for Location 2

Results for Location 2, both elastic modulus and deflection, are presented in the same figure (Figure 20). The result shows that within the PRP area, the elastic modulus is very low, with an average value of 33 MPa (Std Dev 8.09 MPa) compared to the traditional asphalt pavements. The elastic modulus of conventional dense-graded asphalt is almost ten times higher than the elastic modulus of PRPs (Sandberg; Goubert, et al., 2010). So, the deflection was found to be very high (average of 1472 µm). Variation of the elastic modulus in the entire PRP area was observed. These disparities could be due to the presence of vehicle traffic in some areas tested and the absence in others. For example, P-2, P-6, P-9, and P-14 are located in areas (Figure 18b) that consistently experience vehicular traffic; this could be the reason for the lower modulus, as, over time, significant surface distresses were also observed in

these locations. However, P-16, P-20 and some other points rarely experienced vehicular traffic, and less pavement distresses observed, hence the reason for the higher modulus. The transition areas, like points on edges, also show lower elastic modulus along with high deflection. However, the points outside the PRP where the concrete and crumbled asphalt surface existed were observed to have over six times higher elastic modulus than the corresponding PRP. Although for these locations, a higher standard deviation (99.33 MPa) was observed, this can be explained by the variety of materials (concrete and crumbled asphalt) found in these locations. Thus, at those points, deflections were lower. On the edge point, 'P-e-c-37', the elastic modulus was found to be the highest (387 MPa). The probable reason could be the presence of any stone or hard material underneath that point.

4.1.6.2 LWD Results for Location 1

LWD results for Location 1 displays similar results as Location 2 (Figure 21). Here the average elastic modulus is 37 MPa with a standard deviation of 6.8 MPa, and the average deflection was found to be 1575 µm (Std Dev 195.73 µm). ANOVA analysis indicates that there is statistically no significant difference between the stiffness at both locations (P-value 0.2), although they had different pavement structures. It should be noted that the LWD has some limitations with respect to the depth of penetration during testing. This means that the Elastic Modulus of certain layers may not have been accounted for, thus the similarity between results from both locations.

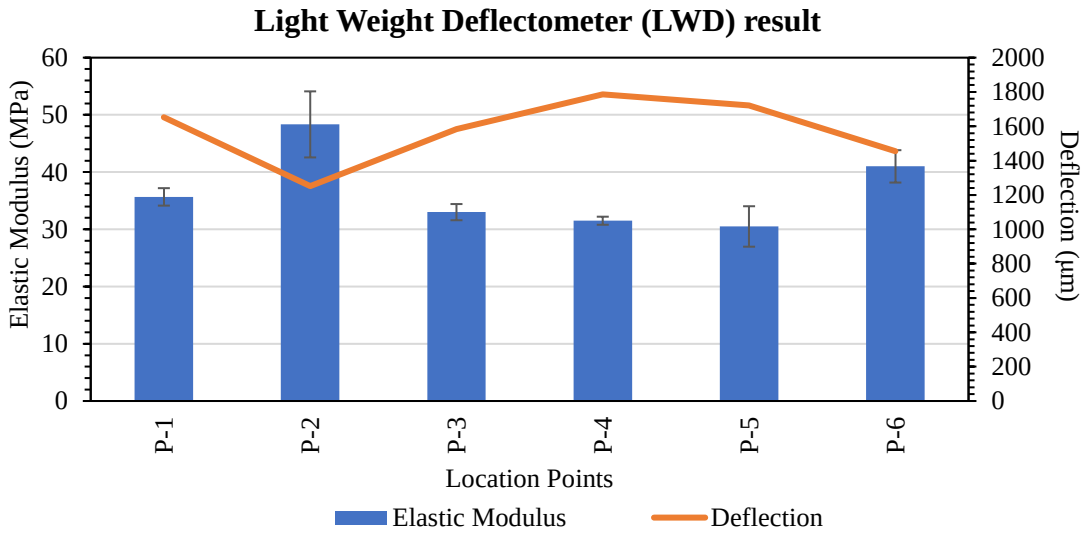

Figure 21 Light Weight Deflectometer Test result for Location 1

4.1.6.3 Friction Test

Friction values obtained using the T2GO and BPT for PRP surface area are presented in Figure 22 and Figure 23, respectively. Points tested by BPT are on the same lines tested by T2GO (Figure 18b). The BPT test was repeated at least five times to obtain an average BPN value for a given point. For the T2GO test, Line 1 is a connected line of points 4, 8, 12, 16 and 19. Line 2 is the connected line of points 1, 5, 9, 13, 17 and 20. Line 3 is the connected line of points 2,6, 10, 14, 18 and 26. Line 4 is the connected line of points 3, 7, 11 and 15, all as shown in Figure 18b.

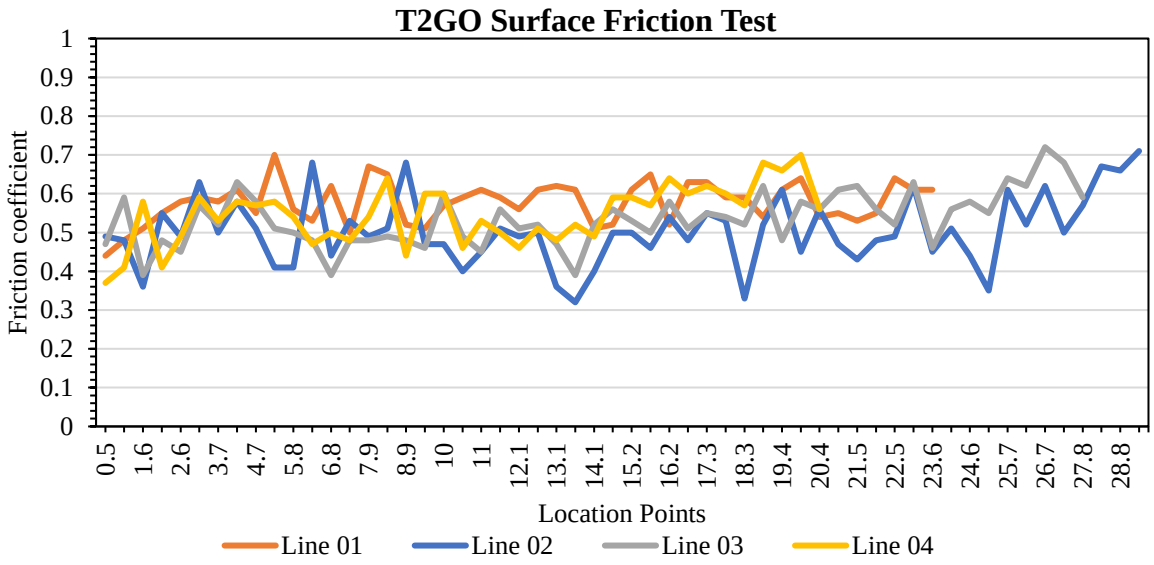

Figure 22 Result from T2Go surface Friction tester

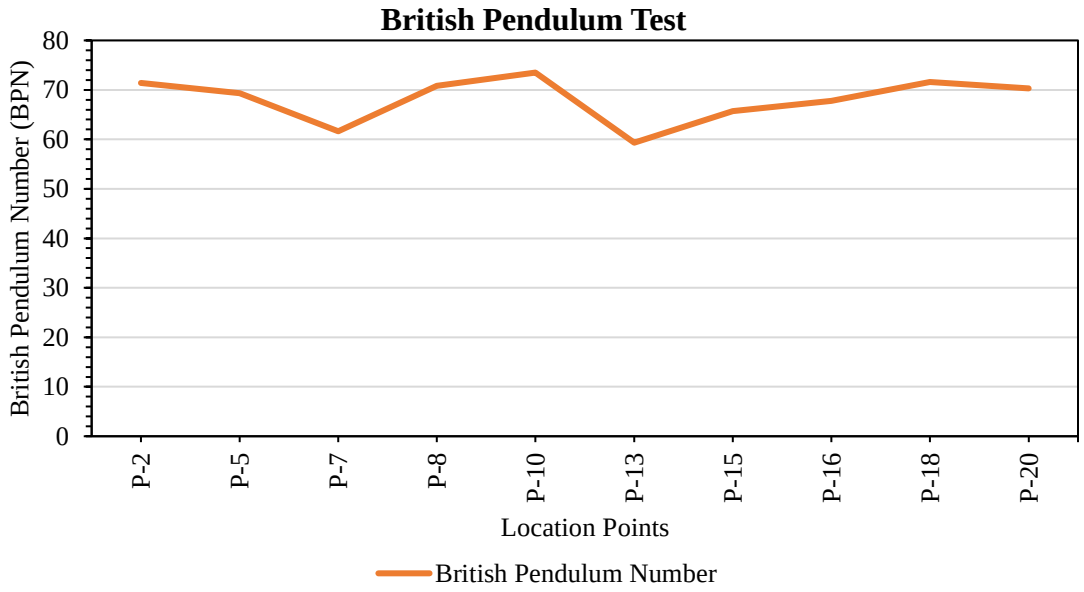

Figure 23 Result from British Pendulum Skid Resistance Tester

The average coefficient of friction was found to be 0.58,0.50,0.53,0.55 for Line 1, Line 2, Line 3 and Line 4, respectively. An average coefficient of friction for the entire area was found to be 0.54 with a standard deviation of 0.079, which shows just a slight variation for the lines.

On the other hand, a higher variation in BPN number was observed. The highest BPN number (74 BPN) was noted at P-10 and the least at P-13 (59 BPN). On average, the BPN value was 68 BPN for the entire location, with a standard deviation of 4.6 BPN. The lower frictional points have been observed to coincide with areas that were directly below the wheel path of service vehicles (Figure 2b) that utilized the parking. On the other hand, areas with higher frictional points were not directly on the wheel path.

Friction values from both types of equipment show a similar trend and magnitude comparing the sags and troughs in Figures 6 and 7 for the T2GO lines and BPN points. However, since more extensive variability is observed for BPN, it could be concluded that the T2GO could produce more consistent data. The friction values for both equipment also depict that the overall friction of the PRP surface is above the lower threshold value. According to the MTO criteria, frictional properties on all sections are acceptable with a Frictional Number greater than 30 (Pickel, 2018). The T2GO values exceed this number while converting the BPN to Coefficient of Friction (COF) according to Safety Direct America

(ranging between 0.66 to 0.85), which also indicates an exceedance of this number (Safety Direct America, 2019). Nevertheless, ravelling could have affected these friction results, which needs to be confirmed by further testing.

4.1.7 Conclusions

This study evaluates the performance of existing Porous Rubber Pavements applied to two parking lots located in Ontario, Canada, in terms of strength and frictional properties. In examining the stiffness of this material, the Lightweight Deflectometer was utilized. The frictional property was studied and compared using British Pendulum Tester and T2GO friction analyzer. The preliminary result shows the following;

- The average Modulus of Elasticity of PRP at Location 1 was 37 MPa, and at Location 2, 33 MPa, with statistically no significant difference between these two locations, even though they had different pavement structures.
- The stiffness of PRP below the wheel path and trafficked areas was found to be lower than in other areas.
- BPN number of PRP ranges between 57 to 74, with frictional values observed to reduce significantly (by 22%) under the wheel path area.
- The T2GO result also shows a lower coefficient of friction (below 0.4) along the wheel path, which indicates the traffic-related abrasion on the surface, with the average coefficient of friction in Location 2 ranging between 0.50 to 0.58.
- Similar trends and magnitude for both T2GO and BPT were observed; however, more variability in results was observed for BPT than for T2GO.

Despite other benefits in terms of environment and safety, the stiffness and friction of PRP are considerably low as a pavement material. This study provides insight into the existing performance of PRP and the basis for future studies to improve its performance for more comprehensive pavement applications.

4.1.7.1 Acknowledgements

The authors of this research gratefully acknowledge Stormflow Surfacing, Canada., Centre for Pavement and Transportation Technology (CPATT) and the University of Waterloo for supporting this research.

4.2 Performance Evaluation of Porous Rubber Pavement (PRP) in the Canadian Climate

This paper was presented at the TAC Conference & Exhibition (2020) in Canada.

4.2.1 Abstract

Permeable pavements are becoming popular in North America, especially in the last decade. Permeable pavements are considered a low environmental impact design and beneficial for best stormwater management practices. Porous Rubber Pavement (PRP) is a comparatively new addition to this type of pavement, which is currently utilized in low-traffic areas and pedestrian walkways as a surface material. PRPs have been used as a surface-wearing course for abating road noise in a few European and Asian countries. The constituents of PRPs are stone aggregates, crumb rubber from recycled tyres, and polyurethane as the binder. As a new pavement material in North America, its performance has not yet been fully quantified for this climatic condition. Because of its higher permeability (27% to 29% of voids), this material can be highly beneficial for preventing hydroplaning, glare, spray and splash on the road surface during surface runoff. Also, as a result of its flexible nature, it has the de-icing capability through the deformation of ice on its surface layers. As part of an extensive study on PRP material, an initial field performance evaluation was conducted on a commercial parking lot located in Kitchener, Ontario, Canada. In this study area, PRP was used as surface material. This paper presents some results obtained during these investigations with a focus on surface roughness, permeability and surface distress of PRP pavements. Two pieces of equipment, SurPRO and Dipstick, were employed to investigate pavement roughness in terms of the International Roughness Index (IRI). The average IRI of the PRP surface was found to be 10 m/km. The average infiltration rate was found to be 30836 mm/h. Ravelling (disintegration of material from the surface) was the significant surface distress observed during visual distress evaluation. Though the PRP shows widespread benefits in terms of environmental and safety issues, there is an opportunity to improve its performance as a pavement material after a thorough evaluation, which can make PRP a good candidate for the low-impact pavement surface. Thus, this investigation can be the basis for the future improvement of this material.

Keywords: Porous Rubber Pavement, Stormwater management, Roughness, Permeability, Surface distress

4.2.2 Introduction

With the building of roads, parking lots, driveways and other similar kinds of structures, impermeable surfaces are expanding in cities. These impermeable surfaces are leading to increased volumes and rates of stormwater runoffs along with accumulation and wash-off from a variety of contaminants. While conventional impermeable paving materials interrupt the natural hydrological system by replacing the natural soil surface, permeable pavement can reduce surface runoff, maintain the underground water table and improve water quality through its filtering capability. Along with the beneficial attributes of permeable pavements for best stormwater management practice, they have widespread environmental and safety benefits (Schaus, 2007).

Permeable pavements have become more common in North America over the last decade. The most common permeable types of pavements in the North American cold climatic region are pervious concrete, porous asphalt and permeable interlocking concrete pavers (Drake; Bradford, et al., 2012, Hein, 2014). Porous Rubber Pavement (PRP) is a comparatively new addition to these types of pavements. This material consists of rubber aggregates, granite aggregates and polyurethane as a binder and is proportioned to attain a very high content of interconnected air voids. PRPs can have a very large percentage of interconnected air voids. This percentage can be up to 40% depending on the variation in the percentage of different components and compaction effort applied during placement (Wang; Liu, et al., 2017). Besides, the use of a substantial amount of crumb rubber makes PRP a highly elastic material. Because of their very permeable nature, PRP pavements could be remarkably beneficial for preventing hydroplaning, glare, spray, and splash on the road surface during surface runoff. Additionally, both permeability and elasticity contribute to better tire-road noise reduction performance than other types of conventional pavements (Kalman; Biligiri, et al., , 2011, Persuade, 2015). Also, as a result of its flexible nature, it has de-icing capability by the deformation of ice on its surface layers, which can reduce snow accumulation on the pavement surface in winter (Wang; Liu, et al., 2017).

In North America, PRPs are used on low-traffic roads and pedestrian walkways as a surface material. It should be noted that this application is in limited areas only, like pathways, driveways, patios, playgrounds etc. However, as a pavement material, its performance is still unexplored in the North American climate. To date, no research has been found in the literature that investigates PRPs for North America. Thus, the properties of PRPs and their performance as pavement materials are still not fully quantified and understood.

4.2.3 Scope

The main objective of this study is to provide information on the current performance of existing PRPs, which will inform decisions that will enable the improvement of PRPs for the Canadian climate as a pavement surface material for low-trafficked areas. This paper presents part of a field investigation, which is a portion of a wide-ranging research. Particularly, surface roughness, infiltration capability and visual distress evaluation from existing PRP pavement are analyzed.

4.2.4 Methodology

The paper is based on the analysis of the in-situ field performance of PRPs in terms of surface roughness, infiltration capability or permeability and surface distress. For surface roughness, the SurPRO walking profiler and Dipstick were used. Using an NCAT permeameter, the permeability of the test surface was investigated. Surface distress was evaluated following The Ontario Ministry of Transportation (MTO) 's SP-024 manual.

4.2.4.1 Test Equipment

SurPRO is an effective device for measuring the surface profile and roughness characteristics of any placed surface. SurPRO uses a rolling inclinometer and measures longitudinal and transverse profiles of a travelled surface (Multipurpose Surface Profiler Operating Manual, 2014). The instrument can be operated at a constant walking speed of up to 2.5 mph (Nazef; Mraz, et al., 2008). Inclinometers of the SurPRO determine the elevation changes between its two wheels and produce profile data of the surface (Pickel, 2018). Then using ProVAL software, this profile data is converted into the IRI value of the tested surface.

The Dipstick is another inclinometer-based profile measurement device, which is traditionally used for profile verification (Karamihas, 2005). The instrument is supported by two legs, which are 305 mm (12 in) apart from each other. Two digital displays at the two ends of the instrument read the elevation of the leg relative to the other leg. The operator walks along the pre-marked surface by alternately pivoting the instrument about each leg (Nazef; Mraz, et al., 2008, Pavement Tools Consortium, 2019). The International Roughness Index (IRI) is calculated automatically from the recorded measurements.

NCAT Asphalt Field Permeameter was used to determine the water infiltration rate. This equipment has four tires of clear plastic. The bottom tire has the largest cross-section, and the cross-section reduces gradually for the upper tires. Permeameter needs to be sealed temporarily at the surface. Then, a given

mass of water is poured into the ring, and the time required for the total water infiltration is recorded. To follow the test standard ASTM - C1701/C1701M, the diameter of the bottom tire is considered. According to test standard ASTM - C1701/C1701M − 17a, at least three test points are recommended for a test area of 2500 m^2. Since the infiltration rate from each point is valid for the localized areas, to determine the infiltration rate of the entire site, the average value should be taken (ASTM C1701/C1701M−17a, 2017). The test points need to be selected in such a way that the first point is near the corner where pores can be clogged, the second point in the middle of the surface, and the third point near the edge where soil or debris can be transported easily (Valeo and Gupta, 2018).

4.2.4.2 Surface Distress Evaluation

Following The Ontario Ministry of Transportation (MTO)'s SP-024 manual for condition rating of flexible pavements, surface distress is assessed (Chong; Phang, et al., 2016). According to the manual's guideline, a visual inspection should be conducted to identify different types of distresses. Afterward, the severity and density of those distresses are categorized according to the guideline. Measurements of those distresses are also taken during the inspection, along with photographs for future reference. Surface distress evaluation helps to rate the surface condition and evaluates its ability to provide the expected service to the users (Chong; Phang, et al., 2016).

4.2.5 Material Properties

In most of the current practices in North America, PRP consists of 45.25% of recycled tires, 45.25% of stone aggregates and 9.5% of polyurethane binder by weight. Typically, it contains 27% to 29% interconnected voids by volume. Crumb rubber chips of a consistent size of approximately 6.35 mm (1/4") to 9.5 mm (3/8") are usually used for PRPs. For stone aggregates, cleaned and kiln-dried stone aggregates of the consistent size of 9.5 mm (3/8") to 19 mm (3/4") are used. Usually, granite is used to avoid water absorption by aggregates, which is detrimental to bonding with polyurethane binder (Porous Pave Inc., 2017). Polyurethane binder is a polymer where carbamate (urethane) links join organic units. Moist-cured polyurethane binder is solid at room temperature. In this study area, a B1—aromatic polyurethane binder was used.

4.2.6 Study Area

Field tests were conducted on a commercial driveway and parking at Kitchener, ON (otherwise referred to as the Study area), as shown in Figure 24 and Figure 25.

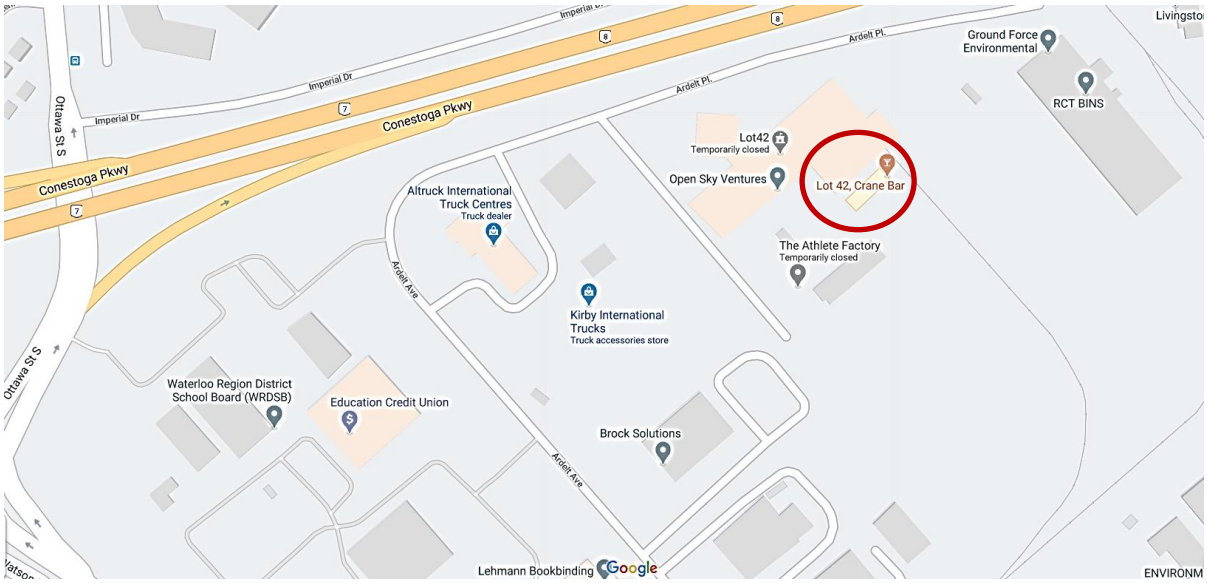

Figure 24 Study area

Source: Google map

The field test was conducted on October 24, 2019, from 10.00 am to 1.00 pm. During that period, the temperature was 11ºC, and humidity was observed at 66%.

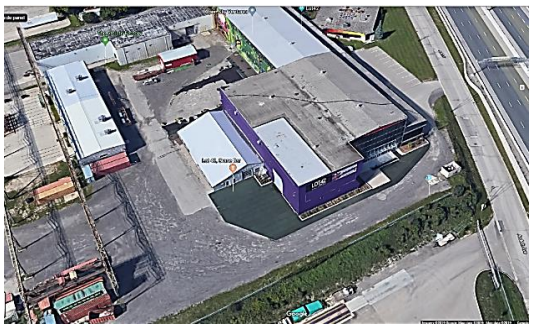

(a) Google earth view of the site

(b) Front view of the site driveway after construction

Figure 25 Photos of the study area

Source: After construction photo, Porous Pave Inc

This parking lot was constructed between July and August of 2017. Within a year of construction, ripples or corrugation were observed on parts of the parking lot. So, the damaged part was cut and replaced by new material using the same construction techniques.

In this study area, 50 mm (2") of PRP material was used over 50 mm (2") of the clean crushed stone subbase. For the PRP surface, a typical standard PRP mix was used. Both structure and mix design are shown in Figure 26. The adjacent areas outside the driveway area consisted of either concrete or crumbled asphalt. Figure 27 shows the detailed plan of the study area with surrounding structures. Heavy traffic areas on the PRP pavement are highlighted with the hatch on the detailed plan.

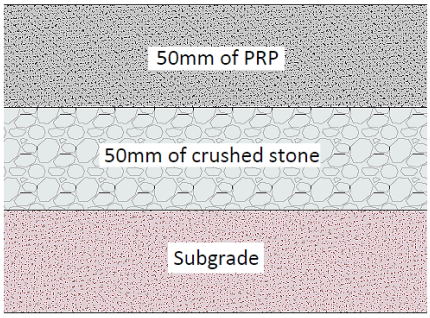

(a) Structure of the study area

Components	% by weight
Rubber Granules	45.25
Granite Aggregates	45.25
Polyurethane binder	9.5

(b) Components in mix

Figure 26 Structure of the pavement in the study area

Figure 27 shows a paved area with PRP by bold black lines. The pavement material of the surrounding area is also shown here. Points P-1 to P-20 indicate the points that were tested within the PRP area. Points ‘P-e-c' indicate the edge points, where outside of the edge is concrete pavement. Points 'P-c' and 'P-ca' indicate the points that are on the concrete surface and crumbled asphalt surface, respectively. The typical traffic type in the study area is delivery trucks and passenger cars.

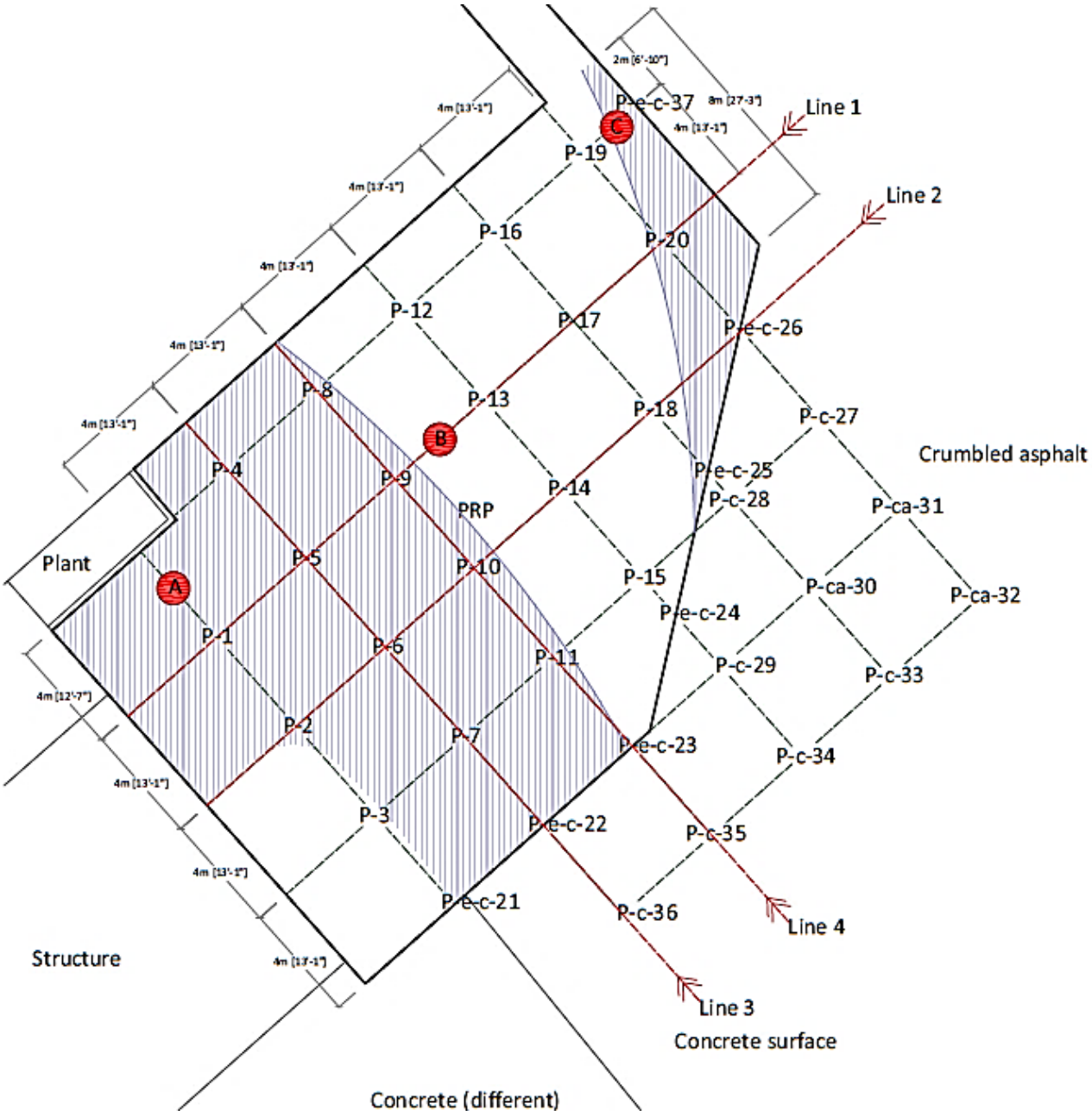

Figure 27 Detail plan of the study area

Figure 28 shows the preparation of the study area for testing according to the plan shown in Figure 27.

Figure 28 Site preparation for testing according to plan

4.2.7 Results

4.2.7.1 Roughness evaluation

The roughness of the PRP surface at the study area was evaluated by using two pieces of equipment, i.e. a walking profiler (SurPRO 2000) and a Dipstick, as shown in Figure 29.

(a) SurPRO 2000 (b) Dipstick

Figure 29 Surface roughness evaluation

IRI value is an indication of surface roughness. Figure 30 can be used for the interpretation of the IRI values obtained from field testing. Where an IRI value of 0 m/km signifies absolute smoothness and 8 m/km represents a rough surface of an unpaved road (Sayers and Karamihas, 1998).

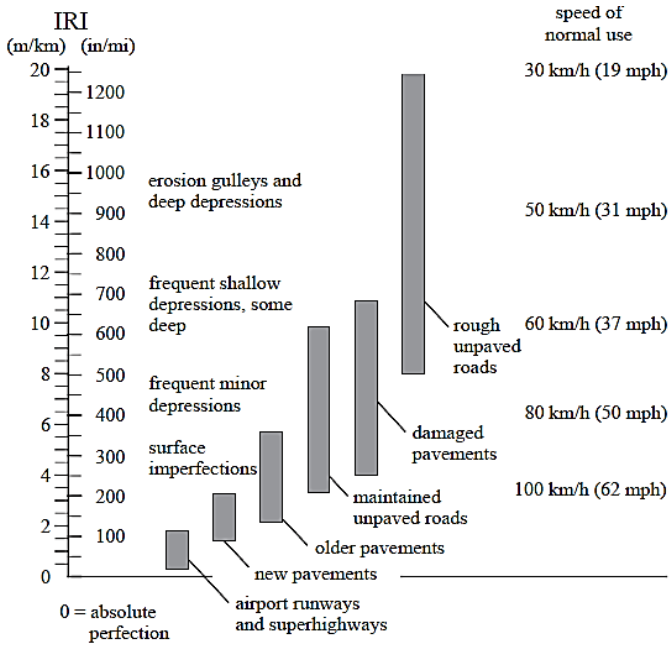

Figure 30 Pavement condition indication by IRI

Source: (Sayers and Karamihas, 1998)

As shown in Table 2, for both SurPRO and Dipstick, the same lines on the pavement surface were used. Tested lines can be identified in Figure 27 using Table 2.

Table 2 Location points for SurPRO and Dipstick testing

	Line 1	Line 2	Line 3	Line 4
SurPRO and Dipstick line connects	P-1, P-5, P-9, P-13, P-17, P-20	P-2, P-6, P-10, P-14, P-18, P-26	P-4, P-5, P-6, P-7, P-22	P-8, P-9, P-10, P-11, P-23

Both types of equipment give a very high average IRI value for the pavement surface, which is 10 m/km. SurPRO results showed a higher standard deviation, whereas Dipstick results showed more consistent values. Higher standard deviations for SurPRO data could be due to continuous

measurements and the presence of surface distress. However, ANOVA analysis indicated that there was statistically no significant difference between the results from both types of equipment (P-value 0.6). The average IRI for each line was also high. Probably under traffic loading, settlement occurred in the base layer. Besides, the construction method, which was not fully mechanized, may have caused unevenness on the surface. For line 3, the average IRI was higher than the rest of the lines. The reason could be that the line fell in the high traffic area, according to Figure 27 (hatched area). Also, it could be the attribution of transverse cracking, depression, and severe ravelling observed during surface distress evaluation along that line, as shown in Figure 33 and Table 6. Unfortunately, there was no initial IRI evaluation performed for the pavement immediately after construction to serve as a baseline for comparison with current IRI values; however, it is assumed that these values were lower than what is currently observed due to the nature of distresses that presently exist.

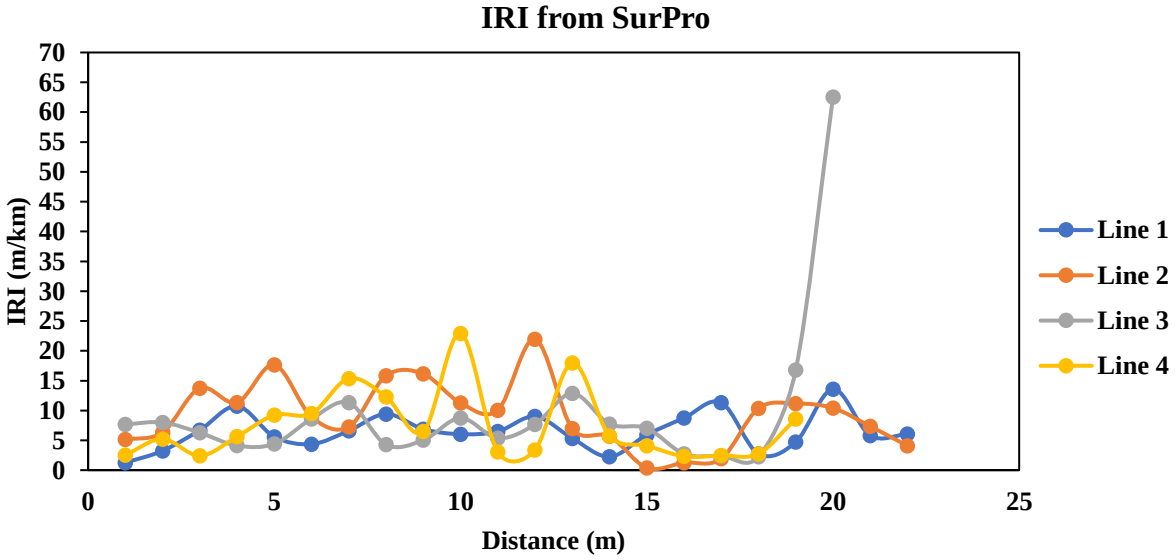

Figure 31 IRI result obtained from SurPRO

Table 3 Result from SurPRO

Line	Average IRI (m/km)	Standard deviation
1	6.52	3.24
2	9.18	5.67
3	13.41	20.55
4	8.68	6.21

Table 4 Result from Dipstick

Line	Average IRI (m/km)	Standard Deviation
1	7.56	0.23
2	10.25	0.10
3	15.77	0.07
4	8.93	0.83

4.2.7.2 Permeability Test

NCAT Asphalt Field Permeameter was used to determine the permeability of the surface at the study area, as shown in Figure 9. According to the test standard ASTM - C1701/C1701M − 17a, three points were selected for testing; A, B, and C. Point A was close to point P-1, as marked on the surface before the test. Point B was on the connecting line of points P-9 and P-13. Point C was very close to the point marked as P-19 (see Figure 4). The points' locations are also given in Table 4. The test area of the study was around 397.78 m^2, for which testing three points were considered sufficient. Since the infiltration rate from each point is valid for the localized areas, the average value should be taken to determine the infiltration rate of the entire site (ASTM C1701/C1701M−17a, 2017). In some cases, if the adjacent areas are unsaturated, water may spread to the adjacent areas. However, during this test, it was found that due to very high permeability, the water did not spread under the plate; instead, it immediately passed through the material.

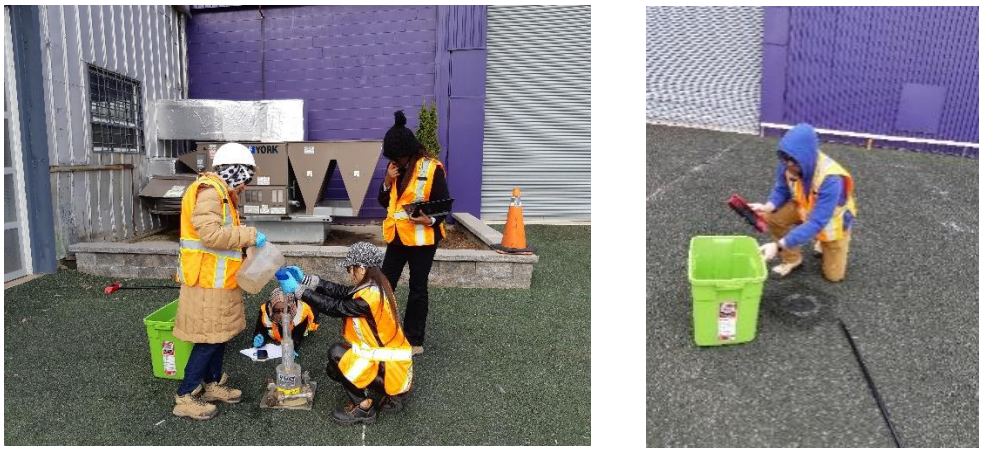

Figure 32 Permeability testing in the study area

The result of the permeability test is presented in Table 4. Points A and B showed a higher infiltration rate compared to point C. Since point C is close to the edge of the pavement surface, the probable reason could be the clogging of pores by debris. The average infiltration for the surface was 30836 mm/h. The intensity duration frequency data for short-duration rainfall shows that the maximum rainfall rate observed for Canada was 298.8 mm/h (Environment Canada, 2019, Henderson, 2012). The permeability rate of this pavement surface was much higher than this value. So, the permeability rate seems to be adequate for the study area. However, no hydrological design was considered during the construction, which would ensure that the pavement's storage or reservoir layer is thick enough to store rainwater for a given period of time and then slowly dissipate it to the subgrade soil. Thus, it was not possible to evaluate the hydrological design of this pavement.

Table 5 Result from Field Permeameter

Point's name	**Infiltration rate, I (mm/h)**
A (Close to P 1)	35508
B (Between P 9 and P 13)	32085
C (Close to P 19)	24915
Average	**30836**

4.2.7.3 Surface Distress Evaluation

There was no adverse structural issue observed during the distress survey. The major concern was ravelling (Figure 10, Figure 11 and Table 5). Most of the PRP surface was affected by ravelling. Lack of adhesion between crumb rubber aggregates and stone aggregates might have contributed to this abrasion loss. Another possible reason could be the rate of compaction or the compaction effort. During construction, only a little compaction effort was applied, which may increase the probability of ravelling on the pavement surface. Besides, the turning movement of vehicles may also have contributed to this ravelling. Other than that, very slight rutting and longitudinal cracking were observed. Slight rutting could be the result of a settlement in the base layer. Sometimes for permeable pavements, water infiltration may deteriorate the situation.

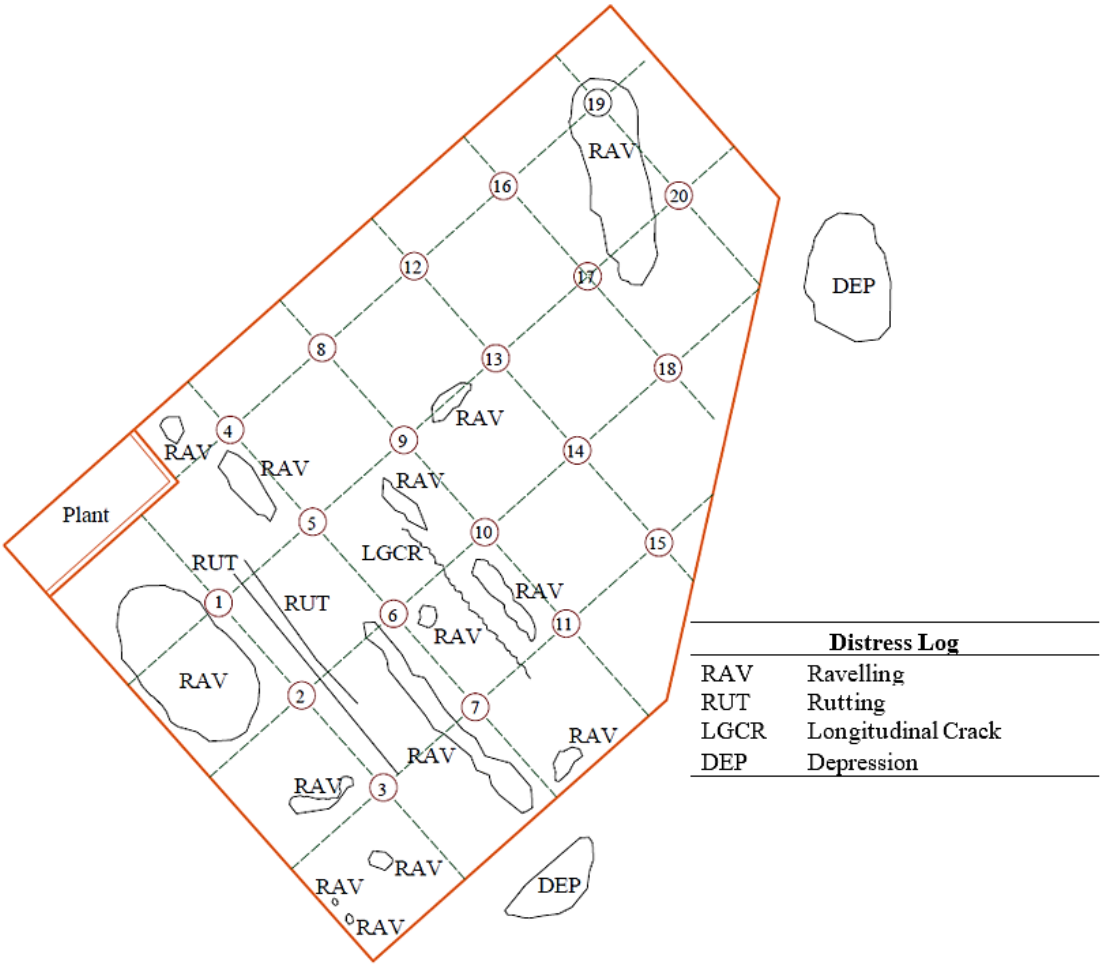

Figure 33 Surface distress mapping for the study area

(a) Ravelling

(b) Rutting

Figure 34 Surface distress at the study area

Table 6 Surface distress evaluation of Site 2

Section	Distress manifestation	Distress type	Severity	Extent	Description
Study area	Surface defects	Ravelling	3 (Moderate)	20 to 50% pavement surface affected (Frequent)	Having a pock-marked appearance. Shallow disintegration of pavement surface on most of the area.
		Ravelling	4 (Severe)	<10% of surface area (Few)	Disintegration with low severity potholes. Mostly in the heavy-traffic area.
	Permanent deformation	Rutting	1 (Very slight)	< 10% area affected (Few)	Barely noticeable, less than 6 mm. Measured rutting is 2 mm.

	Rutting	2 (Slight)	< 10% area affected (Few)	6 to 13 mm without a single longitudinal crack. Measured rutting is 8 mm.
Cracking	Longitudinal crack	2 (Slight)	< 10% area affected (Few)	Single crack from 3 mm to 12 mm. Measured 4 mm.

4.2.8 Conclusion

This paper investigates the performance of the existing pavement surface constructed with Porous Rubber Pavement. The study area was located in Kitchener, ON. The result of surface roughness, permeability and distress evaluation are presented and analyzed in this paper. The roughness of the pavement surface was evaluated by using the SurPRO walking profiler and Dipstick. Results from both types of equipment were compared to validate the result. NCAT permeameter was employed for permeability testing. Surface distress was evaluated by visual inspection. The result can be summarized as,

- The IRI value found from SurPRO was between 6.52 m/km to 13.41 m/km, and for Dipstick, this value was between 7.56 m/km to 15.77 m/km. There was statistically no significant difference between the results from the two pieces of equipment. The average IRI value was found to be 10 m/km.
- IRI value was found higher under the wheel path, in heavy traffic areas and in areas where visible surface distresses were observed. Settlement in the base layer and construction method is probably contributing to the high IRI value. Besides, severe ravelling could also have contributed to the higher IRI value.
- The average infiltration rate found for the pavement surface area was 30836 mm/h, which is significantly higher than the highest rainfall rate in Canada.

- The most visible surface distress for the PRP surface area was ravelling. Moderate to severe ravelling was found all over the study area.
- Lower compaction effort and less adhesion between rubber and stone aggregate were probably contributing to this ravelling or abrasion loss of PRPs.

Porous Rubber Pavement can be a potential alternative to the existing permeable pavement material in Canada. Preliminary investigation shows that its current performance in terms of permeability is adequate to reduce surface runoff during heavy rainfall incidents. However, uneven surface or higher surface roughness may affect riding comfort and maintenance activities. Since this material has typically been used mainly for slow traffic areas like parking lots, and driveways, its higher surface roughness may not affect the safety issues associated with high speed. However, further roughness evaluation is required to assess initial roughness and its progression over time. Also, severe ravelling is a concerning issue that is directly impacting the material's durability. This study is only providing initial insight into the PRP material, which can support the future detailed study and the improvement of the material property. Since performance evaluation in this study was application as a parking lot material, further study could look at improving the PRP material to accommodate higher traffic and speeds.

Chapter 5

Laboratory Mix Preparation and Investigation of Mechanical Behaviour of Polyurethane-bound Porous Rubber Pavement

This chapter is based on the paper submitted to the Journal of Cleaner Material, and the first revision has been submitted.

5.1 Abstract

With increased volumes and rates of stormwater runoffs, permeable pavement is becoming a viable solution for urban stormwater management systems. Polyurethane-bound Porous Rubber Pavement (PRP) is a novel sustainable solution for urban stormwater management systems, consisting of stone and recycled crumb rubber aggregates bound with polyurethane and high air voids (up to 45%). However, research on PRP for colder climates is lacking, making it essential to study its properties and behaviour as a pavement material before broad implementation. The present study explored the mechanical behaviour of PRP, developed techniques for sample preparation and established a method for determining air voids, which currently lacks a standard approach. Compressive strength, indirect tensile strength, and moisture-induced damage tests were conducted to evaluate the PRP's mechanical performance. The mechanical properties were investigated in two scenarios. The first scenario looked at four new mixes with different compositions of ingredients along with a Control Mix, whereas the second looked at four mixes prepared with different binders (aliphatic and aromatic). The study found that increasing the proportion of stone aggregates and binders in the mix improved compressive and indirect tensile strength, while higher rubber aggregate percentages improved retained tensile strength after five freeze-thaw cycles. Nevertheless, all mixes exhibited over 73% retained tensile strength. The type and source of binders resulted in a 59% decrease in indirect tensile strength and a 31% decrease in retained tensile strength across mixes. The mechanical properties indicate that PRP could be a suitable option for low-traffic pavement in colder regions subject to seasonal freeze-thaw cycles.

Keywords

Porous Rubber Pavement, Compressive Strength, Tensile Strength, Moisture-induced Damage

5.2 Introduction

Worldwide inevitable urbanization leads us towards increased impermeable sealed surfaces in urban areas. Also, conventional pavement seals the structure to secure it from moisture damage and other deterioration (Lu; Renken, et al., 2019). Thus, the volume and rate of surface runoff are amplified, and the opportunity to replenish the underground water table is reduced. As a result, it has appeared as a significant threat to the natural ecosystem; and disrupts urban life with disasters and accidents (Törzs; Lu, et al., 2019). Therefore, developing a sustainable system to redirect surface runoff from a sealed surface to the underground has become essential to recreate the natural hydrological cycle (Lu, 2019, Kayhanian; Li, et al., 2019). The construction of permeable pavement is one of the sustainable options that will slow down surface runoff through its water retention effect (Mbanaso; Coupe, et al., 2013). It also increases the water infiltration to the ground, supports efficient urban water management, and re-establish the natural hydrological cycle. However, permeable pavements are weaker than conventional pavements due to their open porosity. Besides, open pores are exposed to different weather conditions like UV radiation, air, water etc. Therefore, it can accelerate their aging process and quickly deteriorate the pavement. Previous studies show that polyurethane binder improves aggregate-to-aggregate mechanical connections and enhances the strength of the permeable material. In some cases, it can also slow down the aging process (Lu, 2019, Lu; Renken, et al., 2019, Scholz and Grabowiecki, 2007, Sun; Lu, et al., 2018, Chu; Tang, et al., 2018). Besides, renewable sources like vegetable oil can produce polyol, which is one of the polyurethane components (Ionescu, 2016).

The new polyurethane-bound Porous Rubber Pavement (PRP) contains different proportions of stone aggregates and rubber aggregates from recycled tires. If tire rubber goes to a landfill, it will take almost 600 years to decompose (Almeida Júnior, A. F. D.; Battistelle, et al., 2012, Singh; Nimmo, et al., 2009, Wang; Schacht, et al., 2017). The recycled rubber-tire crumbs can prevent them from being used as a landfill. PRP producers claim that constructing a 1000 sqft (93 sqm) surface can save about 4100 pounds (1860 kg) of tires from being sent to a landfill (Porous Pave Inc., 2017). Thus, instead of generating more waste from disposing of the scrap tires, their inclusion in PRP saves virgin material. In that way, PRP can contribute to environmental sustainability besides contributing to urban water management as a permeable material.

PRP material was first used in Sweden and then spread to other European countries such as Belgium, Norway, and The Netherlands, where it is commonly known as PoroElastic Road Surface or PERS

(Sandberg; Goubert, et al., 2010, Wang; Liu, et al., 2017). China and Japan also adopted this material as surface wearing course to reduce traffic noise (Wang; Schacht, et al., 2017, Sandberg; Goubert, et al., 2010). The material's flexibility due to the higher percentage of crumb rubber and permeability significantly reduces tire-road noise (Persuade, 2015). Because of its flexibility, it can also accommodate more ground movement and damage caused by root intrusion compared to conventional pavements (Mohammadinia; Disfani, et al., 2018). Additionally, PRP is produced at room temperature (25˚C ± 1˚C), saves energy and reduces Green House Gas (GHG), contrary to the hot mix products.

PRP is a comparatively new material in the North American climate and has been used here for low-trafficked areas, pedestrian paths, playgrounds etc. A thorough exploration of literature associated with PRP asserts some sustainability features of using this material. Besides, cooling-related stresses were measured for similar materials, showing that the cooling-related tensile stresses in this material are very low even when the temperature reached -33˚C (0.05 N/mm^2). Thus, this material can be used in a cold climate (Wang; Liu, et al., 2017). However, as a pavement material, its properties and performance are still unexplored in the North American environment. Although some research and information are available from European countries, those are in their initial stage of examinations. Preliminary field investigations of PRP identified its shortcomings with ravelling resistance, adhesion failure, and durability (Mo; Huurman, et al., 2009, Hagos, 2008, Kabir; Oyeyi; Al-BayatiTighe, 2020b). Besides, due to its recent inception, no consistent method has been developed yet for laboratory sample preparation and field construction, probably leading to varying pavement performance for the same composition. Thus, a consistent construction method, primary mechanical behaviour, and failure criteria must be adequately quantified and understood before widespread application. This research aimed to develop a method for laboratory sample preparation and air void calculation for this type of material. Then it investigated the primary mechanical properties of PRP material as a potential alternative to the conventional pavement in North American climate.

5.3 Materials and Methodology

This paper investigates PRP's strength range, failure criteria, and moisture-induced damage. First, the current commercial mix was examined as the Control Mix. Then, the other four types of mixes were developed through a factorial analysis. Thus, in total, five different mixes were tested. Also, using the proportion of the Control Mix, four polyurethane binders were used to make four different mixes to determine the different binder effects in PRP. In the Control Mix, B1—aromatic binders were used.

B2— aromatic, B2—aliphatic and B3—aromatic were used for the other three types of mixes. Among these binders, only B2— aliphatic was an aliphatic binder; others were aromatic binders. Aromatic binders contain methylene diphenyl diisocyanate (MDI) mixed isomers with aromatic parts in their molecular structure. This aromatic part absorbs ultraviolet rays from lighting. Over time, the binder became yellowish. This phenomenon is commonly known as ambering. However, this discoloration is only problematic for cosmetic issues. Otherwise, it does not impact the mechanical performance of the binder. Besides, the aliphatic binder does not contain any aromatic parts. So those aliphatic binders do not change colour after exposure to ultraviolet rays. Usually, aliphatic binders are more expensive than aromatic ones (Goubert and Sandberg, 2016, Kalman; Leprince, et al., 2015). New mixes and different binder types are listed in Table 7, Table 8 and Table 9. The same aggregates were used for all samples. In this study, all the materials were supplied by the industrial partner Stormflow Surfacing, Canada.

Table 7 Mixes with different compositions

Mixes with different proportions (by weight) of components	**A— Stone Aggregate, R— Rubber Aggregate, B— B1—aromatic Polyurethane Binder**	**Air voids**
Control Mix	A—45.25%, R—45.25%, B— 9.5%	35%–45%
Stone Aggregates (Factor A)	Lower limit— 55%, Upper limit— 75%	Air voids (objective permeability)
Polyurethane Binder (Factor B)	Lower limit— 7.5%, Upper limit— 12%	
New Mix 1	A– 55%, R– 37.5%, B– 7.5%	Within 20%–30%
New Mix 2	A–75%, R– 17.5%, B– 7.5%	
New Mix 3	A– 55%, R– 33%, B— 12%	
New Mix 4	A— 75%, R— 13%, B— 12%	

Table 8 Mixes with different binders

Mixes with different polyurethane binder	Percentages of components (by weight)	Air voids
B1— aromatic— Control Mix	Stone Aggregate– 45.25%, Rubber Aggregate– 45.25%, Polyurethane Binder–9.5%	35%– 45%
B2— aliphatic		
B2— aromatic		
B3—aromatic		

Table 9 Properties of polyurethane binders

Polyurethane binder	Containing group	Composition	Viscosity
B1—aromatic— Control Mix	Aromatic	Two-component commercial polyurethane binder. The two components are polyol mixture (A-component) and methylene diphenyl diisocyanate (B-component).	At 20°C: 3200 mPa.s
B2— aliphatic	Aliphatic		2000-4000 mPa.s (Temp. was not in MSDS)
B2— aromatic	Aromatic		2000-5000 mPa.s (Temp. was not in MSDS)
B3—aromatic	Aromatic		At 23°C: 2300 - 3300 mPa.s

5.3.1 Sieve Analysis

Grading of aggregates helps understand the relationships between porosity and packing. It also confirms whether aggregate sizes meet the specifications (AASHTO T 27-14, 2018). The sieve analysis apparatus (used for aggregates' grading) is shown in Figure 35. The stone (granite) aggregate's gradation is presented in Table 10 and Figure 36. The rubber aggregate's gradation is presented in Table 11and Figure 37. From the sieve analysis, it was found that a narrow range of stone and rubber aggregates were used in PRP mixes that ensure higher permeability. The stone aggregates' size mostly ranged between 4.75 mm to 9.5 mm, and the rubber aggregate's size was between 2.36 mm to 4.75 mm.

Figure 35 Sieve analysis apparatus

Table 10 Stone aggregate's gradation

Stone aggregate	
Sieve no	**Passing %**
12.5 mm	100.0
9.5 mm	95.8
6.7 mm	48.6
4.75 mm	10.4
2.36 mm	0.3
1.18 mm	0.2
No. 100	0.1
No. 200	0.1
Dust	0.0

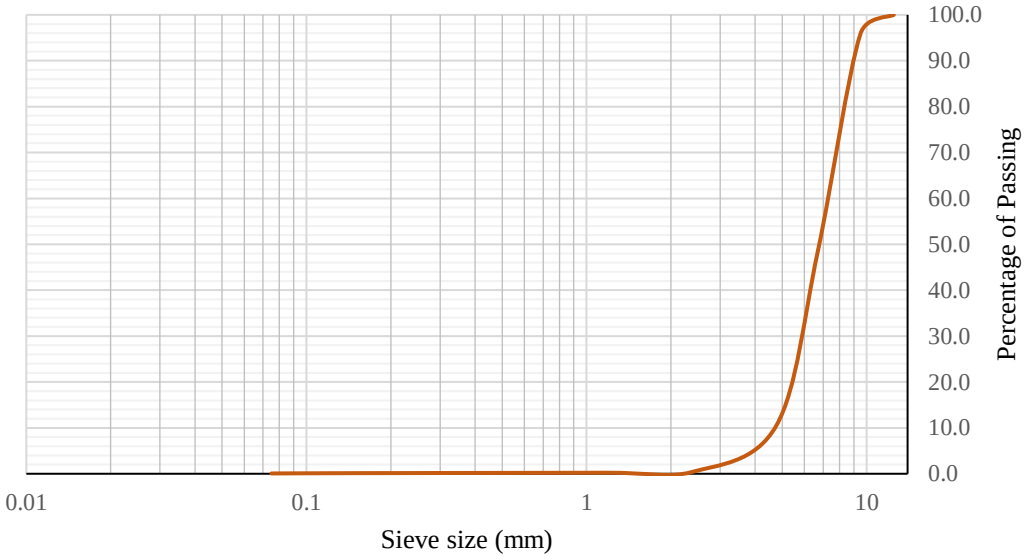

Figure 36 Stone aggregate's gradation

Table 11 Rubber aggregate's gradation

Rubber aggregate	
Sieve no	**Passing %**
6.75 mm	100.0
4.75 mm	99.8
2.36 mm	17.5
1.18 mm	0.1
No. 50(300µm)	0.0
No. 100(150µm)	0.0
No. 200 (75µm)	0.0
Dust	0.0

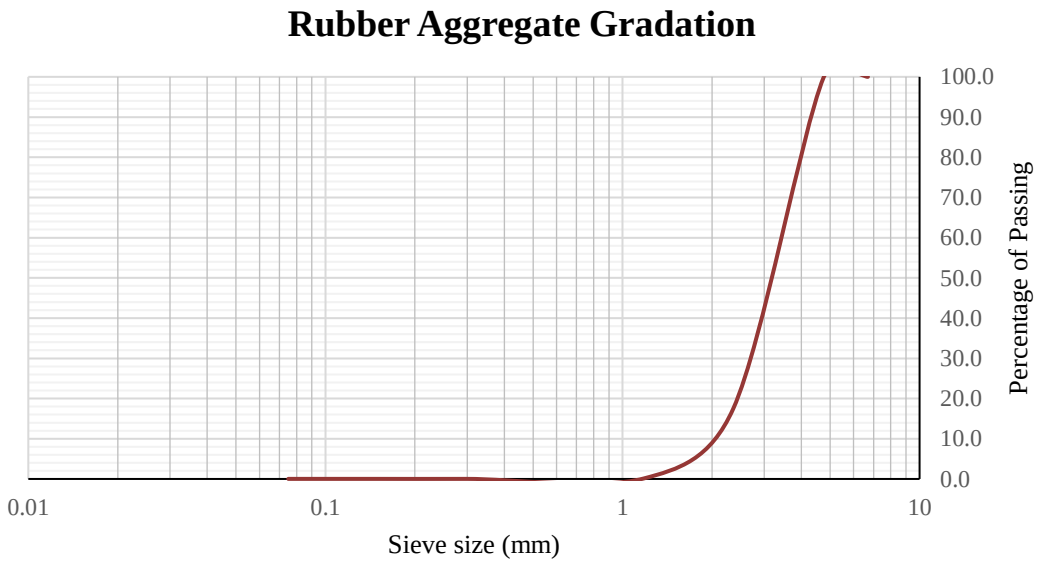

Figure 37 Rubber aggregate's gradation

5.3.2 Relative Density and Absorption of Stone Aggregate

Relative density (Specific Gravity) and absorption value (as shown in Table 12) of stone (granite) aggregate was determined according to ASTM C127 (ASTM C127, 2015). Relative density was found to be 2.83. The absorption for the stone aggregate was found to be 1.02%.

Table 12 Relative density and absorption of stone aggregate

Relative Density (Specific Gravity)	Apparent Relative density (Specific Gravity)	Absorption (%)
2.83	2.88	1.02

5.3.3 Sample Preparation for Lab Testing

Samples were prepared manually for all laboratory testing. Plastic moulds were designed for the test. The shape and sizes of moulds were determined according to the corresponding test protocols. The mixing and casting process was done at room temperature (25˚C ± 1˚C) since the viscosity of the polyurethane binder is not affected that much by the temperature (Lu; Renken, et al., 2019). Dry stone and rubber aggregates were mixed for 30 to 60 seconds. Then liquid polyurethane was added to the dry

mixture and mixed for another 90 seconds to achieve a homogeneous mixture. This mixing time was adopted from the current commercial construction of this type of pavement. However, at the beginning of casting, how much material (by weight) needed to be charged in the moulds to achieve a target air voids range was unknown. So, a few samples were produced, and air voids were tested for those specimens. Then the charging amounts were adjusted to get the target air voids. Vegetable oil was sprayed within the mould to make the de-moulding process easier. Then mixtures were charged into the moulds and compacted with a hand-held vibrator troweling machine, which creates 200 kg of vibrating force with a vibrating frequency of 2840 rpm for 60 seconds. Compaction with a hand-held vibrator troweling machine was applied to imitate the implemented compaction at the construction site and to reduce the air voids. However, after applying compaction effort, it was found that the vibration has minimal impact on compacting the material to achieve reduced air voids. In fact, it is a self-compacting material; densities mainly depend on the composition of mixes. Figure 38 shows the sample preparation process.

(a) Mixing all components in mixer

(b) Spraying mould with vegetable oil

(c) Charging material

(d) Compacting with vibrator

(e) Use of roller to smoothen the surface

(f) Misting the samples

Figure 38 Sample preparation at the lab

After compaction, the samples' top surfaces were smoothened by a wooden roller. After rolling, water mist was sprayed on the casted material to accelerate the curing process. It took about 12 hours to 24 hours to fully cure the specimens. After fully cured, specimens were pushed by a rubber mallet and de-moulded softly.

5.3.4 Maximum Relative Density

As a new material, no established standard is available to determine the Maximum Relative Density (MRD) for loose PRP mixes. Several methods were attempted to determine the MRD for this material. In the liquid state, the polyurethane binder is moisture sensitive, and in contact with moisture, it

becomes solidified and cures quickly. So, MRD was first calculated using an equation (Wakefield, 2020, Mugdha, P.,). The following Equation 1 was used for the calculation.

$$G_t = \frac{100}{\{\frac{100 - W_b}{G_a}\} + (\frac{W_b}{G_b})}$$

Equation 1

Where G_t = Maximum specific gravity of the mix

W_b = Binder content in percent by weight

G_b = Specific gravity of binder

G_a = Average specific gravity of the aggregates

It was not possible to calculate MRD for all the mixes using the equation since the specific gravity of individual components was not available, except for the Control Mix. In the next step of the trial, the standard protocol for the hot mix asphalt was used with modification for calculating MRD. The liquid polyurethane became solidified in contact with moisture after a short period. Thus instead of vacuuming for 10 minutes, loose mixes were vacuumed for 5– 7 minutes and kept in the water bath for another 5– 7 minutes. In this way, it was possible to avoid the solidification of the loose mix (AASHTO T 209-11, 2011). MRD calculated by equation and MRD calculated by the modified method was found to be identical for the Control Mix. Finally, MRD for different mixes was calculated using this modified method. The result is shown in Table 13 and Table 14.

Table 13 MRD for different new mixes

Mix	Maximum Relative Density (MRD)
Control Mix	1.56
New Mix 1	1.67
New Mix 2	1.93
New Mix 3	1.59
New Nix 4	1.78

Table 14 MRD for different mixes with different binders

Mix	Maximum Relative Density (MRD)
B1—aromatic binder - Control	1.56
B2— aromatic binder	1.5
B2— aliphatic binder	1.55
B3—aromatic binder	1.55

5.3.5 Air Void Testing

Calculation of air void for PRP samples is complicated, unlike conventional asphalt or concrete mixes. Even the standard procedures applicable for the Open Graded Friction Course (OGFC) or the pervious material (ASTM D7064/D7064M, 2013, InstroTek, 2011, Montes; Valavala, et al., 2009) do not work for PRPs because of their distinct composition. Some research tried to determine the percentage of air void in a similar product by using the samples' outer dimension and weight (Kalman and Biligiri, 2013). However, since the sample's surface is not smooth enough, the acquired result was not that accurate. Advanced non-destructive technologies like X-Ray computed Tomography (XCT) or other high-resolution cameras could be used to capture the surface and cross-section of the samples. Then the

micro-level structure of the samples could be obtained and analyzed to determine the air voids of the sample (Lu, 2019, Xu; Guo, et al., 2015b, Xu; Guo, et al., 2015a). However, this lengthy procedure could not be adopted for every sample prepared for testing. Also, this is an expensive test needed to be outsourced. Several methods adopted in previous research were also explored. A few research calculated the permeable materials' air voids from the vacuum-sealed density of the compacted samples using the CoreLok machine. Lian and Zhuge combined CoreLok and an equation to determine the air voids. ASTM D 7063 refers to the air void calculation of conventional asphalt mix, and AASHTO T–166 refers to the bulk-specific gravity calculation of conventional asphalt samples. Conventional asphalt sample's air voids are determined using these standards (InstroTek, 2011, Lian and Zhuge, 2010, ASTM D7063/D7063M, 2018, AASHTO T 209-11, 2011, AASHTO T 166, 2013). All the procedures involve the weight calculation of samples submerged in the water. However, due to open pores, the outer surface volume of PRP samples could not be calculated directly by the water displacement. Even the vacuum sealed PRP samples float on water because of their lower density than water. So, to calculate the sample's weight in water, it was necessary to work against the buoyancy effect. Thus, AASHTO T–166 was modified to carry on the test. After vacuuming– sealing, the sample was submerged in the water using a container with a glass lid. A rubber mallet was used to remove bubbles from the water by agitating the container from the outside, and it was easily visible through the glass lid. Following Equation 2 to Equation 7 were used to calculate the air voids. Figure 39 shows the steps in air void testing.

$$T_w^0 = \pm 25^0 C$$

Equation 2

$$R = \frac{A}{M_b}$$

Equation 3

$$A_G = -0.000566 * \mathrm{R} + 0.8121$$

Equation 4

$$V_c = \frac{M_b}{A_G}$$

Equation 5

$$G_{mb} = \frac{A}{A + D - E - V_c}$$

Equation 6

$$P = \frac{G_{mm} - G_{mb}}{G_{mm}} * 100$$

Equation 7

Where A = Dry sample weight in the air before sealing, g

M_b = Dry plastic bag weight, g

$T_W{}^0$ = Water temperature = +/- 25^0C

D = Container + Water + Glass plate weight, g

E = Container + Water + Glass plate + Sample in bag weight, g

R = Ratio

A_G = Plastic bag's Apparent Gravity

V_c = Volume of plastic bag

G_{mb} = Bulk Specific Gravity

G_{mm} = Maximum Relative Density (MRD)

P = % of air voids

(a) Vacuumed–sealed sample

(b) Vacuumed-sealed sample placed into the container

(c) Weighing the sample with a glass plate

Figure 39 Air void testing procedure

5.3.6 Unconfined Compressive Strength (UCS)

The material's compressive strength was tested according to ASTM D1074 Standard. Compressive strength can contribute to the overall mixture characterization and determine its suitability under specific loading and environmental conditions. For this test, specimens of 101.6 mm (4 in.) in diameter by 101.6 mm (4 in.) in height were tested. The test was conducted in axial compression without lateral support at a uniform rate of vertical deformation of 0.05 mm/min·mm (or 0.05 in./min·in.) of height (ASTM D1074 - 17, 2017). The specimen's UCS is then determined as a ratio of the maximum load at failure (P) to the specimen's cross-sectional area (A), as in Equation 8.

$$UCS = \frac{P}{A}$$

Equation 8

Where P = Load at failure

A = Cross-sectional area

The test equipment is shown in Figure 40. Densities and air voids were calculated for all the samples before the compressive strength test.

Figure 40 Test equipment for Unconfined Compressive Strength (UCS)

5.3.7 Indirect Tensile Strength

Low-temperature cracking is one of the dominant pavement deteriorations in cold countries like Canada. The tensile strength test can be one of the measurements for pavement material to determine its resistance against low-temperature cracking (Lu; Renken, et al., 2019). The Indirect Tensile Strength test (ITS) was done on compacted samples following the standard AASHTO T 322-07, as shown in Figure 41. The tensile creep compliance at different loading times, tensile strength, and Poisson's ratio can be calculated from this test. For this test, the sample should be 38 to 50 mm high and 150 ± 9 mm in diameter (AASHTO T 322-07, 2016). The test measures the breaking or the highest force observed on the sample. This resistance capacity of the material is its tensile strength (Lu; Renken, et al., 2019). Equation 9 was used to calculate the tensile strength of each specimen.

$$S_t = \frac{2000 \times P_f}{\pi \times b \times D}$$

Equation 9

Where S_t = Tensile strength of specimen, kPa

P_f = Maximum load observed for specimen, N

b = Thickness of the sample, mm

D = diameter of the sample, mm

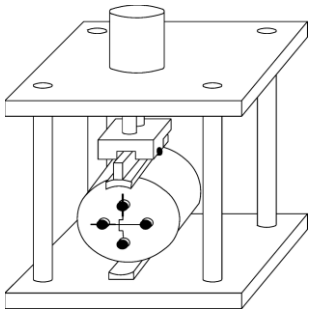

Figure 41 Specimen loading frame for IDT

Source: (AASHTO T 322-07, 2016)

5.3.8 Test for Moisture-induced Damage

After accelerated conditioning with freeze-thaw cycles, a moisture-induced damage test was conducted for the PRP samples. This test evaluated the effects of saturation and freeze-thaw cycles on PRP samples. Numerical indices of retained indirect-tensile properties were calculated by comparing two groups of samples with the same properties (AASHTO T 283-07, 2011). A modified test method was followed for conditioning the samples. A new set of samples were prepared for conditioning which is 150 mm in diameter and 50 mm in height (similar to the indirect tensile test). A partial vacuum of 660mm Hg (26 inches) was applied for 10 minutes to saturate the compacted specimens to whatever saturation level was achieved. Then the specimens were kept submerged in water during freezing cycles to maintain saturation. Samples were frozen at -18˚C for 16 hours and then thawed in 60˚C hot water for 8 hours to complete one freeze–thaw cycle. Instead of one freeze-thaw cycle, the freeze–thaw cycles were repeated five times. Then the tensile strength of the conditioned samples was determined by the indirect tensile test and compared with the indirect tensile strength of unconditioned samples. According to the standards, the retained tensile strength (TSR) should be at least 80 percent (AASHTO T 283-07, 2011, ASTM D7064/D7064M, 2013, Kandhal, 2002). Figure 42 shows the conditioning process of the samples.

Thus, the first group comprised dry samples, and the second group was subjected to moisture and freeze-thaw conditioning. The Tensile Strength Ratio (TSR) was calculated from the Indirect Tensile test results using Equation 10.

$$TSR = \frac{S_2}{S_1}$$

Equation 10

Where S_1 = Average tensile strength of the dry samples

S_2 = Average tensile strength of the conditioned samples

(a) Saturated samples in water

(b) Frozen samples

(c) Thawing of samples

Figure 42 Samples submerged in water, frozen samples, and samples in the hot water bath

5.4 Results and Discussion

5.4.1 Air Void

Air voids were calculated for every sample tested under different protocols with a modified method developed for PRP in this research to ensure all the mixes maintained sufficient permeability. Details are already discussed in the methodology section (5.3.5). A higher percentage of air voids (38% to 45%) was found in the Control samples produced following the current commercial practice. In current practice, a slight vibration is used to compact the material on site. This compaction effort was increased for the new mixes in the laboratory to reduce the void content in the samples. However, samples were prepared with lower and increased vibrations to check their effect on the samples. After calculating void contents for all of the samples, PRP was found to be a self-compacting material. Therefore, increased external vibration has minimal impact on reducing the void contents in the samples. Table 15 shows the calculated void contents for samples with different mixes. Besides, it was also found that mixed compositions primarily determine the void content in the samples. The Control Mix had the

highest percentage of rubber aggregates (45.25%) and the lowest percentage of stone aggregates (45.25%); thus, it contained a higher air void percentage. On the other hand, New Mix 4 contained the maximum percentage of stone aggregates (75%) and maximum percentage of binder (12%), showing a lower percentage of air voids. While the elastic behaviour of rubber aggregates worked against the compaction, stone aggregates and an increased percentage of binder enhanced the compactibility of PRP samples. Different types of binders also showed little impact on compactibility except for B3—aromatic. The use of B3—aromatic in the Control composition indicated a 9% to 12% reduction in air voids. The probable reason could be its lower viscosity than other binders, which probably dispersed more between the aggregates and enhanced its compactibility.

Table 15 Air voids of different mixes

Different mix types	Average air void
Control Mix	38%– 45%
New Mix 1	31%– 38%
New Mix 2	24%– 25%
New Mix 3	27%– 28%
New Mix 4	18%– 29%

Different binder types	Average air void
B1—aromatic—Control	38%– 45%
B2— aromatic	35%– 37%
B2—aliphatic	34%– 37%
B3—aromatic	29%– 33%

5.4.2 Compressive Strength Test

Performance and behavioural differences were expected in PRP than the conventional asphalt and concrete pavement material as its composition and construction method differ. Compressive strength is one of the critical properties of pavement material since it determines the pavement's loading

condition and permanent deformation. The compressive strength test results for the Control and new mixes are presented in Table 16 below.

Table 16 Test results of Unconfined Compressive Strength comparing different new mixes

Mix types	Air voids (%)	Average air void (%)	Compressive strength (MPa)	Average (MPa)	Standard Deviation
Control Mix	41	40	1.1	1.2	0.05
	39		1.2		
	40		1.2		
New Mix 1	33	33	1.7	1.6	0.04
	31		1.6		
	34		1.6		
New Mix 2	24	24	3.7	4.0	0.28
	24		4.1		
	24		4.3		
New Mix 3	27	28	3.7	3.4	0.28
	28		3.5		
	28		3.1		
New Mix 4	19	20	4.1	4.2	0.13
	22		4.1		
	18		4.4		

Because of its very flexible behaviour, though PRP materials showed a low compressive strength, they can carry more loads within the elastic region. The reason is that the deformation in the elastic region is recovered mostly after removing the load. On the contrary, a deformation that occurs in the plastic region is permanent. It was also found that the compressive strength of PRP changed with the change in the composition of the mixes. The result showed that the material's compressive strength increased when the percentage of stone aggregates and binder increased in the mixes. On the other hand, when the percentage of binder and stone aggregates decreased and the percentage of rubber aggregates increased in the mixes, the material's compressive strength decreased. The highest compressive strength was observed in New Mix 4 (4.2 MPa), where the stone aggregate percentage was 75%, the rubber aggregate was 13%, and the binder percentage was 12%. The lowest compressive strength was found in the Control Mix, which was 1.2 MPa. The Control Mix contained the lowest percentage of stone aggregates, i.e., 45.25%, and the highest percentage of rubber aggregates, i.e. 45.25% and 9.5% of binder. New Mix 2 also showed relatively higher compressive strength, i.e., 4.0 MPa, since it contained the highest percentage of stone aggregates (75%) and a lower percentage of

rubber aggregates (17.5%). The factorial analysis also confirmed that increased binder and stone aggregate percentages positively affected compressive strength. In contrast, the increase in rubber aggregates negatively impacted the material's strength. When aggregate increased by 10%, the compressive strength increased by 0.79 MPa. When the binder increased by 2.25%, the compressive strength increased by 0.49 MPa.

A relationship between the air voids and the compressive strength was developed in the graph below (Figure 43). It shows that an increase in air voids decreases the compressive strength of the PRP mixes. Furthermore, linear regression analysis showed that compressive strength and air void had an approximately linear relationship, with an adjusted R^2 of 0.8839 (details in Appendix A).

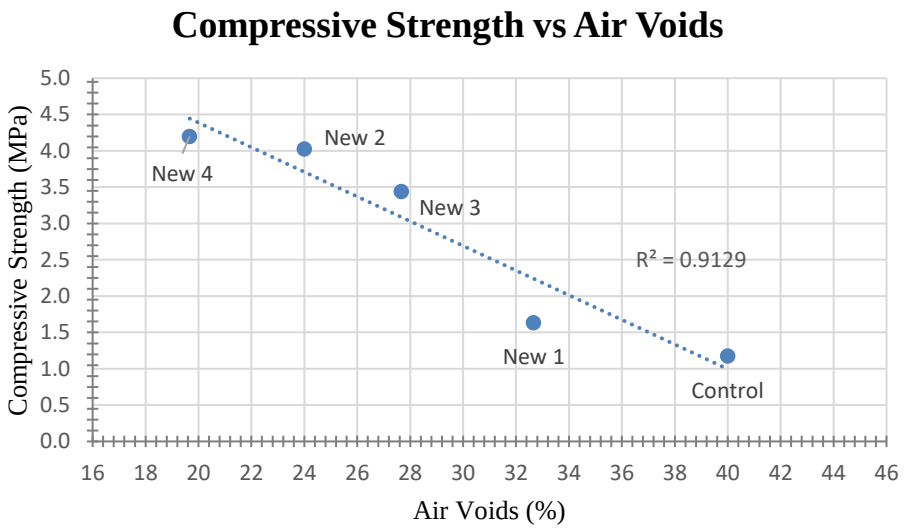

Figure 43 Compressive Strength vs Air Voids

Figure 44 shows the compressive strength development in the different mixes with time.

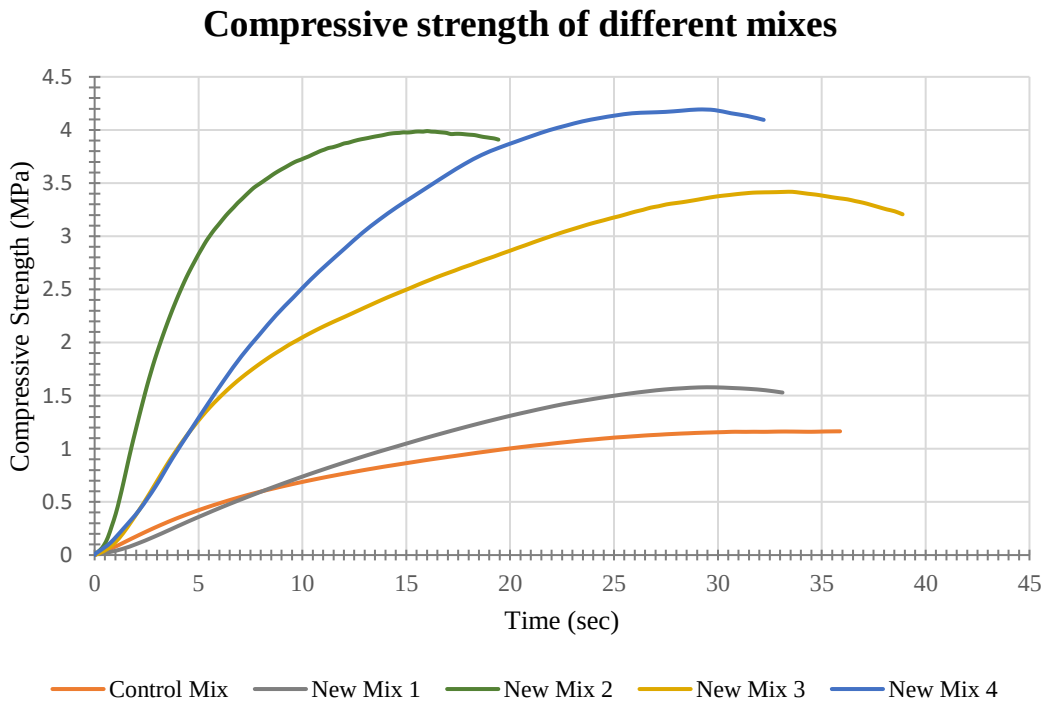

Figure 44 Compressive strength development in the material with time

With the change in the compressive strength, the fracture behaviour of the mixes also changed. The fracture behaviour of the Control Mix (which showed the lowest compressive strength) was different from the New Mix 4 (which showed the highest compressive strength). The Control Mix showed more ductile deformation, while the New Mix 4 showed more brittle behaviour, as shown in Figure 45. The Control Mix contained a higher percentage of rubber aggregates (45.25%) and higher air voids (40%), which can probably explain its ductile behaviour and lower compressive strength. The Control Mix achieved a resilient property due to the elasticity of rubber aggregates, higher porosity and solidified polyurethane binder. Thus it deflected more under compressive loading, enhanced the yielding area (Figure 44) and showed plastic deformation before breaking. On the other hand, New Mix 4 contained a higher percentage of stone aggregates (75%) and a lower percentage of air voids (20%). So, its fracture was mainly dependent on stone aggregates and solidified binders. Thus, it showed brittle behaviour.

(a) Control Mix (b) New Mix 4

Figure 45 Fracture in the Control Mix and Fracture in the New Mix 4

Different mixes of PRP showed that these mixes' compressive strength ranged from 1.2 MPa to 4.2 MPa. However, this range lies between permeable asphalt and permeable concrete. Figure 46 shows the comparison of the compressive strength of different pavement materials. Some research indicates that permeable asphalt pavement's compressive strength could range from 2.4 MPa to 3.6 MPa (Chairuddin; Tjaronge, et al., June 2016). For the permeable concrete, compressive strength was found to be between 3.5 MPa to 28 MPa in the laboratory. The most typical value for permeable concrete is 17 MPa (Pervious Pavement,). In contrast, conventional Portland Cement Concrete (PCC) has a compressive strength between 20.68 MPa and 34.47 MPa (Pavement Tools Consortium, 2019).

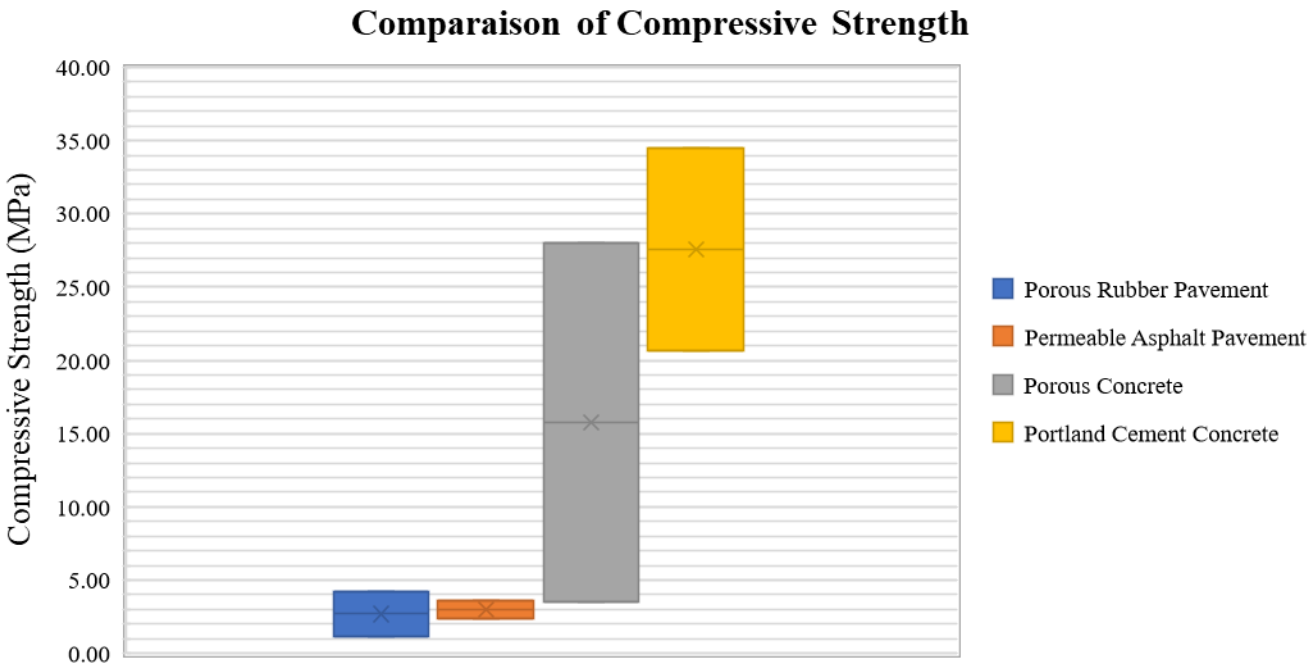

Figure 46 Comparison of compressive strength of different pavement material

The compressive strength test results from the mixes using different binders are presented in Table 17. The highest compressive strength was found in the Control Mix, i.e., 1.18 MPa and the lowest in the mix with B2—aromatic binder, i.e. 0.67 MPa. However, differences in the compressive strength with different binders were shallow. The reason for this difference could be the various sources of the binder.

Table 17 Compressive strength of mixes with different binders

Mix with different binders	Air voids (%)	Average Air void (%)	Compressive strength (MPa)	Average (MPa)	Standard Deviation
B1—aromatic—Control	41	40	1.12	1.18	0.05
	39		1.20		
	40		1.21		
B2— aromatic	35	35	0.82	0.67	0.15
	36		0.65		
	35		0.54		
B2— aliphatic	35	36	1.09	0.96	0.12
	37		0.89		
	36		0.89		
B3—aromatic	30	29	0.98	1.02	0.09
	29		0.96		
	29		1.12		

5.4.3 Indirect Tensile Strength

The Indirect Tensile Strength Test was conducted to determine the tensile strength of the PRP mixes. The test was one of the criteria to assess low-temperature cracking and deformation of the PRP material (Lu; Renken, et al., 2019). Higher tensile strength means a higher resistance against cracking and winter damage (Wang; Liu, et al., 2017). Test results of the Indirect Tensile Strength (ITS) for different mixes are presented in Table 18. The New Mix 2 showed a maximum tensile strength of 565.5 kPa. However, the tensile strength for the Control Mix was determined to be 169.7 kPa, which was the lowest value among the mixes. The mixtures' tensile strength variation was influenced by the percentages of both stone aggregate and binder in the mixes. The tensile strength increased when the stone aggregate and the binder percentages in the mixes increased. Factorial analysis showed that the impact of stone aggregate on tensile strength was higher than the binder contents. When the stone aggregate was increased by 10%, tensile strength increased by 85.16 kPa. However, when the binder percentages were increased by 2.25%, tensile strength increased by 76.29 kPa.

Table 18 Indirect Tensile Strength for different mixes

Mix types	Air voids (%)	Average air void (%)	Indirect Tensile Strength (kPa)	Average (kPa)	Standard Deviation
Control Mix	41	41	155.4	169.7	12.58
	38		182.2		
	45		163.0		
	40		178.1		
New Mix 1	37	37	204.6	205.2	12.56
	38		192.9		
	37		218.0		
New Mix 2	25	25	521.2	565.5	47.29
	24		560.0		
	25		615.3		
New Mix 3	27	27	520.6	547.8	23.60
	28		562.7		
	27		560.1		
New Mix 4	25	25	536.7	528.0	48.10
	21		571.2		
	29		476.2		

Moreover, the percentage of air voids in the mixes affected the tensile strength of the PRP mixes. Figure 47 shows that as the air voids increased, tensile strength decreased. This might be attributed to the fact that when air voids increased, the density of the mixes was reduced, leading to the failure of mixtures at lower stress. A linear regression analysis was conducted to investigate the relationship between the air voids and the tensile strength. The analysis showed (as in Figure 47) that air void and tensile strength had a linear relationship, with an adjusted R^2 of 0.96095 (details in Appendix B). Thus, the increase of rubber aggregates and air voids reduced the tensile strength of the PRP. Analysis of fracture behaviour showed that separations were mostly in aggregates and binders. Figure 48 below

shows the fracture in Control Mix (with the lowest tensile strength) and New Mix 2 (with the highest tensile strength).

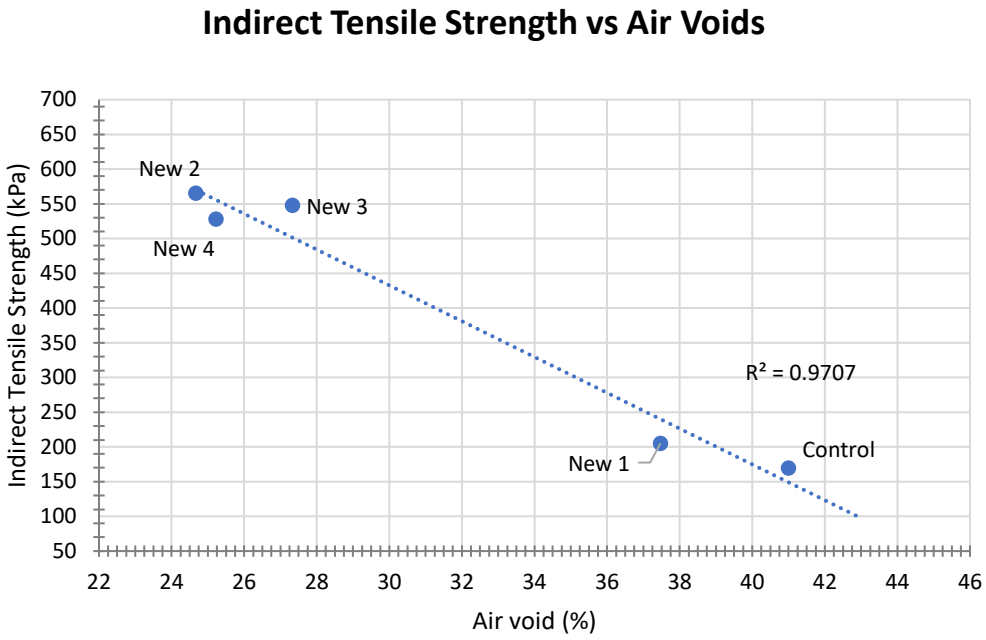

Figure 47 Relationship between Indirect Tensile Strength and air voids

(a) Control Mix (b) New Mix 2

Figure 48 Fracture on Control Mix and New Mix 2

The influence of various binder types on the tensile strength of PRP was also investigated, and the obtained results are presented in Table 19. The results demonstrated that the Control Mix with the B1—

aromatic binder had the maximum tensile strength (169.7 kPa), whereas the samples with the B2—aromatic binder had the lowest tensile strength (70.1kPa). Thus, the material's tensile strength was affected by different sources of polyurethane binder.

Table 19 Indirect Tensile Strength of mixes with different binder

Mix types	Air voids (%)	Average air void (%)	Indirect Tensile Strength (kPa)	Average (kPa)	Standard Deviation
B1—aromatic binder—Control	41	41	155.4	169.7	12.58
	38		182.2		
	45		163.0		
	40		178.1		
B2—aromatic binder	35	36	80.0	70.1	9.51
	36		69.2		
	37		61.1		
B2—aliphatic binder	34	34	150.1	156.4	6.87
	34		163.7		
	35		155.2		
B3—aromatic binder	31	31	84.5	85.0	1.34
	30		84.0		
	33		86.5		

5.4.4 Compressive Strength vs Indirect Tensile Strength

The study findings revealed a strong relationship between PRP's tensile and compressive strength. Mixtures with lower compressive strength showed lower tensile strength as well. Furthermore, the results demonstrated that the material's compressive strength was six to eight times its tensile strength, as shown in Table 20.

Table 20 Compressive Strength and the Indirect Tensile Strength of new mixes presented in the same unit

Mix type	Compressive Strength (MPa)	Indirect Tensile Test (kPa)	Indirect Tensile Test (MPa)	Times
Control Mix	1.2	170	0.17	6.9
New Mix 1	1.6	205	0.205	8.0
New Mix 2	4.0	566	0.566	7.1
New Mix 3	3.4	548	0.548	6.3
New Mix 4	4.2	528	0.528	8.0

5.4.5 Moisture-induced Damage

Permeable pavement has lower strength than conventional pavement related to its high porosity. Besides, unlike impermeable pavement, permeable pavement allows water to go through it. Prolonged saturation is also a common phenomenon for this type of pavement. Consequently, premature failure of permeable pavement often occurs due to moisture-induced damage. Thus, durability and performance often reduce quickly (Huang; Wu, et al., 2010, Lu, 2019). In the cold regions, moisture-induced damages are accelerated with freeze-thaw cycles. Hence, this research compared two sets of samples to determine the moisture-induced damage from freeze-thaw cycles, where the first set of samples tested for indirect tensile strength without conditioning. The second set of samples was conditioned with five freeze-thaw cycles before being tested for indirect tensile strength. Then the ratio of the conditioned and unconditioned samples was calculated. The result is presented in Table 21. The tensile strength of the samples was expected to decrease after being conditioned. However, PRP showed good resistance to moisture-induced damage due to freeze-thaw cycles. Calculated Tensile Strength Ratio (TSR) showed that all samples with different compositions retained more than 73% of the tensile strength.

Table 21 Retained tensile strength of different mixes

Mix	ITS before conditioning (kPa)	ITS after conditioning (kPa)	Tensile Strength Ratio, TSR
Control Mix	169.7	141.2	0.83
New Mix 1	205.2	215.7	1.05
New Mix 2	565.5	410.6	0.73
New Mix 3	547.8	458.1	0.84
New Mix 4	528.0	395.4	0.75

Xu H. et al. (2015) explained that during freeze-thaw cycles, the internal structures of pavement material change in three ways, i.e. existing pores enlarge, separate voids merge, and new voids form (Xu; Guo, et al., 2015a, Xu; Guo, et al., 2015b). Hence, the mixes that attained lower internal changes after freeze-thaw cycles retained more strength than others. On the other hand, the mixes that reached more internal changes after freeze-thaw cycles lost more strength due to a loss in their density with more voids. This study observed that retained tensile strength was higher in those mixes where the percentage of rubber aggregates was higher. That indicates rubber aggregates resisted their internal changes. The retained tensile strengths of New Mix 1, New Mix 3 and Control Mix were 105%, 84% and 83%, respectively. These mixes comprise 37.5%, 33%, and 45.25% rubber aggregates. New Mix 1 showed the highest retained strength since it contained a lower percentage of stone aggregates (55%) and a relatively higher percentage of rubber aggregates (37.5%). Test results obtained from the relative density and absorption of stone aggregates (as in 5.3.2) also supported the moisture-induced damage of this section. The relative density of the stone aggregates used in these mixes was found to be lower, and absorption was slightly higher (1.02%). So, the mixes containing more stone aggregate lost their strength easily after conditioning. Besides, only a small amount of disintegrated material (loose aggregate) was found for all the samples after conditioning. Furthermore, all samples showed minimal discoloration after the freeze-thaw cycles, as presented in Figure 49.

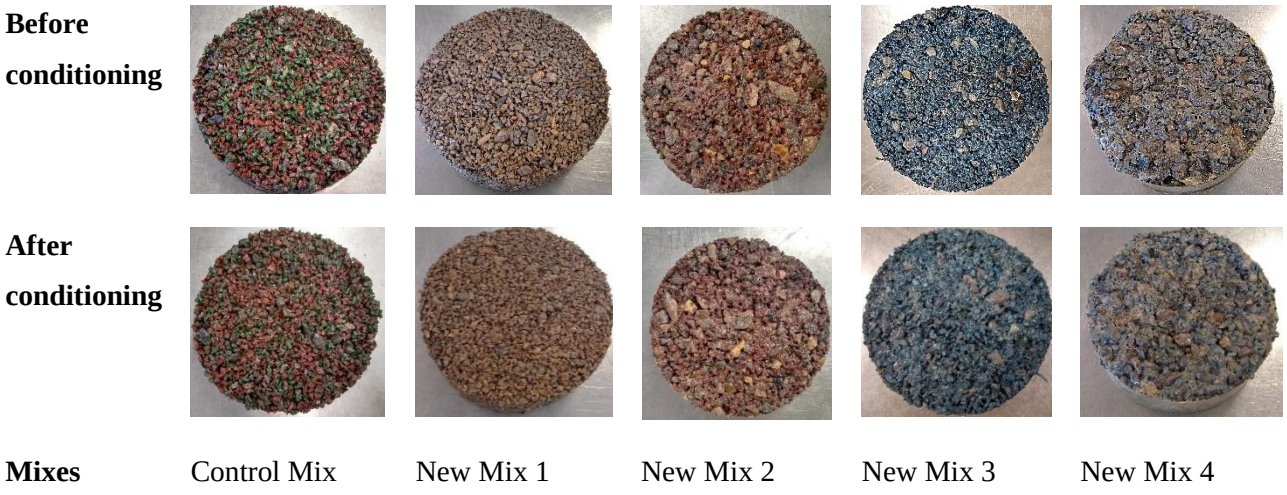

Figure 49 Samples before and after conditioning

The moisture-induced damage results for the mixtures with different binders are presented below in Table 22. The results revealed that the Control Mix with the B1—aromatic binder had the highest maintained strength following freeze-thaw conditioning, which was 83%. In contrast, the mix with the B3—aromatic binder had the lowest retained strength (57%). However, the reduction in strength in all the mixes was significant except the Control Mix after freeze-thaw conditioning. Single Factor ANOVA analysis was conducted for the Tensile Strength Ratio (TSR) in samples with different binders. The P-value for the interaction was found to be 0.0058 at an alpha level 0.05, which is statistically significant (details in Appendix C). It revealed a considerable impact of binder types on the retained tensile strength in the samples.

Table 22 Retained Tensile Strength for mixes with different binder

Mixes with different binders	ITS before conditioning (kPa)	ITS after conditioning (kPa)	TSR
B1—aromatic—Control Mix	169.7	141.2	0.83
B2— aromatic	70.1	46.2	0.66
B2—aliphatic	156.4	110.2	0.70
B3—aromatic	85.0	48.9	0.57

5.5 Conclusions

This research aimed to investigate the preliminary mechanical behaviour of PRPs with various compositions of components and different types of binders, as well as to develop a consistent method for sample preparation and air void calculation. The results are summarized below:

1. A consistent method has been developed for laboratory sample preparation. This study suggests limiting the laboratory mixing time to 90 seconds after adding the binder to prevent its foam formation. During the process, it was also revealed that the compaction properties of PRPs were found to primarily depend on the mixture's composition rather than external vibratory compaction efforts, thus classifying PRP as a self-compacting material.
2. A novel method is developed for calculating the air voids of PRP materials which are characterized by having open pores and exhibit a lower density than water, resulting in a buoyancy effect when submerged.
3. A higher percentage of stone aggregates and binder in the PRP mixes increased the compressive strength by 71% and indirect tensile strength by 70%. An increase of air voids within the PRP sample reduced the material's compressive and tensile strength, indicating a negative correlation between the air voids and the material's strength.
4. A higher percentage of rubber aggregates increased the retained tensile strength of PRP mixes after conditioning with freeze-thaw cycles. Regardless of their composition with different percentages of components, all the PRP mixes retained more than 73% of their original tensile strength after being conditioned.

5. The incorporation of various binder types and sources resulted in a reduction of 59% in the indirect tensile strength, 43% in the compressive strength and 31% in the retained tensile strength in the PRP mix.

The primary mechanical performance analysis results indicate that PRP material may be a viable alternative to traditional pavements for low-traffic areas. The utilization of PRP material in these settings has the potential to confer significant benefits in terms of environmental impact, safety, and sustainability. Moreover, the PRP material exhibited good moisture-induced damage resistance in saturated conditions. Thus, it is expected to perform well in harsh environmental conditions such as freeze-thaw cycles with substantial temperature fluctuations in cold climates.

Chapter 6

Durability Evaluation of Porous Rubber Pavement

The paper outlined in Chapter 6 has not yet been published.

6.1 Abstract

Permeable pavements became a viable alternative to typical pavement solutions to address the surface runoff in urban areas. Water penetration through the permeable pavement replenishes the groundwater table along with bearing the traffic load. Porous Rubber Pavement (PRP) is a novel permeable pavement that can significantly reduce surface runoff because of its very high permeability (up to 45%). This material consists of stone aggregates, recycled crumb rubber and polyurethane as the binder. Since it uses recycled crumb rubber instead of virgin material, it supports environmental sustainability. Water passes through the permeable PRP materials and goes through freeze-thaw cycles during winter in the Canadian climate; thus, often durability of this pavement is compromised. This paper evaluates the durability of PRP for different compositions and polyurethane binders. Samples of the material and its individual components were tested to assess the durability of the PRP material. Stone aggregates' abrasion loss was tested to evaluate the contribution of stone to the material's durability. The Hamburg Wheel Tracking test was conducted to assess the permanent deformation and stripping-related abrasion condition. For both conditioned and unconditioned samples, abrasion losses were evaluated through Los Angeles Abrasion test. Finally, how materials' permeability changes with the change in material composition and binder were also assessed. The obtained results demonstrated that the stone aggregates abrasion loss was found to be 22.25%, which was relatively high compared to the usual range of 17% to 20%. PRP materials showed good rutting resistance ranging from 0.3 mm to 2.8 mm in different mixes. Thus, Due to rutting and moisture-induced damage, stripping-related abrasion was also found to be very low, ranging from 0.1% to 2.6%. Also, the Hamburg Wheel Tracking test for different types of binder showed that samples with an aliphatic binder (B2—aliphatic - 1.1 mm) were more rutting resistant than aromatic binder (B2—aromatic - 2.6 mm and B1—aromatic - 1.4 mm). However, another aromatic binder from a different source, B3—aromatic, could not withstand the impact of the Hamburg Wheel Tracking Test load and temperature (53 ˚C) for a long time, resulting in samples failing after 4000 cycles. In terms of moisture-induced damage and stripping-related abrasions, the outcomes were negligible (0.3% to 0.6%) in both the aromatic and aliphatic binders except for B3—aromatic. For

conditioned samples, abrasion loss was found to be the highest in the New Mix 2, 25.31%. The lowest value was in New Mix 3, which is 6.49%. For unconditioned samples, the highest abrasion loss was found in New Mix 2 (13.23%) and the lowest in New Mix 3 (4.54%). After conditioning, samples with different binders deteriorated differently. In unconditioned samples, the highest abrasion loss was found in samples with B1—aromatic binder (9.94%) and the lowest in the samples with B2—aliphatic (2.75%). Samples with B2—aromatic showed a very high abrasion loss of 15.37% after conditioning. B2—aliphatic samples showed the lowest abrasion loss after conditioning which was 7.53%. For permeability measurement, New Mix 2 showed the highest value, 168080 mm/h, and the lowest permeability was observed in New Mix 3 (98628 mm/h). For the sample with different binders, permeability does not differ very much. They all ranged between 130082 mm/h to 130082 mm/h.

Keywords

Porous Rubber Pavement, Durability, Permanent Deformation, Abrasion Resistance, Permeability

6.2 Introduction

Inevitable urban growth increases the impermeable surfaces in urban areas. Sealed surfaces inhibit the retention of groundwater tables and disrupt the natural hydrological management and ecosystem. As one of the solutions to this problem, permeable pavements are designed for both traffic load bearing and water management (Scholz and Grabowiecki, 2007, Lu; Wang, et al., 2020). It reduces surface runoff, increases the seepage capacity and enables in-situ stormwater management, which is imperative in municipal areas. It also filters water before entering the groundwater table. Since water passes through the material, its durability is often compromised. Thus, the research on permeable pavement always seeks an optimum solution to target strength and durability. In this regime, Porous Rubber Pavement is a novel type of pavement material. It adds supplementary environmental benefits by using recycled crumb tires, partially replacing virgin material. However, the inappropriate disposal of tire waste could be responsible for significant environmental degradation because of its nonbiodegradable aspects and shape. Porous Rubber Pavement consists of stone aggregates, crumb rubber aggregates and polyurethane binder, proportioned to create a higher percentage of interconnected air voids. The shifting rigid-flexible behaviour of the PRP could withstand more unanticipated deformation induced on the pavement (Mohammadinia; Disfani, et al., 2018). Besides, the use of polyurethane synthetic binders with permeable pavement can be considered a feasible solution (Törzs; Lu, et al., 2019).

Estimating service life is critical in determining the benefit of permeable pavement material. This pavement's open porous nature often leads to weaker pavement and ravelling. The service life of the pavement material could be estimated from the laboratory testing and trial sections (Goubert and Sandberg, 2016). This paper investigates PRP's strength range, failure criteria, and moisture-induced damage to estimate the material's durability. One current commercial mix (Control Mix) and four news mixes developed in the laboratory were tested. In addition, Control Mixes prepared with four different types of the binder were also tested.

6.3 Materials and Methodology

6.3.1 Mix Design

In this research, the Control Mix refers to the current mix that has been used commercially. New four types of mixes were also tested in the laboratory, determined through factorial analysis. In these four new mixes, the different proportions of stone aggregates, rubber aggregates and polyurethane binder were used other than the Control Mix. The polyurethane binder also can perform differently in the mixes if their types and sources are changed. Thus, four mixes with different types of the binder were also tested, where the proportion of the material in these mixes was kept the same as the Control Mix. For the Control Mix, B1—aromatic binder was used in both cases (i.e. mixes with different compositions and mixes with different binders). New mixes and different binder types are listed in Table 23 and Table 24. All the mixes used the same rubber and stone aggregates that the industrial partner of this research supplied.

Table 23 Mixes with different compositions

Mixes with different components	Stone Aggregate	Rubber Aggregate	B1—aromatic Polyurethane Binder	Objective air voids	Achieved air voids
Control Mix	45.25	45.25	9.5	35% - 45%	38% to 45%
Stone Aggregates (Factor A)	Lower limit - 55%, Lower limit - 55%				
Polyurethane Binder (Factor B)	Lower limit - 7.5%, Upper limit - 12%				
New Mix 1	55	37.5	7.5	Within 20%-30%	18% - 38%
New Mix 2	75	17.5	7.5		
New Mix 3	55	33	12		
New Mix 4	75	13	12		

Table 24 Mixes with different binders

Mixes with different Polyurethane Binder	Percentages of components	Objective air voids	Achieved air voids
Control Mix – B1—aromatic	Stone Aggregate - 45.25%, Rubber Aggregate - 45.25%, Polyurethane Binder - 9.5%	35% -45%	38% to 45%
B2—aliphatic			
B2—aromatic			
B3—aromatic			

6.3.2 Abrasion Loss of Stone Aggregate

The same granite aggregates were used for all mixes that were prepared for testing. Aggregates' resistance to abrasion was determined using the Micro-Deval apparatus. The test was conducted according to ASTM D6928–17. Steel balls were added with aggregate samples and rolled inside the

Micro-Deval apparatus to abrade the aggregates for this test. Then after washing, the aggregates' abrasion loss was determined (ASTM D6928−17, 2017).

6.3.3 Hamburg Wheel Tracking Test

To evaluate the rutting, stripping and moisture susceptibility of the compacted specimen, the Hamburg Wheel Tracking Test was used. The test was conducted in accordance with AASHTO T324-17. The permanent deformation rate from moving concentrated loads could be derived for the submerged samples through this test. This method is used to determine the premature failure of the sample mixture. The weakness of the aggregates structure, low binder stiffness or moisture damage is the reason for this premature failure. Rut depth and the number of passes to failure are obtained through the test, and the stripping inflection point (SIP) could be calculated from those measures, as shown in Figure 50 (AASHTO T 324-17, 2017). It is important to simulate real traffic on the pavement to get the actual result. The load applied on the Hamburg wheel tracking machine wheel is 705 ± 4.5 N (158 ± 1.0 lb) (AASHTO T 324-17, 2017). The test temperature is 53 ± 1°C.

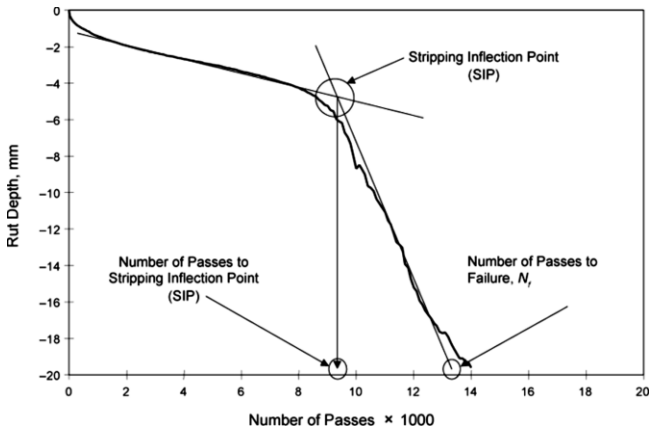

Figure 50 Hamburg Wheel Test Curve

Source: (AASHTO T 324-17, 2017)

6.3.4 Los Angeles Abrasion Resistance test

The abrasion resistance test was done by following ASTM C1747/C1747M – 13, 'Standard Test Method for Determining Potential Resistance to Degradation of Pervious Concrete by Impact and Abrasion.' Materials' resistance to degradation due to the combined effect of impact and abrasion is determined through this test in a rotating steel drum. Mass loss of the specimen is considered to determine the

abrasion loss of the material shown in Figure 51 (ASTM C1747/C1747M − 13, 2013). Usually, three specimens are placed in the Los Angeles machine without steel spheres. The device usually rotates for 30 to 33 mins to complete 500 revolutions. However, Los Angeles Machine was unavailable in the lab during this research. So, a medium-sized concrete mixer was used for conducting this test. This particular piece of equipment needed to run at least 13 mins to complete 500 revolutions. For this test, 500 revolutions were repeated three times. That means the samples were abraded in the machines three times. Each time was prolonged for 13 mins. Initially, the samples' weights were recorded. Then, after every 13 mins, the samples' weight was again recorded to determine the abrasion loss.

(a) Abrasion Loss Machine (b) Loose material (c) Abraded sample

Figure 51 Abrasion Loss machine and procedure

6.3.5 Permeability Test

The permeability of the PRP samples was tested using NCAT Asphalt Permeameter. ASTM C1701/C1701M was followed to perform the test. A fixed amount of water was poured onto the sample and allowed to penetrate through the sample using the small tire of the permeameter (ASTM C1701/C1701M−17a, 2017).

6.4 Result and Analysis

6.4.1 The Durability of Stone Aggregate

The Micro-Deval abrasion test determined the abrasion loss of aggregates, as shown in Figure 52. The abrasion loss of granite aggregate was found to be relatively high. The usual range for Micro-Deval

abrasion loss is 17% to 20% (ASTM D6928−17, 2017). However, abrasion loss for the stone aggregate that has been used in the current PRP mixtures was found to be 22.25%, which indicates that this aggregate was not strong enough to ensure the strength of the PRP surface.

Figure 52 Micro-Deval abrasion loss test at the lab

6.4.2 Rutting and Stripping

6.4.2.1 Rutting for Different Mixes

Hamburg wheel test was conducted to determine the rutting resistance and moisture susceptibility of the PRPs mixtures. In total, 20 specimens were prepared (four specimens for each mixture) and tested using the Hamburg wheel tracking machine.

The PRP mixes showed a good rutting resistance, as shown in Table 25. The average rutting deformation for different types of mixes ranged from 0.3 mm to 2.8 mm. The results are demonstrated in Figure 53 and Figure 54. During the 10000 cycles, some more considerable rut depths were found but were mostly temporary. The reason behind this behaviour was that the PRPs are very flexible materials which possess elastic behaviour. Thus, deflection occurred during the loading conditions on the material's surface; however, the deflection disappeared when the load was removed. The highest rutting deformation was recorded for New Mix 4, and the lowest was recorded for New Mix 2. There was no correlation observed with the rutting results of different mixes. Even no correlation was possible to establish between air voids and rutting.

Figure 53 Permanent deformation due to rutting on different mixes

Table 25 Rutting results from different mixes

Hamburg Wheel Tracking Test				
Mixes	**Depth 01 (mm)**	**Depth 02 (mm)**	**Average (mm)**	**Standard Deviation**
Control Mix	1.6	1.2	1.4	0.26
New Mix 1	1.6	0.7	1.2	0.62
New Mix 2	0.2	0.4	0.3	0.16
New Mix 3	0.8	0.9	0.8	0.13
New Mix 4	3.0	2.7	2.8	0.25

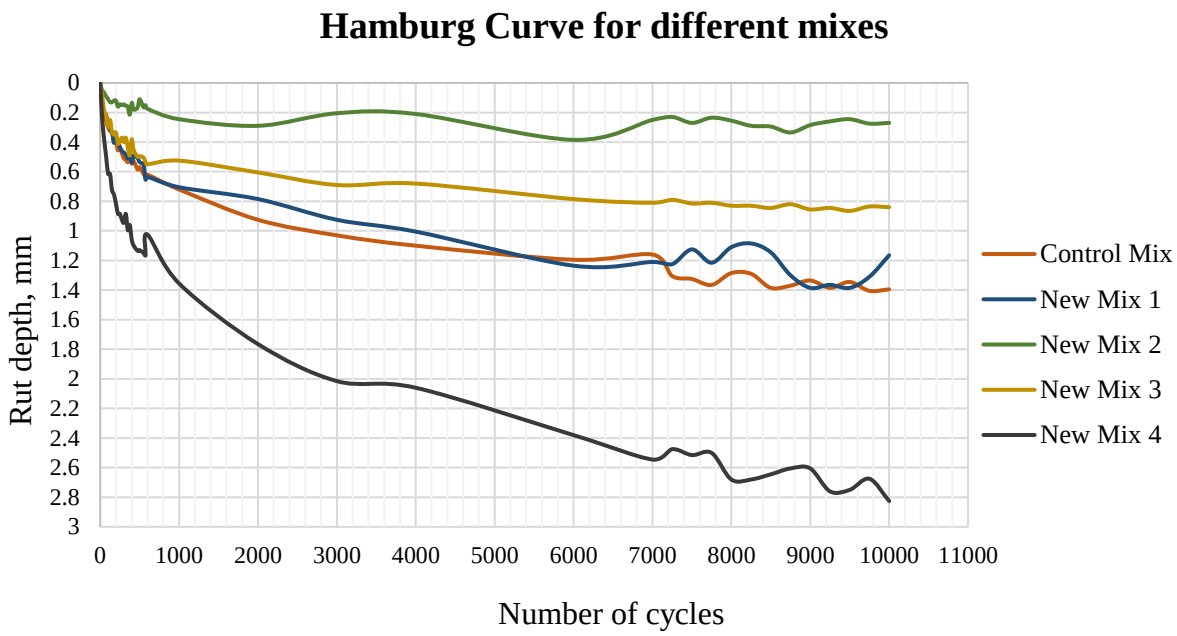

Figure 54 Rutting curve

6.4.2.2 Stripping Related Abrasion for Different Mixes

Due to rutting and moisture-induced damage, stripping-related abrasion was also found to be very small. It was found that moisture is absorbed by the stone aggregates of the samples. So, immediately after the test, the weight of the samples was found to be higher than the initial weight. However, after drying out the samples, there was little reduction observed in the weight of the samples, which ranged between 2.6% to 0.1%, as shown in Figure 55 and Table 26.

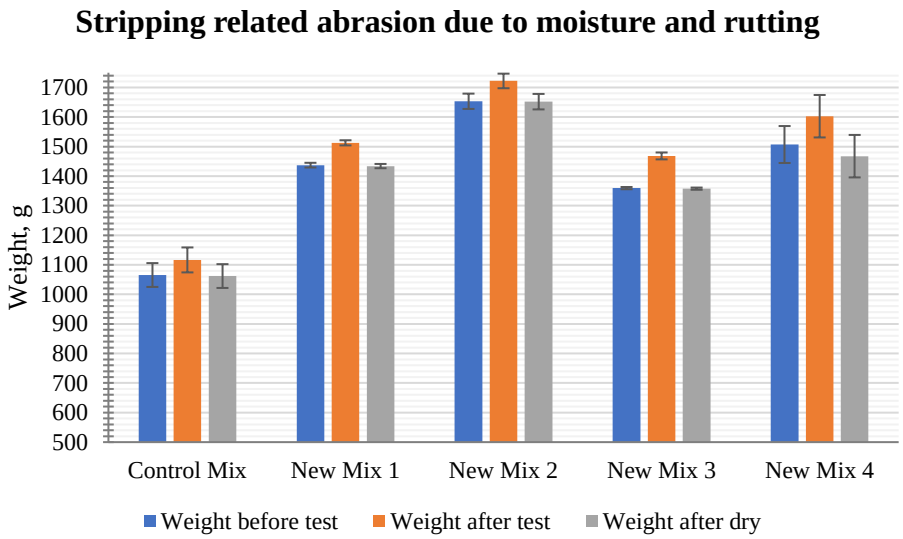

Figure 55 Stripping-related abrasion for different mixes

Table 26 Weight loss after rutting and stripping

Mixes	Weight loss after rutting test
Control Mix	0.3%
New Mix 1	0.2%
New Mix 2	0.1%
New Mix 3	0.1%
New Mix 4	2.6%

6.4.2.3 Rutting for Different Binders

The Hamburg Wheel Tracking test was conducted on four samples for each different binder types. In total, sixteen samples were tested. Except for B2—aliphatic, all other samples were aromatic binders, but their sources differed. Samples with B2—aliphatic binder showed the lowest permanent deformation compared to other samples, which was 1.1 mm. B2—aromatic and B1—aromatic binder Samples showed permanent deformation of 2.6 mm and 1.4 mm, respectively. However, samples with

B3—aromatic showed the highest deformation and failed after the test. The results are presented in Figure 56, Figure 57 and Table 27.

Table 27 Rutting results from mixes with different binders

Hamburg Wheel Tracking Test				
Different binder	**Depth 01 (mm)**	**Depth 02 (mm)**	**Average (mm)**	**Standard Deviation**
B1—aromatic	1.58	1.21	1.4	0.26
B2—aromatic	2.41	2.78	2.6	0.26
B2—aliphatic	0.85	1.28	1.1	0.30
B3—aromatic	11.5	15.74	13.6	3.00

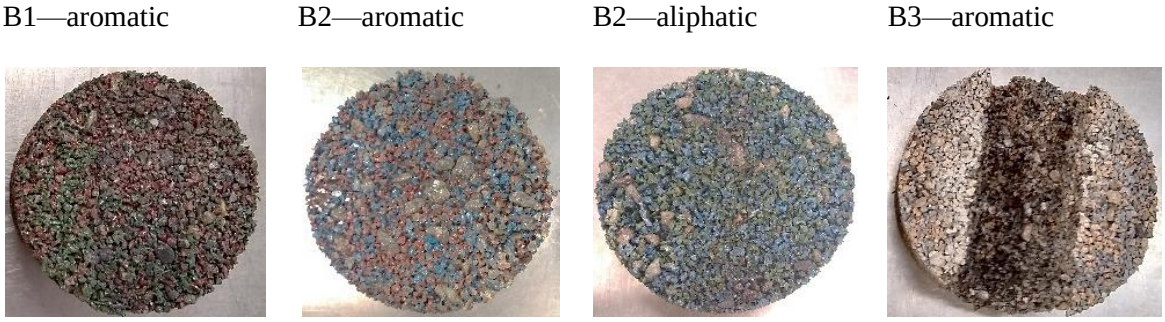

Figure 56 Rutting result with different binders

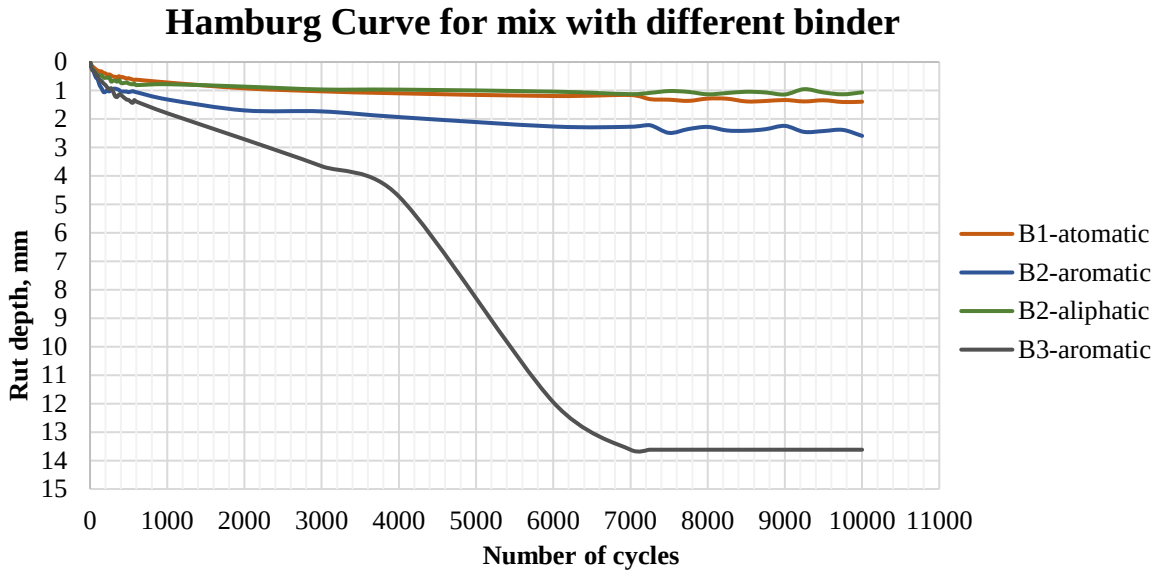

Figure 57 Rutting curve

6.4.2.4 Stripping Related Abrasion for Mixes with Different Binder

Stripping-related abrasion due to permanent deformation and moisture-induced damage was calculated for the samples with different binders after Hamburg Wheel testing. For the samples with B1—aromatic, B2—aromatic and B2—aliphatic binder, the abrasion loss percentage was found to be small, ranging between 0.3% to 0.6%. However, samples with B3—aromatic failed after the test and abrasion loss was found to be 30.3%. Results are shown in Table 28 and Figure 58. All the samples were prepared with the same stone aggregates, and the absorption for this aggregate was a little higher. Thus, just after the test samples' weight for the first three types of binder, i.e. B1—aromatic, B2— aliphatic and B2—aromatic, were higher than the initial weight. However, weight losses were measured after drying the tested samples to determine the abrasion loss. Further testing was conducted for high-temperature tensile strength to explain the failure of the sample with B3—aromatic. It was found that the B3—aromatic binder was temperature sensitive. Indirect Tensile Strength at room temperature for this sample was found to be 85 kPa. However, right after conditioning the samples at 60°C for two hours, the Indirect Tensile Strength result was found to be 34.07 kPa. This lower tensile strength indicates that the probable reason for the failure of samples with B3—aromatic was the temperature sensitivity of the binder. The Hamburg Wheel Tracking test uses a conditioning water temperature of 53˚C.

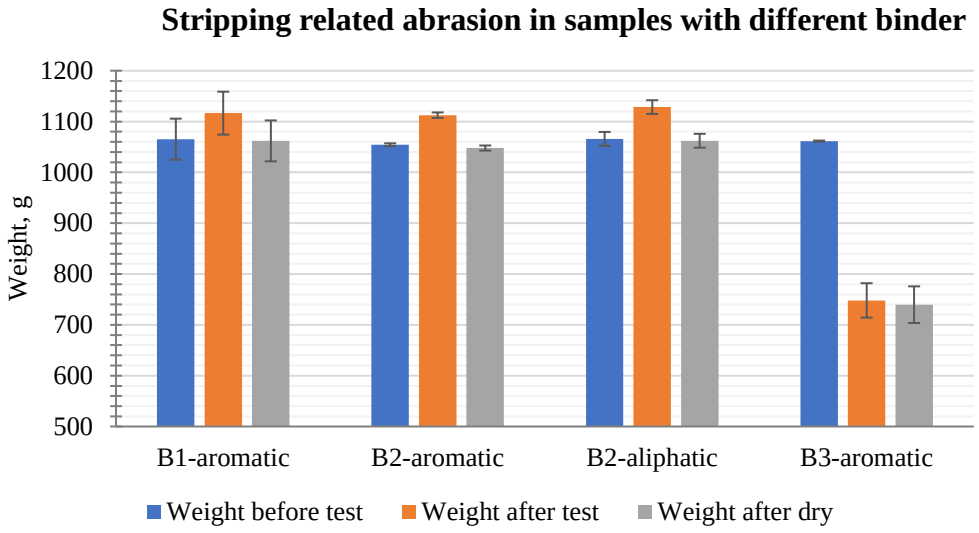

Figure 58 Stripping-related abrasion in samples with different binders

Table 28 Stripping-related abrasion loss in samples with different binders

Mixes	Weight loss after rutting test
B1—aromatic	-0.3%
B2—aromatic	-0.6%
B2—aliphatic	-0.3%
B3—aromatic	-30.3%

6.4.3 Ravelling Resistance

Ravelling resistance is a critical performance for PRP materials; since it directly influences the durability of the pavement material exposed to traffic loading. From the study of the previous research and evidence from the field applications, it was found that PRP is not very ravelling resistant. For this study, the ravelling resistance was conducted for both conditioned and unconditioned samples. One group of samples was tested after five harsh freeze-thaw conditioning. For conditioned samples, abrasion loss was found to be the highest in New Mix 2 (25.31%) and the lowest in New Mix 3 (6.49%). Unconditioned samples also showed consistency in the result. For unconditioned samples, the highest abrasion loss was found in New Mix 2 (13.23%) and the lowest in New Mix 3 (4.54%). The amount of

stone aggregate and binder in mixes influenced the material's abrasion resistance. The factorial analysis showed that, for conditioned samples, when aggregate was increased by 10%, abrasion was increased by 3.84 g. When the binder was increased by 2.25%, abrasion was decreased by 5.57 g.

On the other hand, for unconditioned samples, when aggregate was increased by 10%, abrasion was increased by 1.65 g; when the binder was increased by 2.25%, abrasion was decreased by 2.68 g.

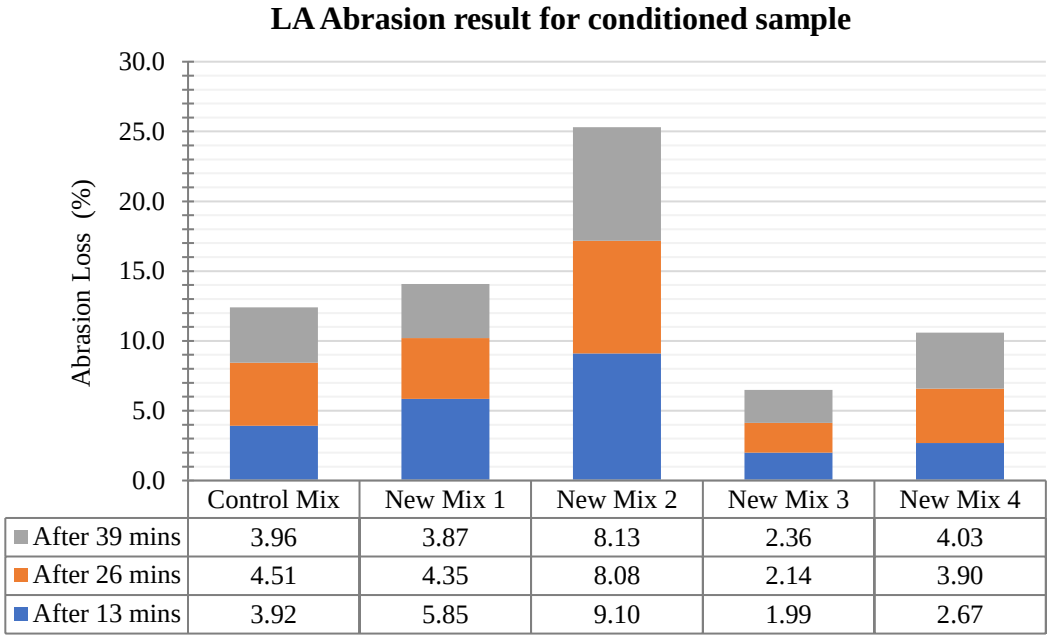

	Control Mix	New Mix 1	New Mix 2	New Mix 3	New Mix 4
After 39 mins	3.96	3.87	8.13	2.36	4.03
After 26 mins	4.51	4.35	8.08	2.14	3.90
After 13 mins	3.92	5.85	9.10	1.99	2.67

Figure 59 Ravelling for conditioned sample

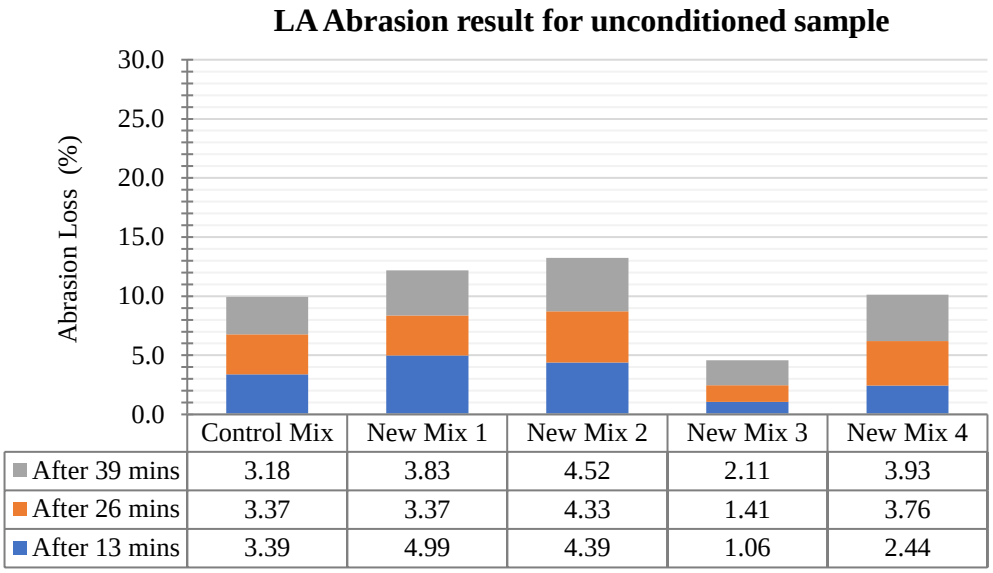

	Control Mix	New Mix 1	New Mix 2	New Mix 3	New Mix 4
After 39 mins	3.18	3.83	4.52	2.11	3.93
After 26 mins	3.37	3.37	4.33	1.41	3.76
After 13 mins	3.39	4.99	4.39	1.06	2.44

Figure 60 Ravelling for unconditioned sample

For the use of different binders in the conditioned and unconditioned sample, it was found that the B2—aromatic binder deteriorated more than other binders after freeze-thaw conditioning. In unconditioned samples, the highest abrasion loss was found in samples with B1—aromatic binder (9.94%) and the lowest in the samples with B2—aliphatic (2.75%). Unconditioned samples with B2—aromatic showed an abrasion of 3.76%. After conditioning, samples with B2—aromatic showed a very high abrasion loss of 15.37%. However, all other samples with different binders showed increased abrasion loss after conditioning the sample. For the B1—aromatic binder, this loss was 12.4%, B2—aliphatic was 7.53%, and B3—aromatic was 8.89%.

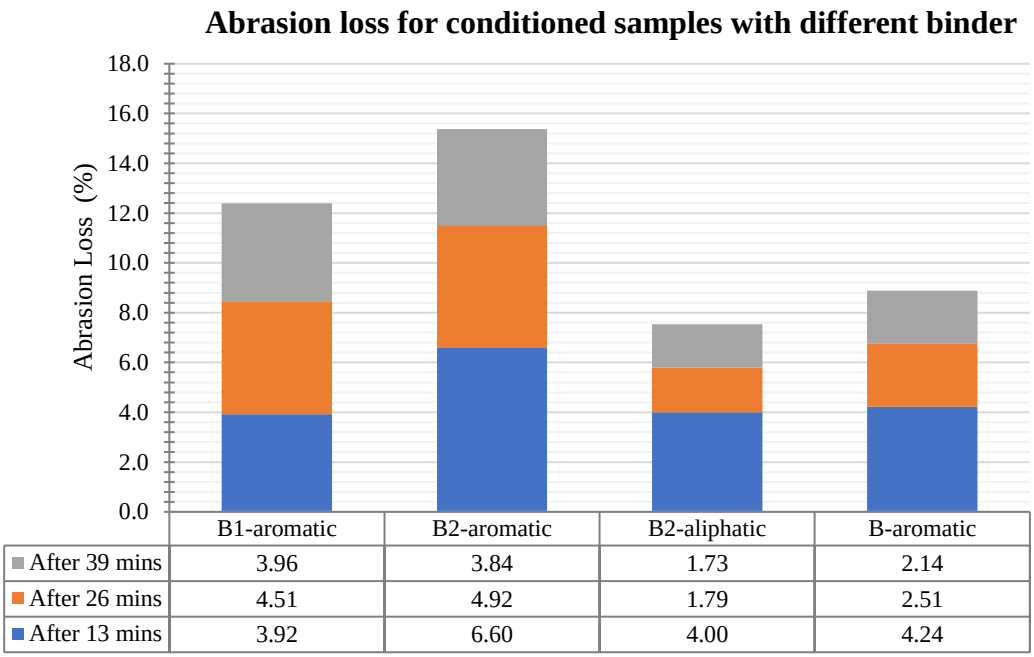

	B1-aromatic	B2-aromatic	B2-aliphatic	B-aromatic
After 39 mins	3.96	3.84	1.73	2.14
After 26 mins	4.51	4.92	1.79	2.51
After 13 mins	3.92	6.60	4.00	4.24

Figure 61 Abrasion loss for conditioned samples with different binder

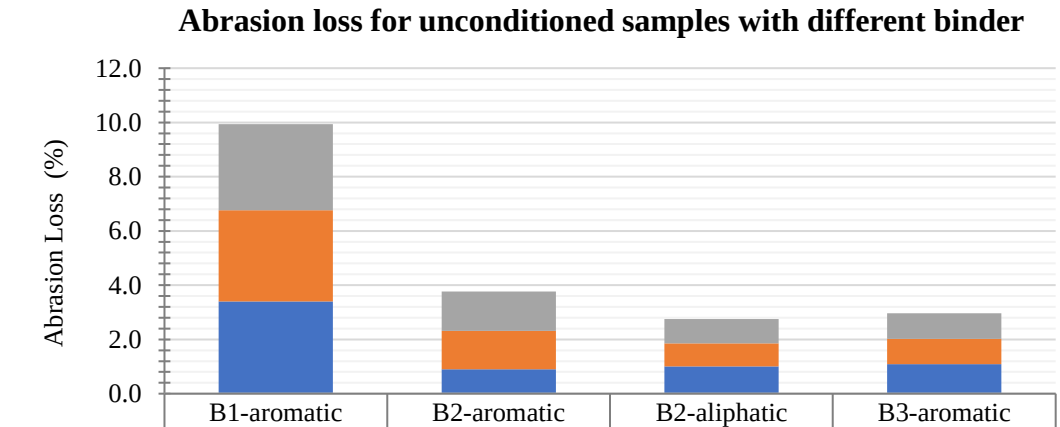

	B1-aromatic	B2-aromatic	B2-aliphatic	B3-aromatic
After 39 mins	3.18	1.45	0.89	0.95
After 26 mins	3.37	1.41	0.85	0.93
After 13 mins	3.39	0.90	1.00	1.08

Figure 62 Abrasion loss for unconditioned samples with different binder

6.4.4 Permeability

The permeability of porous pavement could depend on the material's interconnected air voids, internal structure, and base and subgrade conditions. However, the laboratory test of Porous Rubber Pavement for permeability was mostly affected by the materials' interconnected air voids and internal structures. It gives comparative information among different types of mixes. When the permeability of different new mixes was measured, New Mix 2 showed the highest permeability, which was 168080 mm/h, as shown in Table 29. The lowest permeability was observed in New Mix 3 (98628 mm/h). The probable reason could be the composition differences in the mixes that also contributed to the internal structure and porosity of the material. New Mix 2 consists of the highest percentage of stone aggregate (75%), a lower percentage of rubber aggregate (17.5%) and the lowest percentage of binder (7.5%). Thus, larger stone aggregates formed comparatively rigid and large interconnected voids, leading to a higher permeability. However, New Mix 3 consists of a lower percentage of stone aggregates, a higher percentage of rubber aggregates and the highest percentage of the binder. The gradation of the rubber aggregates was smaller than 4.75 mm and created smaller interconnected flexible voids, which reduced the permeability of the mixes. Besides, a portion of the highest percentage of binder became foam during cure time with the contact of moisture, clogged some pores, and was also responsible for lower permeability. For the sample with different binders, permeability did not differ very much. They ranged between 125393 mm/h to 130082 mm/h.

Figure 63 Permeability test at the laboratory

Table 29 Permeability of different new mixes

Mix type	Infiltration rate, I (mm/h)
Control Mix	127695
New Mix 1	139067
New Mix 2	168080
New Mix 3	98628
New Mix 4	128923

Table 30 Permeability of mixes with different binders

Mix type	Infiltration rate, I (mm/h)
B1—aromatic—Control	127695
B2—aliphatic	130082
B2—aromatic	125393
B3—aromatic	130082

6.5 Conclusions

Durability testing is critical for permeable pavement material before its widespread application. PRP is a novel pavement material in the North American climate, and its durability-related properties are not fully identified. The mechanical behaviour of different PRP mixes was investigated in the first part of this research. The evaluation of durability properties in this part created a guideline for the researcher to select optimum mixes for further testing through the trial section construction. First, abrasion loss was determined for the granite stones that were used for all the mixes. Then different mixes and control

samples with different binders were tested for Hamburg Wheel Tracking Test, Loss Angeles abrasion test, and permeability. The results are summarized below:

1. A relatively high abrasion loss was found for the granite stones that were used for all the sample preparation.
2. PRP materials for different compositions showed good rutting resistance, which ranges from 0.3 mm to 2.8 mm in different mixes. Moisture-induced damage, stripping related abrasion was also found to be very small, ranging from 2.6% to 0.1%.
3. The use of different binders from different sources showed that the B2—aliphatic binder could withstand more rutting than other binders. After 10000 cycles, only 1.1 mm rutting was found in B2—aliphatic samples. However, among all the aromatic binders, B3—aromatic samples failed after 4000 cycles and deteriorated quickly at a higher temperature. Except for B3—aromatic, moisture-induced damage and stripping-related abrasions were found to be between 0.3% to 0.6%.
4. Los Angeles abrasion loss testing gave an indication of the ravelling resistance of the samples. In the conditioned situation, New Mix 2 showed the highest abrasion, which was 25.31%, and the lowest was found in New Mix 3, 6.49%. For unconditioned samples, the highest abrasion loss was reduced in all cases, which was consistent with the mix types. Thus, the highest in New Mix 2 (13.23%) and the lowest in New Mix 3 (4.54%).
5. Deterioration of samples with different binders occurred differently in the conditioned and unconditioned situations and was inconsistent in the mixes. In unconditioned samples, the highest abrasion loss was found in samples with B1—aromatic binder (9.94%). After conditioning, samples with B2—aromatic showed a very high abrasion loss of 15.37%. However, before conditioning, the abrasion loss for B2—aromatic was only 3.76%.
6. Based on the mix composition, the permeability result was different. New Mix 2 showed the highest permeability, which was 168080 mm/h and the lowest permeability was observed in New Mix 3. However, permeability does not differ very much for samples with different types and sourced binders. They ranged between 125393 mm/h to 130082mm/h.

The durability of PRP differs for different mix compositions and binder types. Durability was also impacted by the quality of aggregates used for all the mixes. Sources of the binder were critical to tolerate a wide temperature range, a common phenomenon in the Canadian climate.

Chapter 7

Construction of Polyurethane-bound Porous Rubber Pavement (PRP) Trial Section in Canadian Climate and Understanding its Behaviour Based on Field Performance Evaluation

This chapter is based on the paper published in the Journal of Sustainability, Special Issue—Pavement Materials and Sustainability.

7.1 Abstract

Porous pavements are designed and used in current construction practices to address environmental and safety issues related to wet weather. Porous Rubber Pavement (PRP) is a novel porous pavement material consisting of recycled crumb tire rubbers, stone aggregates, and polyurethane binders. The higher permeability (up to 45% of air voids) of PRP and its composition offers excellent benefits to the urban hydrological system and environment. Due to its recent outset in the Canadian climate, its properties and performance are not investigated yet. This research investigates PRP's properties and performance as pavement material through the construction of two trial sections incorporating three newly developed PRP mixes along with a Control mix. Samples were obtained from the field and tested in the laboratory to determine the mechanical and durability properties, including indirect tensile strength, moisture-induced damage due to freeze-thaw cycles and permanent deformation. Field evaluation was also performed three times: right after construction, three weeks later, and after seven months to determine stiffness, frictional properties, roughness, and permeability. The results revealed that all PRP mixes exhibited excellent permeability and retained more than 68% of tensile strength after five freeze-thaw cycles. Although PRP showed significantly lower initial elastic modulus than conventional pavement material ranging between 28 MPa to 59 MPa, in the springtime, none of them went below 23 MPa. Material composition, site geometry and subgrade conditions were found to be the main factors influencing field performance of PRP pavement.

Keywords: Porous Rubber Pavement; Trial Section Construction; Mechanical Properties; Durability; Stiffness; Frictional Property; Permeability

7.2 Introduction

Rapid urbanization is part and parcel of modern civilization and leads toward covering permeable surfaces for new development. Thus, the seepage capacity of urban surfaces have been declined and can lead to a noticeable distortion in the natural ecosystem (Törzs; Lu, et al., 2019). To respond to the effect and mitigate the risk of increased surface runoff through construction, the use of porous pavement is becoming popular (Lu, 2019). Porous pavements contribute significantly to reducing surface runoff and replenishing the groundwater table. Besides, it can address safety issues related to wet weather by reducing spray, splash and hydroplaning during rain and snow. Porous Rubber Pavement (PRP) is a novel addition to this type of pavement material. PRP consists of recycled crumb tire rubbers, stone aggregates, and polyurethane binders and contains a higher percentage of air voids (up to 45%). Besides, PRP replaces the use of virgin material by using recycled tires. Thus, the higher permeability of PRP and its composition can offer excellent benefits to the urban hydrological system along with its environmental advantages. However, there is very limited research, development and information available on these systems. Although a few studies were identified from some European and Asian countries, they are also in the very initial stages of examining this material (Kalman; Biligiri, et al., , 2011, Sandberg, August 24, 2015, Wang; Liu, et al., 2017) . Moreover, the use of PRP has been added to contemporary Canadian construction practice very recently. PRPs are used in this climatic region on low-traffic roads and pedestrian walkways as a surface material. It should be noted that this application is in limited areas only. Due to its recent outset in the Canadian climate, its properties and performance as a pavement material are not investigated yet for this climatic condition. Hence, it is essential to understand the properties and performance of PRP from laboratory and field investigation before its widespread application in Canada.

Along with laboratory investigation and development, the construction of trial sections is critical to verify the material's laboratory performance under actual conditions. Any pavement can perform differently in a natural ecological environment. Surrounding conditions, soil types, water quality, sub-surface layers, traffic load, etc., all work together to affect permeable pavement performance. For instance, if the pores of permeable pavement are partially saturated with water, hydromechanical interactions occur during traffic load and influence the durability of permeable pavement (Lu, 2019). Besides, many steps are involved in trial section construction, from preparing construction drawings to pouring the material. These steps and process clarifies many issues, enrich the construction knowledge and influence pavement performance.

Thus, extensive research was planned for both the laboratory and field to investigate and improve the properties and performance of PRPs in the Canadian climate. Prior research was conducted for preliminary field investigation, developing different compositions of PRPs and testing their performance in laboratory facilities. This research is designed to investigate PRP's properties and performance from two field applications for selected mixes. Besides, samples were prepared from field mixes to investigate the properties and durability of field mixes under laboratory conditions; and to determine their deviations from laboratory mixes.

7.3 Trial Section Construction

7.3.1 Location

The trial section is located at 1400 Greenwood Hill Rd, Wellesley, ON N0B 2T0. The location is situated within the Township of Wellesley. It is a north-western pastoral township of the Regional Municipality of Waterloo in Ontario, Canada (Google Maps, 2021). It is about 23 km from the City of Waterloo. Figure 64 and Figure 65 show the location's bird's eye view and view from the entrance, respectively.

An agricultural and farm products manufacturing and distributing company is located at the site. Other small rental businesses are also operated at the site.

Figure 64 Location of the trial section: Bird's eye view

Source: Google Map, 2022

Figure 65 Sites' view from the entrance

Source: Google Map, 2022

7.3.2 Site Selection

Two sites were selected at this location. Site A is the dedicated parking area for the businesses on site. Mostly, cars are parked there during peak hours. Site B is the driveway to the drop-off and pickup point. This site is a sloped driveway leading towards the loading-unloading dock. All sorts of vehicles use this driveway, from small cars to heavy trucks. However, the vehicles' driving speed is slow on the driveway, ranging between 30 km/h to 40 km/h. Figure 66 and Figure 67 show the surroundings of Site A and Site B

(a) (b)

Figure 66 Site A: Before construction with the parked vehicle; (a) View from the side, (b) View from the front

(a) (b)

Figure 67 Site B: Before construction and heavy vehicle at pickup dock; (a) View from the front, (b) Heavy vehicle parked at Site B

7.3.3 Weather Conditions

The trial sections were constructed on October 2, 2021. At 8:30 am, the temperature was 15˚C. The wind speed was 14 km/h (SW), and the wind gust was 25 km/h. By the time of construction at 10:30 am, the temperature had reached 19˚C. The wind speed was 15 km/h (SW), and the wind gust was 27 km/h.

7.3.4 Planning Before Construction

Before construction, Site A and Site B plans were prepared with all necessary dimensions. It was also essential for the construction workers to obtain the exact measurements to prepare the ground for construction. Cross-sectional drawings for the pavements were also produced. Figure 68 and Figure 69 show the plan for Site A and Site B, respectively. Figure 70 shows the cross-section of the trial section.

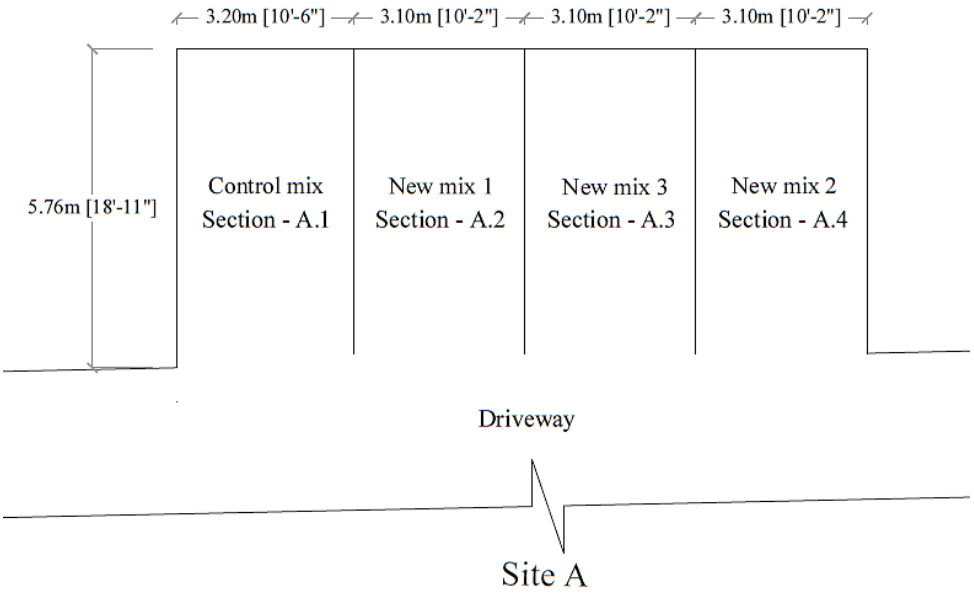

Figure 68 Site A plan

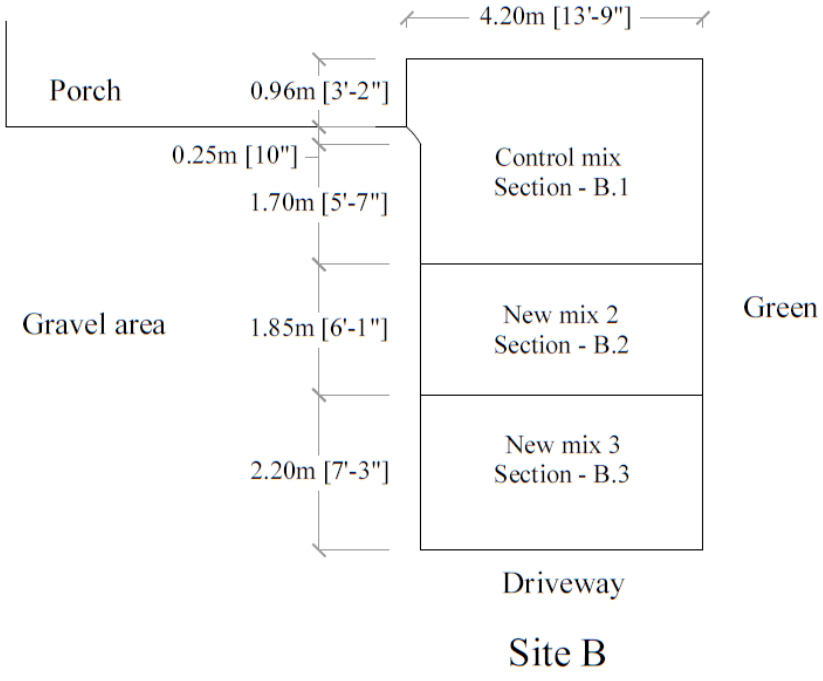

Figure 69 Site B plan

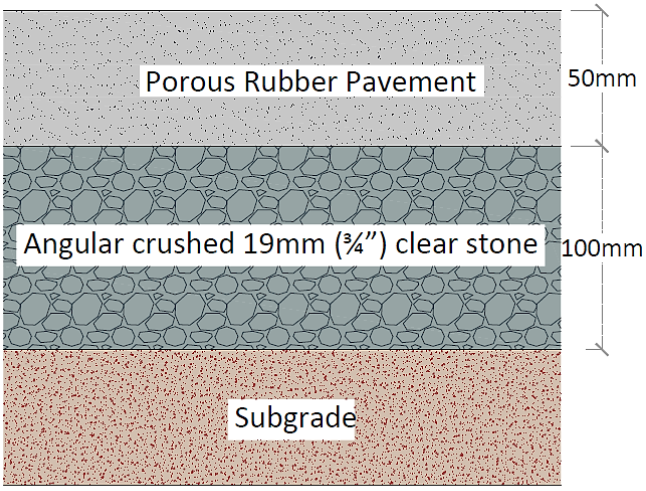

Figure 70 Cross Section of the trial section

7.3.5 Mixes Used for Placement

PRP materials consist of stone aggregates, rubber aggregates and polyurethane binder. Table 31 shows the basic properties of the components used in this research.

Table 31 Basic properties of the components

	Rubber aggregates	Stone aggregates	Polyurethane binder
Basic properties	Recycled crumbed tire rubber	Granite aggregates	B1—aromatic Binder
Size of aggregates	1.18 to 2.36 mm	4.75 to 6.75 mm.	

Three new mixes with varied compositions and the Control Mix were employed to build the different segments of the trial sections. These new mixes were chosen based on their mechanical performance and durability as determined by a series of lab tests in the prior research. The mixes that were selected for the trial section are shown in Table 32.

Table 32 Mixes used for trial section construction

Mixes with different proportions of components	A -Stone Aggregate, R -Rubber Aggregate, B – B1—aromatic Polyurethane Binder	Air voids
Control Mix	A - 45.25%, R - 45.25% B - 9.5%	38% -45%
New mix 1	A - 55%, R - 37.5% B - 7.5%	Within 24%-38%
New mix 2	A - 75%, R - 17.5%, B - 7.5%	
New mix 3	A - 55%, R - 33%, B - 12%	

7.3.6 Weather Station Installation

On the day before construction work commenced, a weather station comprising a tipping bucket rain gauge and a solar radiation shield was put in place at the site to capture meteorological weather occurrences. The solar radiation shield houses a data-logging device that captures rainfall and temperature-related events. The device was programmed to collect temperature data hourly, with an accuracy of ±2% for precipitation rates of up to 2 inches per hour (Novalynx Corporation, 2009). A suitable location for the weather station was selected to receive maximum sun, rain and wind exposure. It was installed on a concrete block close to Site A, in the middle of vacant land, that is seasonally used for growing kitchen vegetables (as shown in Figure 71).

(a) (b)

Figure 71 Weather station near Site A; (a) Different parts of the weather station, (b) Location of the weather station

7.3.7 Subgrade and Base Preparation

Following the drawing, section outlines were marked on Site A and Site B, as shown in Figure 72. Then, using an earth excavator, the existing surface layers were removed up to 150mm (6 inches).

(a) (b)

Figure 72 Marked on the existing surface layer; (a) Site B marking, (b) Site A marking

After removing the surface layer from both sites, the subgrade soil was collected for CBR (California Bearing Ratio) testing. The CBR test is essential to determine the soil's stability and strength. Then, the uneven subgrade was further levelled manually. After levelling, an angular crushed stone of 19 mm

was placed to the thickness of 100mm and compacted with a small compactor, as shown in Figure 73. Then, plastic edges were placed on different sections with pegs to create different segments.

(a) (b) (c) (d)

Figure 73 Preparing subgrade with crushed stone; (a) Removing surface soil, (b) Collecting soil samples, (c) Marking of crushed stone layer, (d) Compactor to compact crushed stone layer

7.3.8 Construction Technique, Equipment and Placement

After preparing the subgrade and base layers, the different mixes were prepared on-site. Each mix was prepared for both sites at the same time to maintain the consistency of the mix. Mix preparation followed a consistent method. First, stone and rubber aggregates were measured and mixed using a medium-sized mixer for 60 seconds. After 60 seconds, the polyurethane binder was added according to the measurement. Then all the materials were mixed again for 180 seconds. Finally, loose mixes were carried to the site using a dumper. The processes are shown in Figure 74.

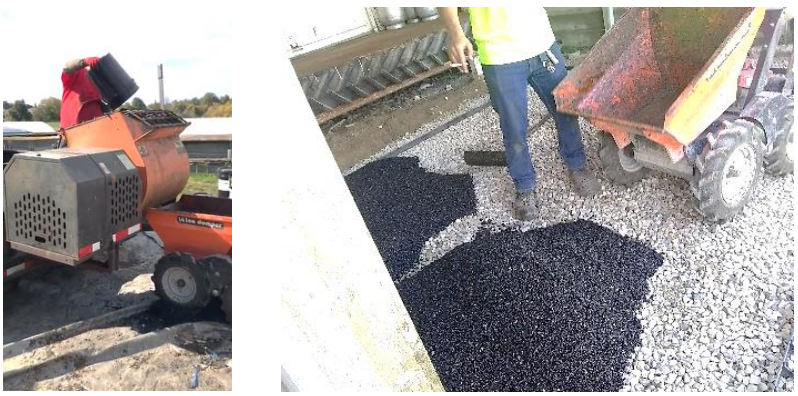

(a) (b)

Figure 74 Construction equipment and placement of material; (a) Mixer, (b) Dumper

After pouring the loose mixes on the relevant sections, the mixes were spread over the entire area with a trowel and screed to achieve a thickness of 50mm. Then using a flat plate with vibration, the surface was smoothened further. Later a small amount of mist was applied to the surface to accelerate the curing process. After misting, the surface was again smoothened with a roller. PRP is a self-compacting material, and crumb rubber aggregate possesses elastic properties. Thus, the external vibration to compact the material has little effect on reducing air voids. However, vibration enhances the bonding among different components. Therefore, as planned, the vibration time was increased more than regular practice. Then the surface was left undisturbed for curing. Figure 75 shows several construction steps.

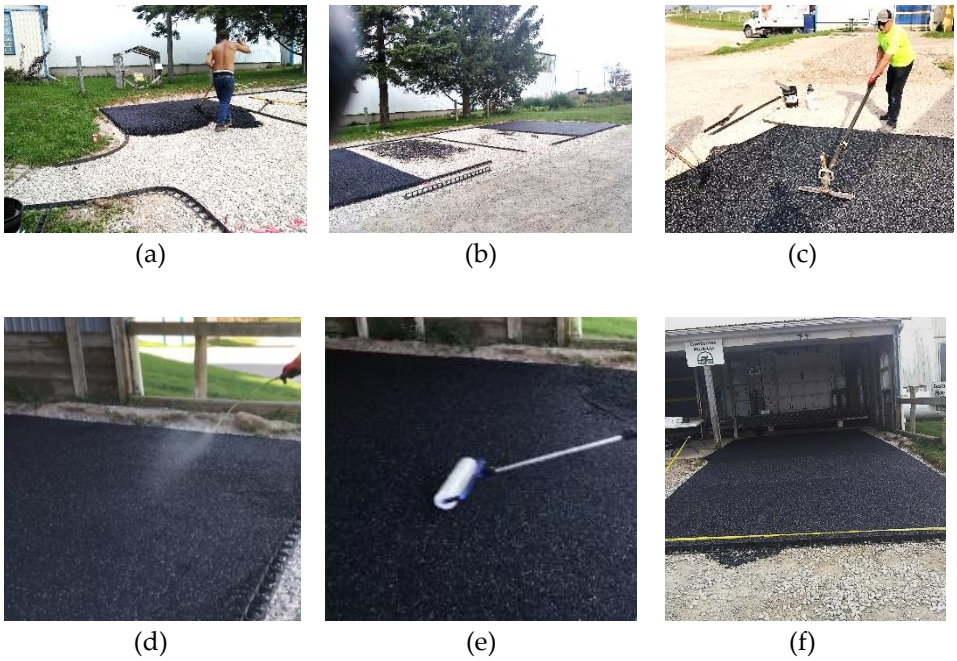

(a) (b) (c)

(d) (e) (f)

Figure 75 Several steps of construction; (a) Spreading material on the site, (b) Different mixes were poured on different sections, (c) Smoothing the surface, (d) Water spray on the material, (e) Smoothing the surface with a roller, (f) Completed section

7.3.9 Preparing Samples for Lab Testing

During the construction of the sections, samples were also prepared for further lab testing. The sample preparation followed the procedure developed in the prior research, as shown in Figure 76. Ideally, lab test results show the materials' consistent and actual properties. However, the material's performance

can be different during actual construction due to differences in workmanship, construction procedure, ambient environment, handling of large amounts of materials, etc. Thus, it is crucial to prepare samples during trial section construction and test them in the lab facilities. This helps to identify the performance gaps and room for improvement during construction.

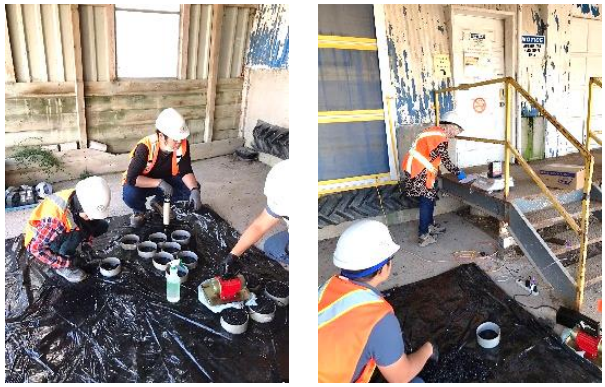

(a) (b)

Figure 76 Preparing sample from trial section mixes; (a) Pouring material into the molds, (b) Weighing the material for pouring into the mold

7.3.10 Opening for Traffic

The trial sections were kept undisturbed for 24 hours to be cured after completion of construction. Then, before entirely opening for traffic, the pavements were tested to evaluate their initial condition and performance. Finally, the sections were opened for all sorts of traffic after being fully cured.

7.4 Lab Testing of Samples Prepared on the Construction Site

7.4.1 Methodology for Laboratory Testing

7.4.1.1 Laboratory Compaction Characteristics of Subgrade Soil

The laboratory compaction method, ASTM D 698, was used to investigate the relationship between water content and dry unit weight of soil. Method C was used in this test based on the soil's gradation. In this case, 30% or less soil material was retained on the 19mm sieve by mass. A mould of 152.4 mm was used to compact the soil into three layers. On each layer, 56 blows were applied (ASTM - D698, 2012).

7.4.1.2 California Bearing Ratio (CBR) test

The standard test method ASTM - D1883 – 16 was followed to examine the subgrade soil's California Bearing Ratio (CBR). This method determines the strength of subgrade soil with a maximum particle size of less than 19mm. It also investigates soil's linear swelling after soaking with water (ASTM - D1883, 2016).

7.4.1.3 Indirect Tensile Strength

The Indirect Tensile Strength (ITS) test was conducted following the standard AASHTO T 322-07. ITS was performed using 50mm high and 150mm diameter samples (AASHTO T 322-07, 2016). The estimated resistance capacity of the sample is considered as the material's tensile strength (Lu; Renken, et al., 2019). Thus the breaking or the highest force observed on the sample was obtained to calculate the material's tensile strength. The following equation was used for the calculation.

$$S_t = \frac{2000 \times P_f}{\pi \times b \times D}$$

Equation 11

Where S_t = Tensile strength of specimen, kPa

P_f = Maximum load observed for specimen, N

b = Thickness of the sample, mm

D = diameter of the sample, mm

7.4.1.4 Moisture Induced Damage Test

The moisture-induced damage test was conducted for the trial section samples. Two groups of samples involved in this test had the same properties. The first group of samples was tested for ITS without any conditioning. The second group of samples was conditioned with five freeze-thaw cycles (freezing at -18 ˚C and thawing at 60 ˚C) and then tested for ITS. Then, the calculated numerical indices of retained indirect-tensile properties indicated the moisture-induced damage to the material (AASHTO T 283-07, 2011). A modified test method was followed for freeze-thaw conditioning of the sample, as developed in earlier research. In this modified method, a partial vacuum of 660 mm (26 inches) Hg was applied for 10 minutes to saturate the samples, which were then submerged in water during freezing cycles to maintain saturation. According to the standards, the retained tensile strength (Tensile Strength Ratio or

TSR) of at least 80 percent indicates good resistance to moisture-induced damage (AASHTO T 283-07, 2011, ASTM D7064/D7064M, 2013, Kandhal, 2002).

From the test results, the TSR was calculated using the following equation.

$$TSR = \frac{S_2}{S_1}$$

Equation 12

Where S1 = Average tensile strength of the dry samples

S2 = Average tensile strength of the conditioned samples

7.4.1.5 Hamburg Wheel Tracking Test

The Hamburg wheel tracking test was conducted following AASHTO T 324-17 to investigate the permanent deformation (rutting) and moisture susceptibility of the trial section samples. The rate of permanent deformation from moving concentrated loads can be derived for the submerged samples. The test temperature was 53 ± 1˚C. In addition, moisture-induced stripping was calculated from the samples' material loss. Premature failure of the sample due to weakness of aggregate structure, low binder stiffness or moisture damage can be determined through this test (AASHTO T 324-17, 2017).

7.4.2 Lab Testing Results

7.4.2.1 Determination of Moisture Content for Subgrade Soil

The optimum moisture contents of the subgrade soil of both sites were obtained using the laboratory compaction method ASTM D 698 (Method C). The test steps are shown in Figure 77. The obtained optimum moisture content information was used to prepare samples for CBR testing. The optimum moisture content values for Site A and Site B soils were found to be at 6% and 5.9%, respectively (as shown in Figure 78 and Figure 79).

(a) (b) (c)

Figure 77 Laboratory compaction characteristics of the soil; (a) Measured Material, (b) Compacted soil, (c) After demolding the compacted soil

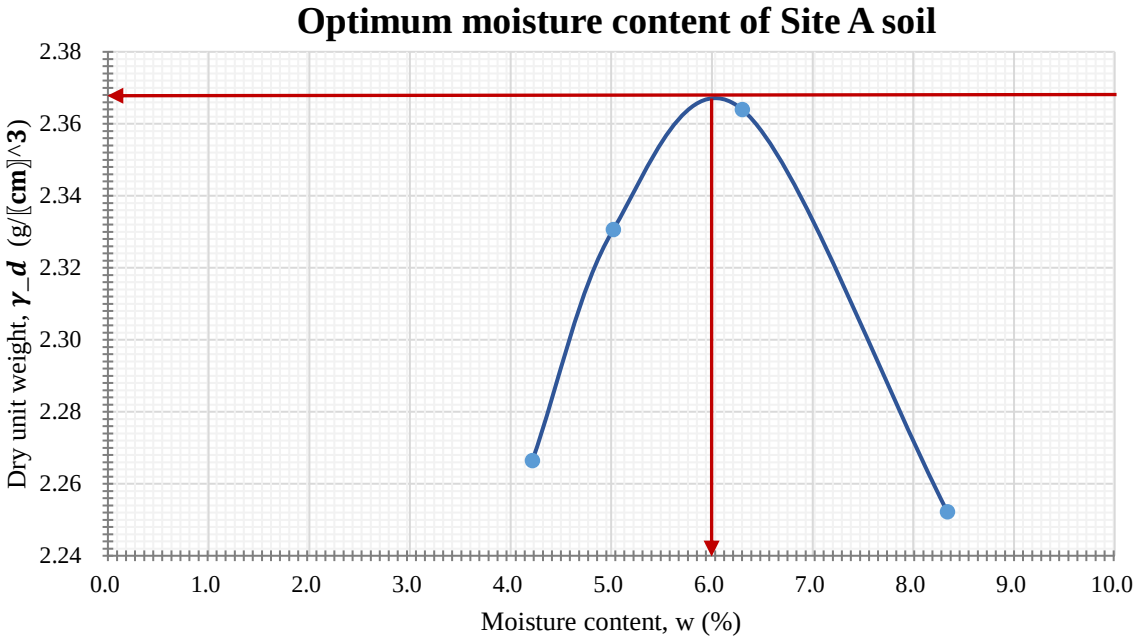

Figure 78 Optimum moisture content of the Site A subgrade soil

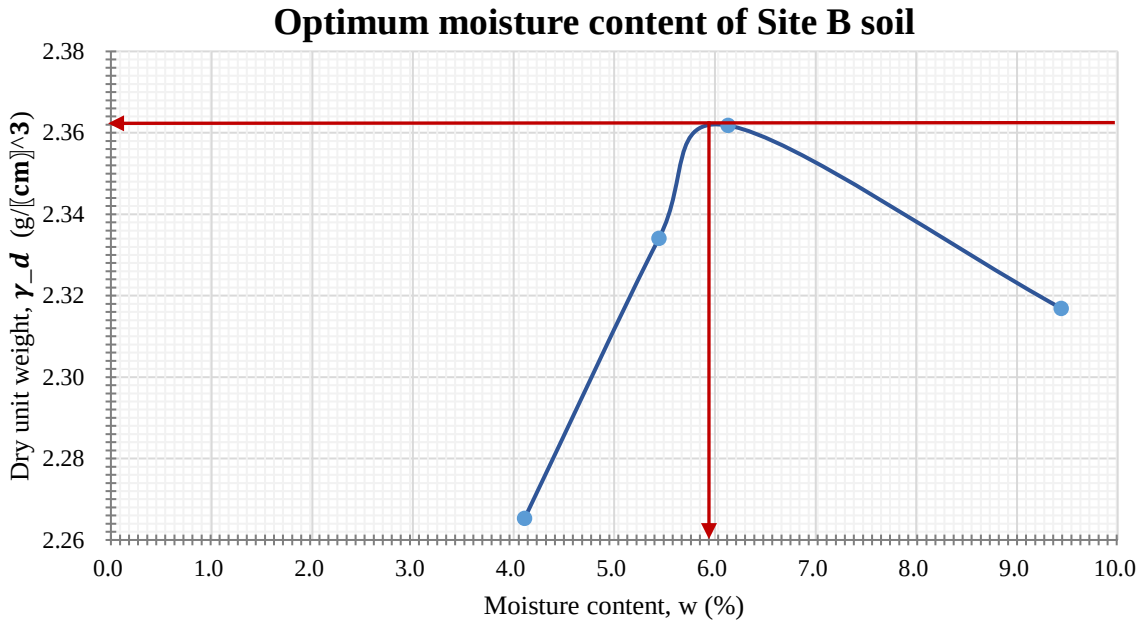

Figure 79 Optimum moisture content of the site B subgrade soil

7.4.2.2 California Bearing Ratio (CBR) of the Subgrade Soil

The CBR value for subgrade soil explains the bearing capacity of the subgrade. The procedure of the test is shown in Figure 80. The subgrade soil types of Site A and Site B are shown in Table 33. The subgrade soil of Site A was coarse-grained soil falling into the category of SM (sands with fines). It contained sands with an appreciable amount of fines. In addition, silty sands and sand-silt mixtures are also found in this type of soil. Besides, the fines can be non-plastic or can be characterized by low plasticity.

The subgrade soil of site B falls within the category of SW (clean sands). The SW is coarse-grained soil with clean sand and slight fines. Well-graded sands, gravelly sands, and little or no fines are found in this type of soil. A wide range also characterizes this soil type in terms of grain sizes and substantial amounts of all intermediate particle sizes (USDA - NRCS, 2012).

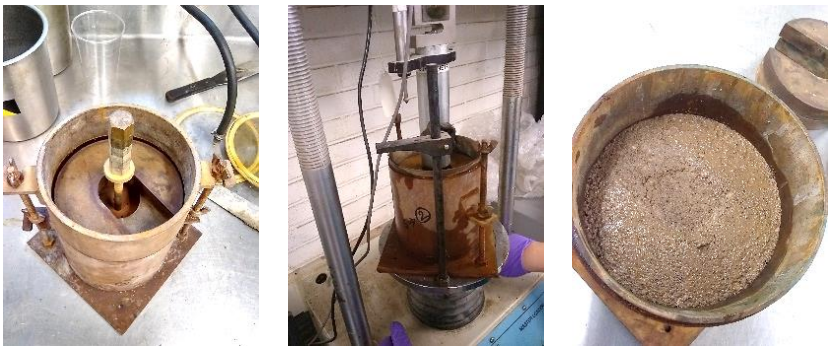

(a) (b) (c)

Figure 80 CBR test procedure, (a) Prepared sample, (b) CBR testing, (c) Sample after test

Table 33 Subgrade soil category for Site A and Site B

	CBR of trial sites		
Site	**Average CBR**	**Standard Dev.**	**Soil type**
Site A	18.2	1.5	SM
Site B	24.3	4.3	SW

7.4.2.3 Indirect Tensile Strength

In a cold climate, low-temperature cracking and deformation are critical factors with respect to the durability of pavement material. However, the pavement material's tensile strength could be one indicator of durability against low-temperature cracking (Lu; Renken, et al., 2019). Among the mixes used in the trial sections, New Mix 3 showed the highest tensile strength, 682.4 kPa. However, this result was higher than the previously found results in laboratory mix samples (547.8 kPa). Table 34 shows the result of the Indirect Tensile Strength test. The Control Mix showed the lowest tensile strength, i.e., 299.3 kPa. New Mix 3 contained a higher percentage of binder (12%), which influenced the increase in tensile strength. New Mix 2 also showed a relatively higher tensile strength of 518.7 kPa. New Mix 2 contained the highest percentage of stone aggregate (75%) but the lowest percentage of binder (7.5%). Probably, a higher stone aggregate percentage contributed to this strength. The factorial analysis in the prior research revealed that both stone aggregate and binder percentages influence the tensile strength of the PRP material. It showed that a 10% increase in stone aggregates

increased the tensile strength of the PRP material by 85.16 kPa. Besides, an increase of binder by 2.25% increased the material's tensile strength by 76.29 kPa.

Table 34 Indirect Tensile Strength result

Mix Types	Air voids	Average Air void	Indirect Tensile Strength (kPa)	Average (kPa)	Standard Deviation
Control Mix	38	38	296.0	299.3	8.86
	39		292.5		
	38		309.3		
New Mix 1	31	31	332.8	306.1	23.11
	31		292.7		
	32		292.8		
New Mix 2	26	24	571.4	518.7	45.86
	18		497.0		
	29		487.7		
New Mix 3	23	23	648.9	682.4	29.69
	22		692.9		
	22		705.4		

7.4.2.4 Relationship Between Indirect Tensile Strength and Air Voids

Indirect Tensile Strength (ITS) and air voids exhibited a polynomial equation with a high R^2 value of 0.98 after plotting the result. It was found that the increase of air voids in the sample gradually decreased the material's tensile strength, as shown in Figure 81. Furthermore, the regression model showed that the adjusted R^2 value was 0.93, along with a P-value of 0.15 at an alpha level of 0.05, which means the interaction between ITS and air void was not statistically significant (details in Appendix D).

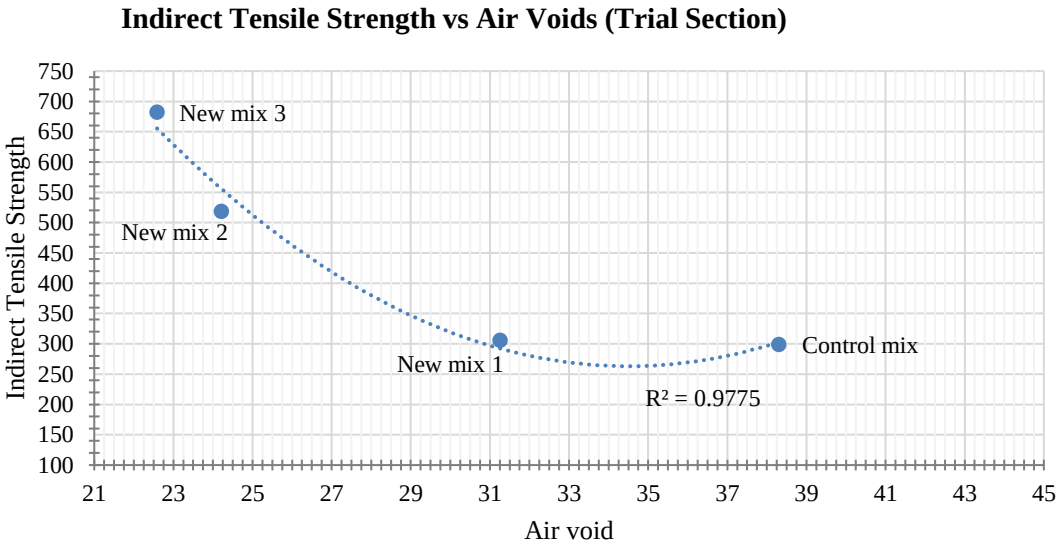

Figure 81 Relationship between Indirect Tensile Strength and air voids

7.4.2.5 Moisture-induced Damage Test

Moisture-induced damage is a common phenomenon for permeable pavement. Water penetrates through the pore structures and gets saturated quickly for the time being if the pores are clogged. In a cold climate, the freeze-thaw cycles further deteriorate this condition and cause premature pavement damage (Huang; Wu, et al., 2010, Lu, 2019). The moisture-induced damage in the PRP mixes was obtained from retained tensile strength in the samples after conditioning with five freeze-thaw cycles, as shown in Table 35. The retained tensile strength for all the mixes was found to be more than 70%, except for the New Mix 2. Higher retained tensile strength in samples could be correlated to the higher percentage of rubber aggregates and binders in the mixes. The Control Mix showed the highest retained tensile strength (80%) since it contained the highest percentage of rubber aggregates (45.25%) and a higher percentage of binder (9.5%). The New Mix 3 also showed a higher retained strength (76%) since it contained 33% rubber aggregates and 12% binder. On the other hand, New Mix 2 contained the lowest percentage of rubber aggregates (17.5%) and binder (7.5%), thus showing the lowest retained strength. The retained tensile strength calculated for the New Mix 2 was 68%.

Table 35 Moisture-Induced Damage – Tensile Strength Ratio

Mix	ITS before conditioning	Standard Deviation	ITS after conditioning	Standard Deviation	TSR	Standard Deviation
Control Mix	299.3	8.86	238.8	4.7	0.80	0.02
New Mix 1	306.1	23.11	224.2	8.1	0.73	0.03
New Mix 2	518.7	45.86	351.4	16.2	0.68	0.03
New Mix 3	682.4	29.69	515.4	36.5	0.76	0.05

7.4.2.6 Hamburg Wheel Tracking Test Result

The rutting resistance of the PRP material was investigated through the Hamburg Wheel Tracking test. The average rutting results for different mixes ranged from 0.81 mm to 0.99 mm, as shown in Table 36, which indicated that all the mixes showed good rutting resistance compared to the conventional pavement material. The analysis of the rutting result indicated that from 0 cycles to 10000 cycles, several temporary rutting occurred on the samples, as shown in Figure 82. However, this temporary rutting mostly disappeared after the removal of the wheel load from the samples. Material's elastic properties due to rubber aggregates and the large percentage of air voids could probably explain this phenomenon. Hence, the samples got room for deflection under loading conditions by compressing the air voids. However, after the load's removal, the material's elasticity helped it return to its original condition.

Table 36 Hamburg Wheel Tracking Test

Trial Section Hamburg Wheel Tracking Test				
Mixes	Depth 01 (mm)	Depth 02 (mm)	Rutting average (mm)	Standard Deviation
Control Mix	0.72	0.89	0.81	0.12
New Mix 1	1.18	0.6	0.89	0.41
New Mix 2	1.4	0.58	0.99	0.58

New Mix 3	0.81	1.09	0.95	0.20

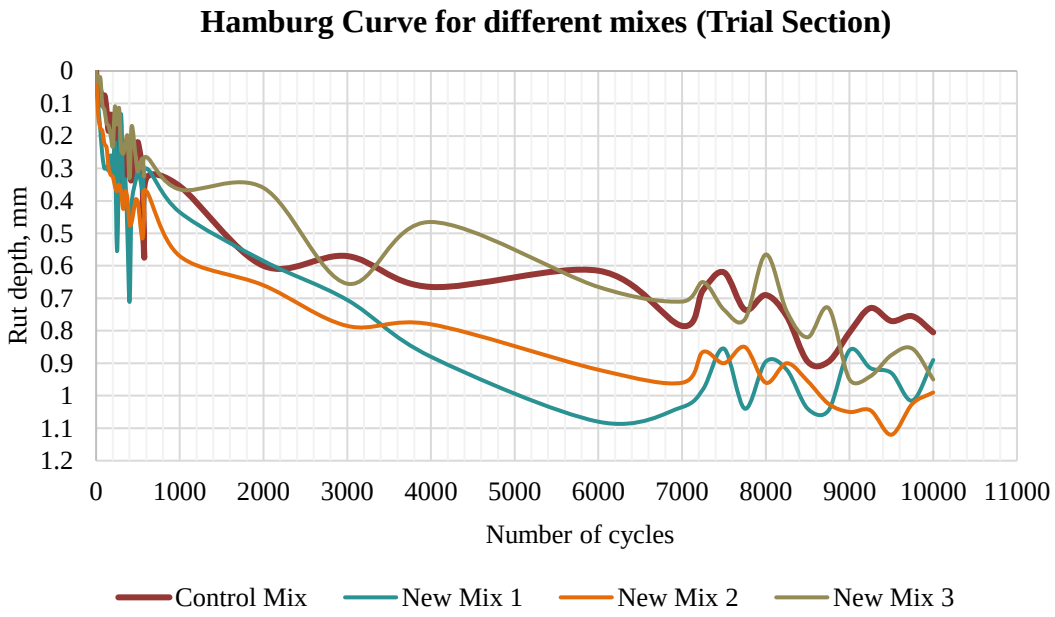

Figure 82 Hamburg curve for different mixes

Stripping-related abrasion was also obtained from the Hamburg Wheel Tracking test, as shown in Figure 83 and Table 37. Samples' weights were measured before and after the testing and after the drying of the samples. However, right after the test, all the samples showed a higher weight than the initial weight. The increased weight was due to water absorption by the sample's stone aggregates during the test. However, after drying the samples, a small amount of weight loss was observed than the initial weight. These weight losses ranged from 0% to 0.3%, indicating the mixes' stripping-related abrasion. However, the New Mix 3 showed a 0.7% increase in weight even after drying the sample. The probable reason could be this mix's higher percentage of binder and stone aggregates. Along with water absorption by the stone aggregates, binder components probably chemically changed under the wheel pressure and water, resulting in increased weight. However, this change was negligible.

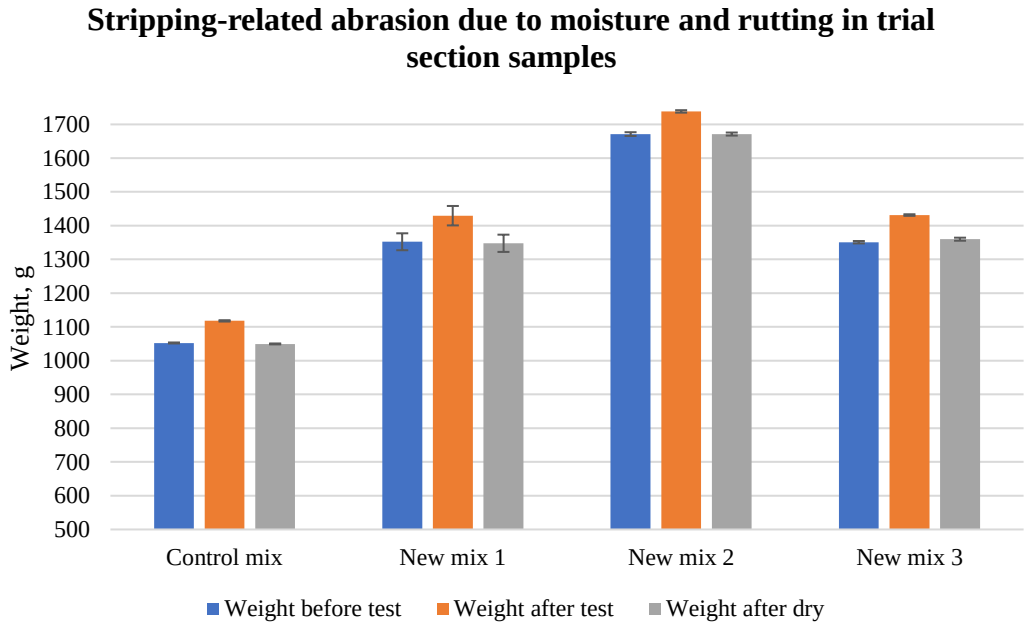

Figure 83 Stripping-related abrasion

Table 37 Stripping-related abrasion in percentage in trial section sample

Mixes	Weight loss after rutting test
Control Mix	-0.3%
New Mix 1	-0.3%
New Mix 2	0.0%
New Mix 3	0.7% (increased)

7.5 Field Test on the Trial Section

7.5.1 Field Testing Methodology

7.5.1.1 Light Weight Deflectometer

Light Weight Deflectometer (LWD) was used to determine the deflection due to a falling weight that was held at a constant height by a release mechanism. First, the deflection value was measured using the falling weight that transmits the impact of the load to the pavement surface. Then, the stiffness

modulus of the pavement was calculated using the deflection value (Elhakim; Elbaz, et al., 2014, Mallick, R. B. and El-Korchi, T., 2018).

7.5.1.2 British Pendulum Test (BPT)

A British Pendulum tester was used to measure the energy loss when its sliders were propelled over the pavement's surface. A higher British Pendulum Number (BPN) is related to a more significant energy loss, which is associated with a higher frictional value of the pavement (ASTM E303−93, 2018, Pickel, 2018). However, BPT can only measure the frictional properties at low speeds (Saito and et al, 1996). All the frictional values were measured after wetting the surface to obtain the results in wet conditions.

7.5.1.3 Rut Depth from Dipstick

The Dipstick is an inclinometer-based profile measurement device supported by two legs 305 mm apart. This piece of equipment measures the relative elevation difference of the legs. Usually, the Dipstick calculates the International Roughness Index (IRI) value (Karamihas, 2005, Nazef; Mraz, et al., 2008, Pavement Tools Consortium, 2019). However, the trial sections' length was insufficient to determine the IRI value using this equipment. Thus, Dipstick calculated only the rut depths from the trial sections at different times.

7.5.1.4 NCAT Field Permeameter

NCAT Asphalt Field Permeameter was used to determine the trial sections' water infiltration rate following ASTM - C1701/C1701M. The permeameter's bottom tire (cross-section area is 167.53 cm^2) was used for testing. Four litres of water were poured on each point at least three times, and the average value was considered for calculation. According to the test standard ASTM - C1701/C1701M − 17a, at least three (3) test points are recommended for a test area of 2500 m^2. Since the infiltration rate from each point is valid for the localized area, the average value was taken to determine the infiltration rate of the entire site (ASTM C1701/C1701M−17a, 2017).

7.5.2 Field Testing Schedule

The 1st field test was conducted on the trial sections from October 4, 2021, to October 7, 2021, right after construction, before fully opening for traffic. After the 1st field test, trial sections were fully opened for traffic. The 2nd field test was conducted on October 23, 2021, about two weeks after the 1st field test. Finally, the 3rd field test was carried out on May 13, 2022, about six months after the 2nd field test.

Between the 2nd and 3rd tests, the trial sections experienced one winter. Schedule for field testing is shown in Table 38.

Table 38 Schedule for field testing

Date	Construction	Testing
02-Oct-2021	Phase 01	
04-Oct-2021		1st Testing
05-Oct-2021	Phase 02	
07-Oct-2021		
23-Oct-2021		2nd Testing
13-May-2022		3rd Testing

7.5.3 Weather Station Data

Weather data from the trial section construction time to the 3rd field testing is presented here. Figure 84 shows the daily maximum, minimum and average temperature from September 15, 2021, to May 13, 2022. The temperature ranged from 25˚C to -25˚C. Thus, the PRP pavement experienced a temperature difference of 50˚C from 1st to 3rd field testing. In addition, Figure 85 shows the rainfall data for the same period, indicating that in September 2021, the pavement received more precipitation.

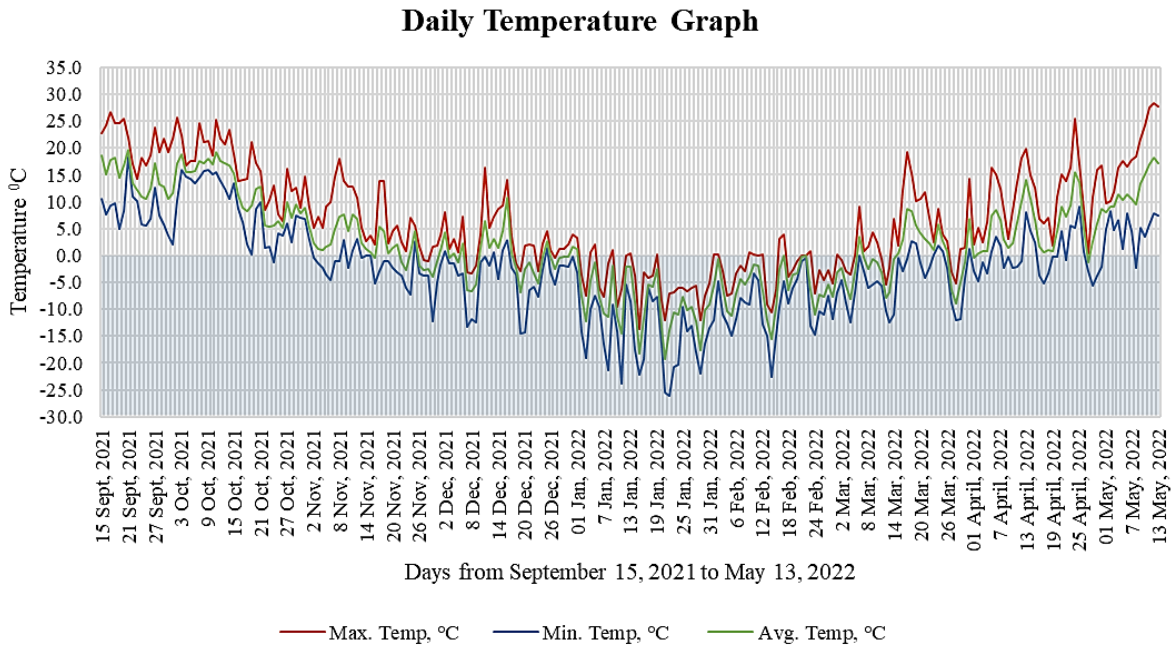

Figure 84 Temperature data from the weather station

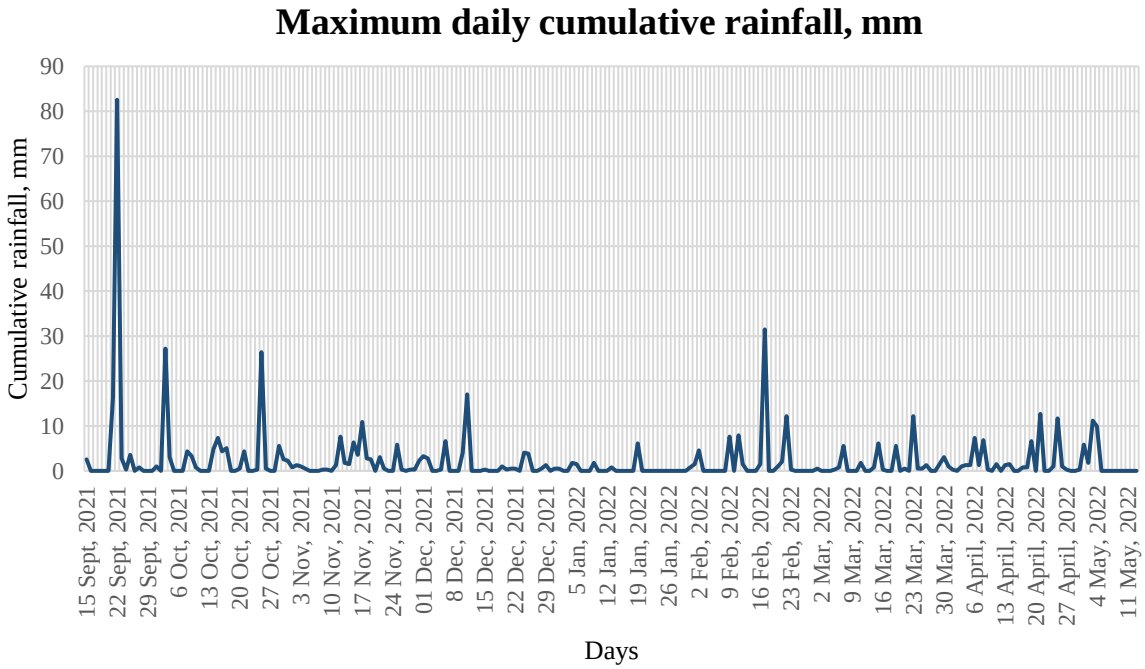

Figure 85 Precipitation data from the weather station

7.5.4 Detailed Drawings for Field Testing

Detailed drawings of Site A and Site B are shown in Figure 86 and Figure 87, respectively. The figures also show the points that were tested during field testing.

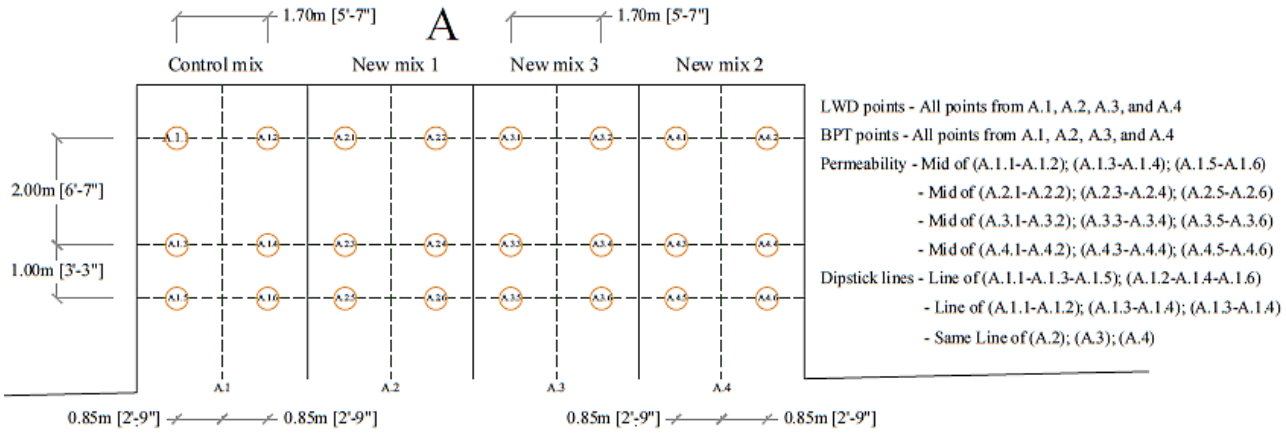

Figure 86 Site A detail for testing

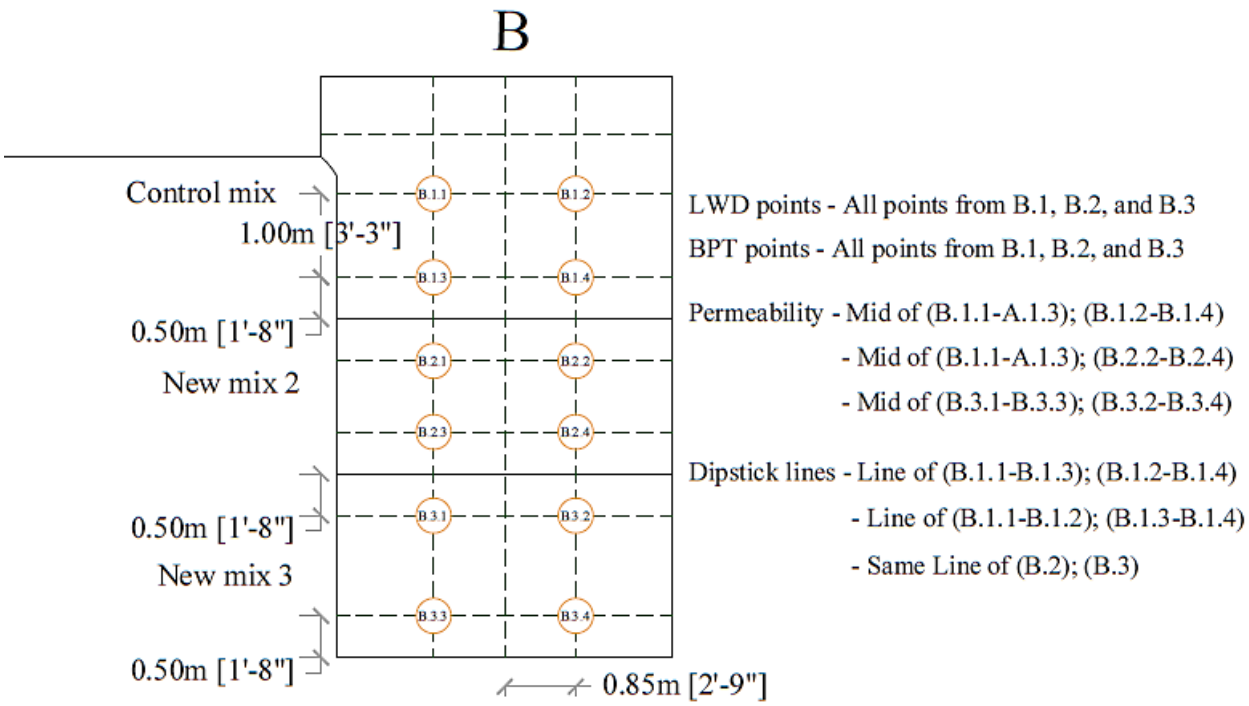

Figure 87 Site B detail for Testing

7.5.5 Field Test Result

7.5.5.1 Light Weight Deflectometer (LWD) Results

Site A and Site B were tested with LWD to measure the pavement's deflection and elastic modulus. At Site A, six points were tested on each section, and at Site B, four points were tested on each section. As expected, where elastic moduli were found to be higher, deflection values were found to be lower and vice versa. The trial sections were tested with LWD three times after the construction, as mentioned in Table 38. Among the three tests, a general trend was observed for all sections. During the 2nd test, elastic moduli were found to be higher than in the 1st. After the 1st test, vehicular traffic was fully opened, and further compaction on the pavement occurred under traffic loading. However, after the 3rd test, all the sections showed lower elastic modulus than in the 2nd. The timing of the 3rd test could probably explain the lower elastic modulus value. The 3rd test was conducted on May 13, 2022, in springtime. During the Spring, subgrade soils are usually in their weakest condition due to thawing. Therefore, it was reflected in the pavement's elastic modulus, showing a lower elastic modulus during the 3rd test (Table 39 and Table 40; Figure 88 to Figure 93).

Besides the test timing, the mixes with a higher percentage of rubber aggregates and binders compacted more than other mixes after opening for traffic. The Control Mix contained a higher percentage of rubber (45.25%) and binder (9.5%); thus, it compacted more after opening for traffic, resulting in a higher elastic modulus value during the 2nd test. Although initially, the average elastic modulus of the Control Mix was 36 MPa, during the 2nd test, it reached 45 MPa. New Mix 1 also contained a comparatively higher percentage of rubber aggregates (37.5%) and showed more compaction than other mixes (from 1st to 2nd test).

The LWD results differed for the same mixes at Site A and Site B. The reason could be the differences in the pavement's sub-grade soil types and their strength. The CBR test revealed that the bearing capacity of the Site A (CBR 18.2%) subgrade is lower than the Site B (CBR 24.3%) subgrade. Thus, all mixes showed higher initial elastic moduli at Site B than at Site A. Besides, New Mix 2 showed the highest elastic modulus at Site B despite containing a lower percentage of rubber aggregates (17.55%) and binder (7.5%), as shown in Table 40. Probably the presence of hard rocks under this section contributed to this result.

Table 39 Elastic Modulus and Deflection of Site A

Trial section - Site A						
Mixes	**Elastic Modulus (MPa)**					
	1st test	**Standard dev.**	**2nd test**	**Standard dev.**	**3rd test**	**Standard dev.**
Control Mix	36	12	45	15	39	11
New Mix 1	32	6	38	10	28	3
New Mix 3	34	10	34	8	28	2
New Mix 2	28	3	29	3	23	5
Mixes	**Deflection (μm)**					
	1st test	**Standard dev.**	**2nd test**	**Standard dev.**	**3rd test**	**Standard dev.**
Control Mix	1335	309	1174	374	1350	356
New Mix 1	1530	264	1342	298	1771	172
New Mix 3	1474	341	1470	321	1729	153
New Mix 2	1682	182	1629	175	1715	775

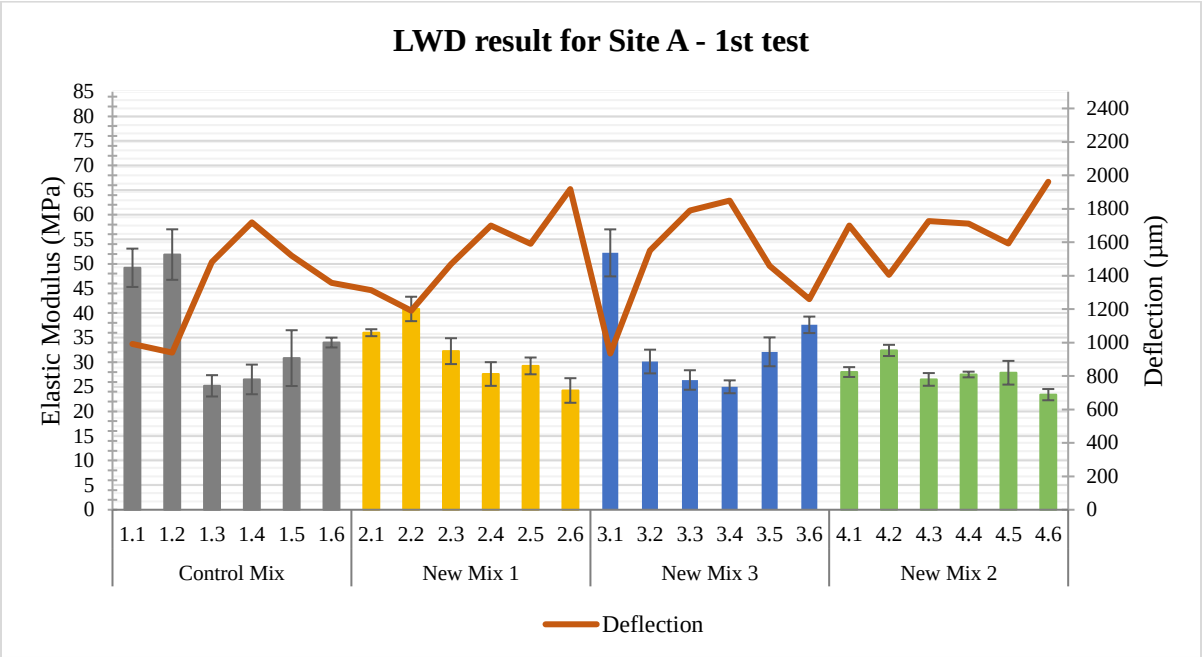

Figure 88 Elastic Modulus and Deflection during the 1st test at Site A

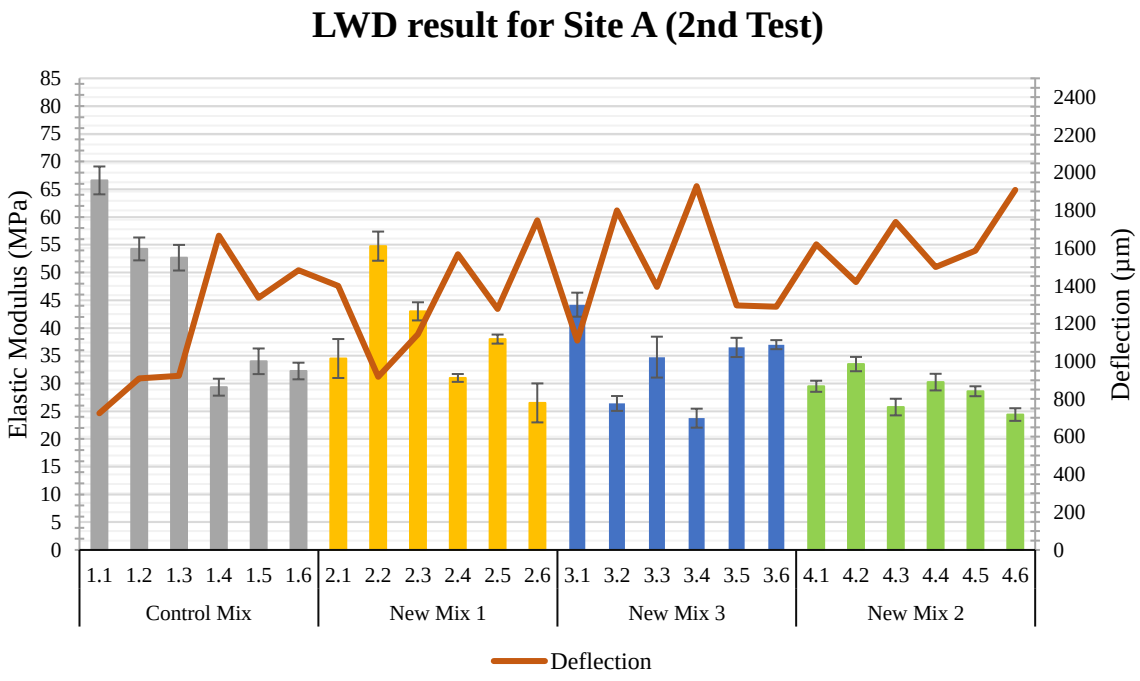

Figure 89 Elastic Modulus and Deflection during the 2nd test at Site A

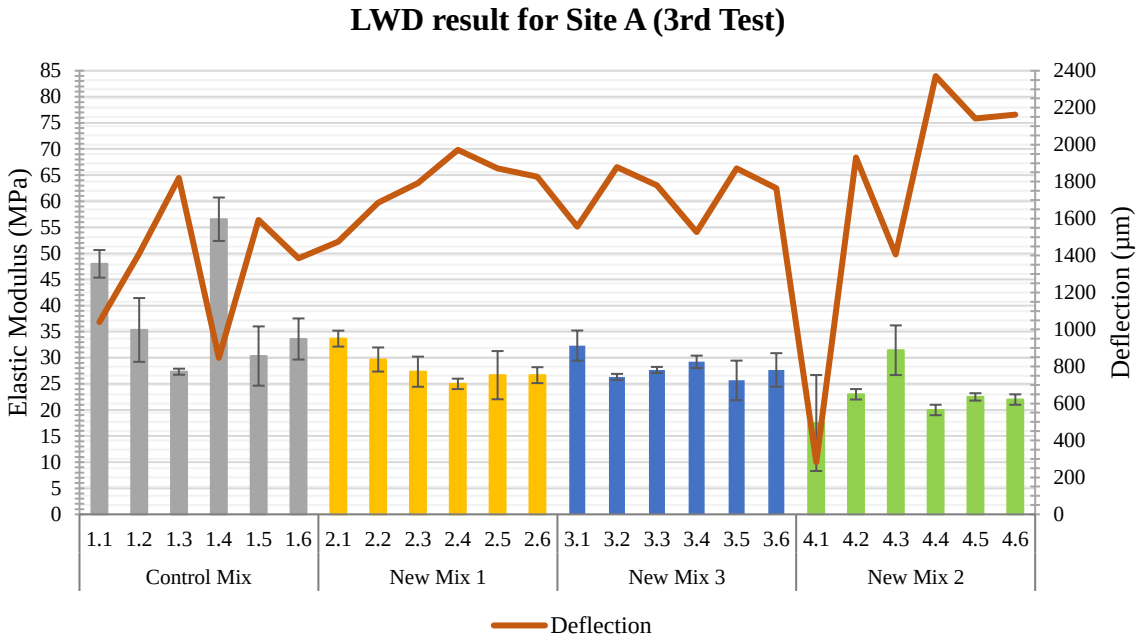

Figure 90 Elastic Modulus and Deflection during the 3rd test at Site A

Table 40 Elastic Modulus and Deflection of Site B

Trial section - Site B						
Mixes	**Elastic Modulus (MPa)**					
	1st test	**Standard dev.**	**2nd test**	**Standard dev.**	**3rd test**	**Standard dev.**
Control Mix	42	10	38	7	36	10
New Mix 2	59	15	73	9	64	9
New Mix 3	41	3	68	6	55	7
Mixes	**Deflection (µm)**					
	1st test	**Standard dev.**	**2nd test**	**Standard dev.**	**3rd test**	**Standard dev.**
Control Mix	1265	252	1307	276	1430	317

New Mix 2	967	204	667	76	824	104
New Mix 3	1359	119	725	66	935	113

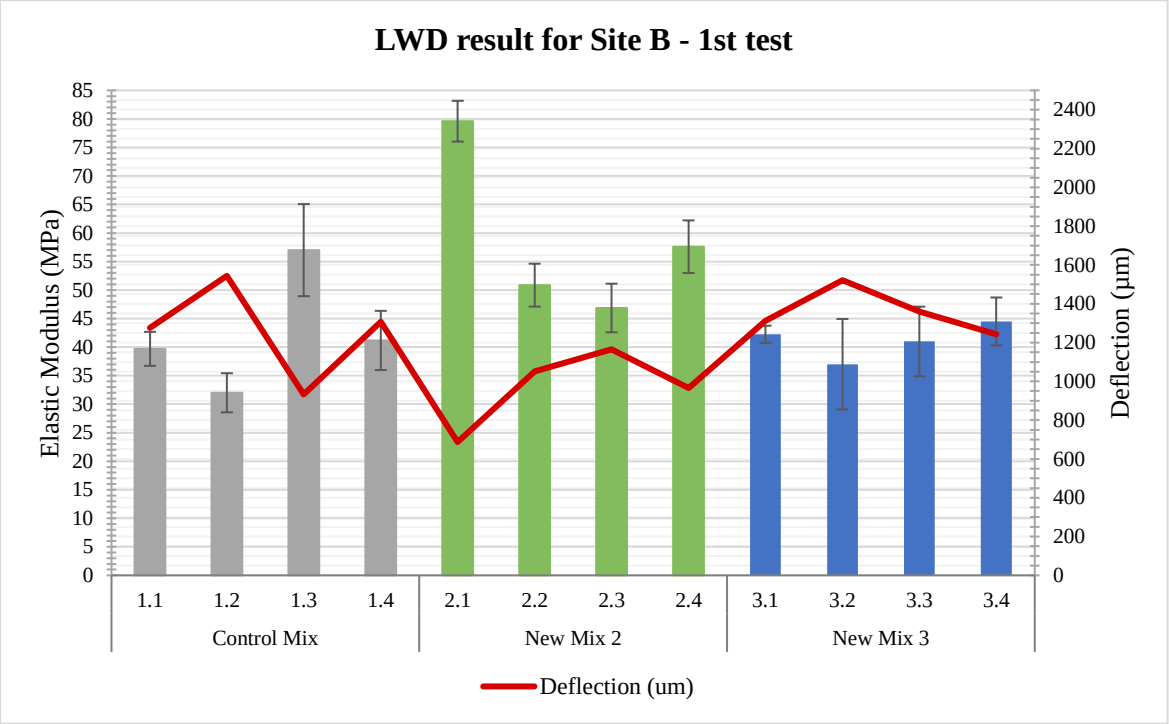

Figure 91 Elastic Modulus and Deflection during the 1st test at Site B

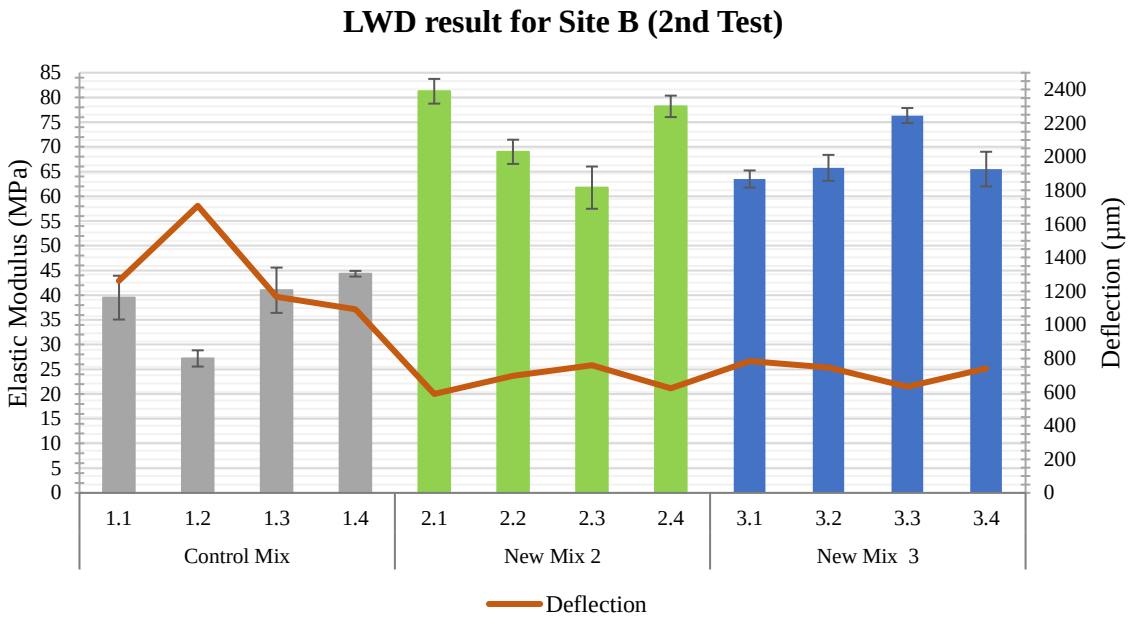

Figure 92 Elastic Modulus and Deflection during the 2nd test at Site B

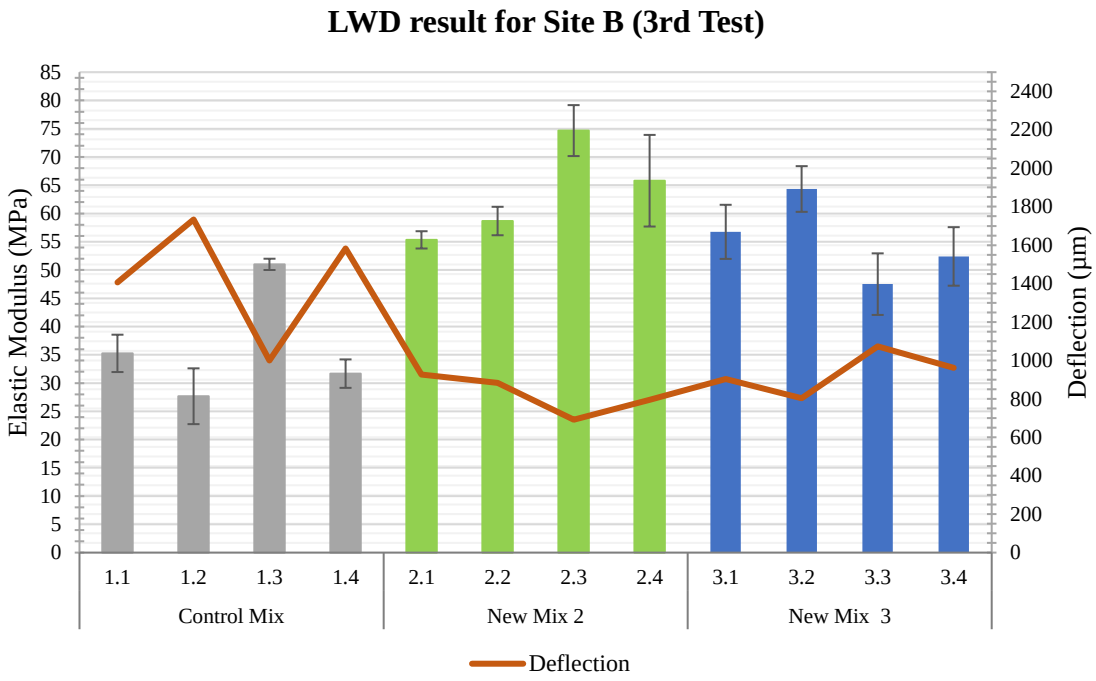

Figure 93 Elastic Modulus and Deflection during the 3rd test at Site B

Single-factor ANOVA analysis (with a confidence interval of 95%) was conducted on the LWD data collected at sites A and B. The results for Control Mix, New Mix 1 and New Mix 3 at Site A showed that there was no significant effect of the time (from 1st to 3rd field test) on the elastic modulus of these mixes. That is proven by the P-value, as the obtained P-value is higher than 0.05. However, there was a significant effect of time on the elastic modulus of the New Mix 2 at Site A, as the obtained P-value was 0.032, which is less than 0.05. Also, there was a significant effect of time on the elastic modulus of the New Mix 3 at Site B (P-value is 0.00032).

Furthermore, a two-factor ANOVA analysis was conducted for sites A and B. The two investigated parameters were the location and type of mixes. The obtained results showed that there was a significant effect of the location on the elastic modulus of the mixes. These differences were found in their initial stiffness and changes in stiffness over time.

7.5.5.2 British Pendulum Test

British Pendulum Numbers (BPN) for different sections were obtained from the British Pendulum Test. A higher BPN is related to a more significant loss of energy and higher friction value (Pickel, 2018). The measured frictional property of the pavement surface is associated with the micro-texture of the pavement surface (ASTM E303−93, 2018). Besides, the Ministry of Transportation Ontario (MTO) recommended minimum value for pavement surface friction is 30 BPN (Pickel, 2018). The results from the 1st to the 3rd field test showed that all the sections met this MTO requirement exceeding the 30 BPN threshold. However, very high BPN values were obtained for several sections, which was associated with surface ravelling and particles' movement from the surrounding areas. Hence, surface ravelling and particles' movement from the vicinities can threaten the pavement's durability.

Additionally, all the sections showed a common trend from the 1st to the 3rd test. Higher BPN values were obtained for all the sections during the 1st test, whereas the values were reduced in the 2nd. This reduction was because the PRP surfaces were compacted and polished further by the vehicular traffic after the 1st testing, which probably smoothened the pavement surface. However, during the 3rd test (in Spring, after seven months of construction), surfaces ravelled and loose particles were transported from the site's surroundings, increasing the BPN number again. The mixes with a higher percentage of stone aggregates and binders showed lower frictional values than those with a lower percentage of binder and a higher percentage of rubber. The Control mix showed the highest BPN values (73 at Site A and 69 at Site B) since it contained a higher percentage of rubber aggregates (as shown in Table 41, Table 42,

Figure 94 and Figure 95). On the other hand, the New Mix 2 contained the highest percentage of stone aggregates (75%) and binder (12%), resulting in lower BPN values (60 at Site A and 59 at Site B).

Table 41 British Pendulum Test Result from Site A

Trial section - Site A						
Mixes	**British Pendulum Number (BPN)**					
	1st test	**Standard dev.**	**2nd test**	**Standard dev.**	**3rd test**	**Standard dev.**
Control Mix	73	10	60	4	64	28
New Mix 1	69	8	55	5	72	9
New Mix 3	58	6	48	4	45	15
New Mix 2	60	6	50	3	55	22

Table 42 British Pendulum Test Result from Site B

Trial section - Site B						
Mixes	**British Pendulum Number (BPN)**					
	1st test	**Standard dev.**	**2nd test**	**Standard dev.**	**3rd test**	**Standard dev.**
Control Mix	69	6	64	2	67	9
New Mix 2	59	8	67	6	83	6
New Mix 3	62	13	60	3	84	7

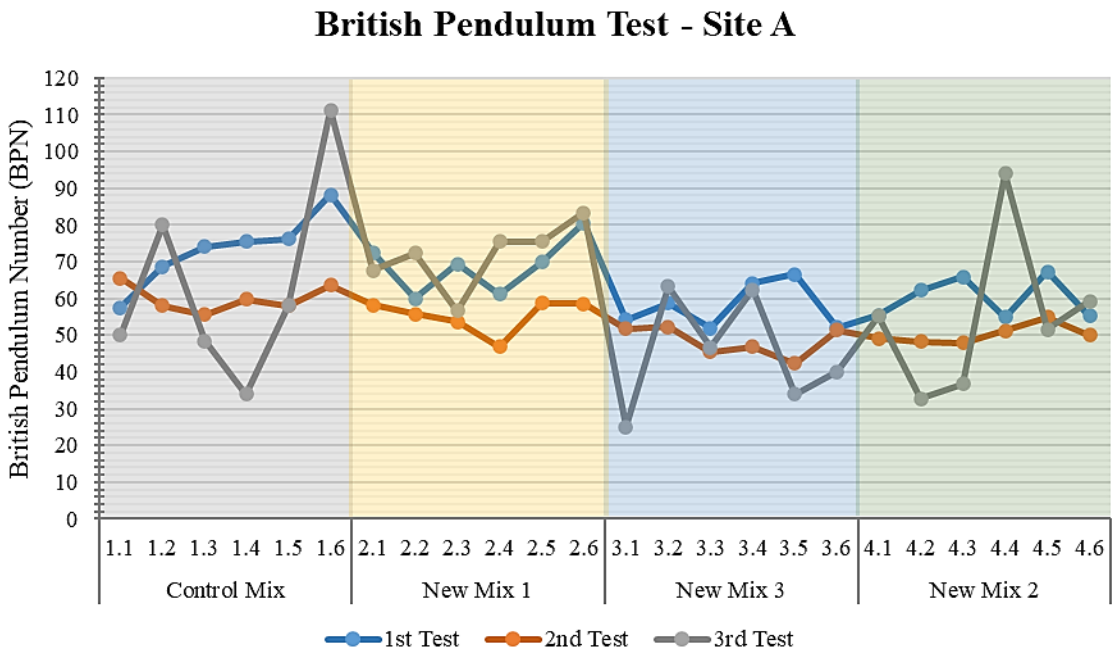

Figure 94 British Pendulum Test for Site A

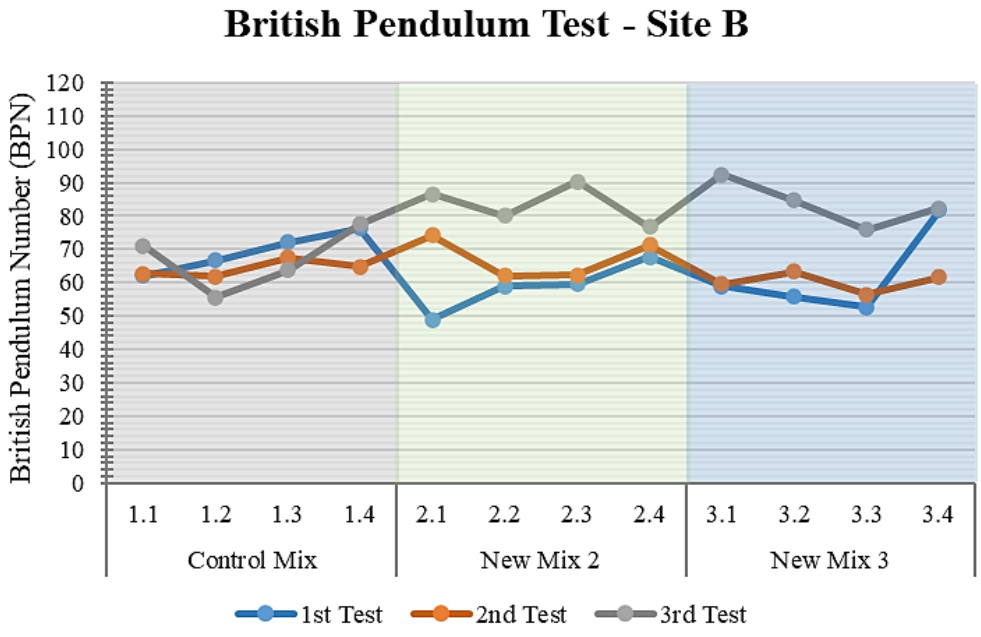

Figure 95 British Pendulum Test for Site B

Single-factor ANOVA analysis (with a confidence interval of 95%) was conducted on the BPT data collected at Site A and Site B. The results showed that there is no significant effect of the time (from the 1st test to the 3rd) on the BPN values of the Control Mix, New Mix 2 and New Mix 3 at Site A. This was proven by the P-values, as the obtained P-values were higher than 0.05. However, there was a significant effect of time on the BPN value of the New Mix 1, as the obtained P-value was 0.003, which is less than 0.05. Besides, the time factor had no significant effect on the BPN value of the Control Mix (P-Value 0.58) at Site B. However, the time significantly affected the BPN value of New Mix 2 and New Mix 3 at Site B (as the P-Value was less than 0.05).

Furthermore, a two-factor ANOVA analysis was conducted for sites A and B. The two investigated parameters were location and time. The results showed that the location factor did not significantly affect any mixes in their changes in BPN number over time.

7.5.5.3 Rut Depth from Dipstick

The International Roughness Index (IRI) is calculated automatically from recorded Dipstick measurements. However, trial sections were very small to calculate IRI using the Dipstick. IRI can only be calculated if at least 37 readings (minimum 9.25m) can be obtained from the Dipstick. Therefore, only the average rut depth was possible to calculate using the Dipstick. Rut depths were calculated for Site A and Site B during the 1st and 2nd tests. Initial rut depths on Site A for different mixes ranged from -7.0 mm to -8.7mm (Table 43 and Figure 96). For Site B, this range was -5.8 mm to -10.7mm (Table 44 and Figure 97). The probable reason for this initial rut depth could be the workmanship, the site's slopes and the undulating surface.

After fully opening for traffic, greater rut depths were found on each section under the wheel paths. These rut depths ranged from -22.5mm to -26.0mm for Site A and from -19.6mm to -24.4mm for Site B. Hence, compaction occurred under the wheel path, resulting in a larger rut depth.

Table 43 Rut depth result from Site A

Rut depth from Dipstick -Site A		
Mixes	**Avg. Depth of Rut (mm) - 1st test**	**Avg. Depth of Rut (mm) - 2nd test**
Control Mix	-7.7	-22.5
New Mix 1	-7.9	-23.6
New Mix 3	-7.0	-22.6
New Mix 2	-8.7	-26.0

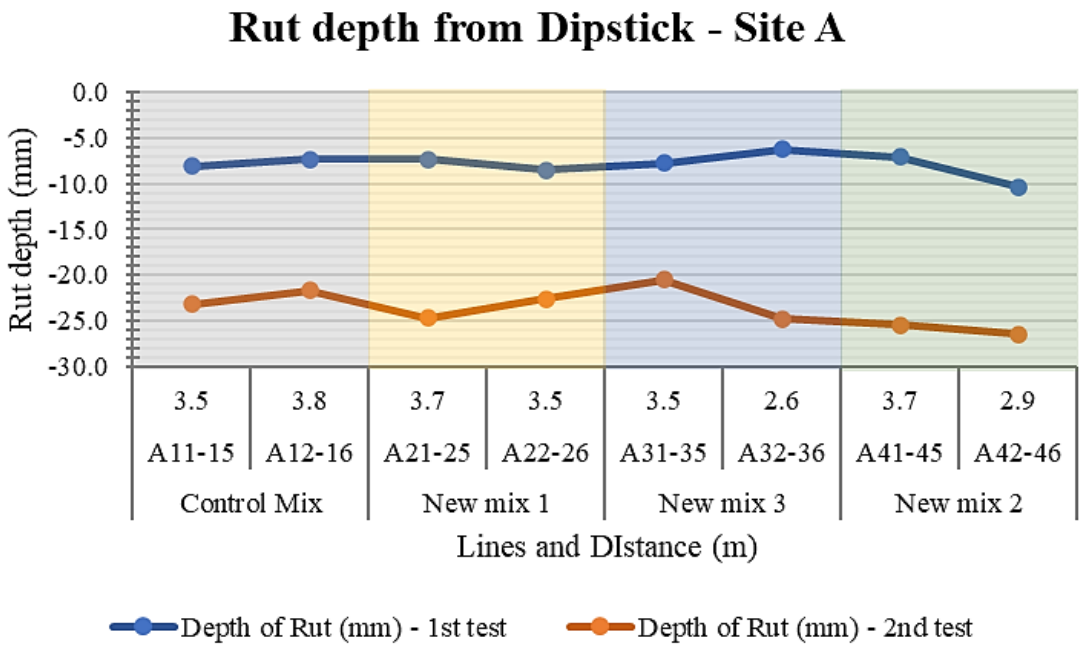

Figure 96 Comparison of rut depth between tests on Site A

Table 44 Rut depth result from Site B

Rut depth from Dipstick -Site B		
Mixes	**Avg. Depth of Rut (mm) - 1st test**	**Avg. Depth of Rut (mm) - 2nd test**
Control Mix	-10.7	-24.4
New Mix 2	-6.6	-19.6
New Mix 3	-5.8	-21.5

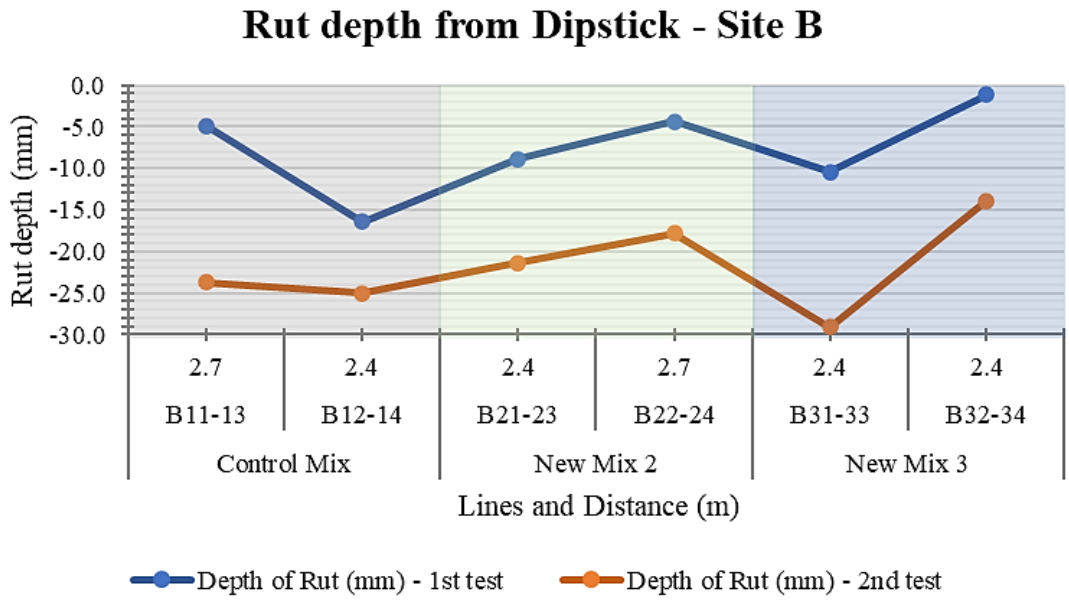

Figure 97 Comparison of rut depth between tests on Site B

A single-factor ANOVA analysis was conducted on the rut depths data collected at Site A and Site B (with a confidence interval of 95%). The result showed that rut depths at Site A for different mixes were changed significantly (P-value was less than 0.05) with time (between 1st and 2nd test). In contrast, the rut depths on Site B for different mixes did not change significantly between the tests. The probable reason could be the sites' location and differences in the stiffness of the subgrade soil. Table 33 showed that the bearing capacity of the Site A subgrade soil was lower than that of Site B. Besides, a two-factor ANOVA analysis was conducted for Site A and Site B. The two investigated parameters were location

and time. The result showed that all the mixes were performed similarly at both sites (P-value is above 0.05).

7.5.5.4 NCAT Field Permeameter

The permeability of different sections at Site A and Site B was tested three times (right after construction, three weeks after construction, and seven months later). Sections on both sites showed a common trend during these three tests. All sections showed more permeability in the 2nd test than the 1st test at both locations, except for New Mix 3. It is assumed that all the sections showed a certain permeability right after construction, before opening for traffic, based on the types of mixes. However, after three weeks of construction, due to environmental effects, traffic loading and interaction among the components, internal connectivity could have been changed, and new voids formed. Hence, the permeability of the sections was increased during the 2nd test. However, the New Mix 3 contained the highest percentage of binder (12%), probably resulting in greater compaction, reducing the interconnected air voids. Furthermore, the changes in the permeability of the sections at Site A and Site B differed in 3rd test.

The permeability of the Control Mix and the New Mix 1 at Site A further increased in the 3rd test. In contrast, the permeability of the New Mix 2 and the New Mix 3 at Site A decreased in the 3rd test (Table 45). The probable reason could be the expansion of existing voids or the creation of new voids in the Control mix and the New Mix 1 after winter. However, more compaction or clogging probably occurred in the New Mix 2 and the New Mix 3 after the winter.

All the sections at Site B showed reduced permeability during the 3rd test (Table 46). This can be explained based on field observation. Site B was constructed on a slope and surrounded by an unpaved area with loose gravel. Thus, lots of dirt particles were transported to the site from the surrounding area, reducing the sections' permeability. Even the lowest part of the site (section with the New mix 3) was found to be fully clogged with debris in the 3rd test.

A two-factor ANOVA analysis was conducted for the permeability data collected at Site A and Site B. The result showed no significant difference in the performance of the mixes at Site A and Site B (the P-value is higher than 0.05 at an alpha level of 0.05). However, the permeability rates in the trial sections were significantly higher than the highest rainfall rate in Canada, which is 298.8 mm/h (Environment Canada, 2019, Kabir; Oyeyi; Al-BayatiTighe, 2020a, Henderson, 2012).

Table 45 Permeability of Site A

Permeability of Site A						
Mix	**Average Infiltration (mm/h)**	**Standard deviation**	**Average Infiltration (mm/h)**	**Standard seriation**	**Average Infiltration (mm/h)**	**Standard deviation**
	1st test		**2nd test**		**3rd test**	
Control Mix	45605	6845	48428	10956	57715	9502
New Mix 1	44785	2019	62741	2313	74805	13139
New Mix 3	28368	5183	24695	7555	22658	6639
New Mix 2	39608	5970	45476	4409	40244	24851

Table 46 Permeability of Site B

Permeability of Site B						
Mix	**Average Infiltration (mm/h)**	**Standard deviation**	**Average Infiltration (mm/h)**	**Standard deviation**	**Average Infiltration (mm/h)**	**Standard deviation**
	1st test		**2nd test**		**3rd test**	
Control Mix	39681	3070	48334	3808	25468	18009
New Mix 2	37698	1991	50998	3357	11029	8394
New Mix 3	30469	262	21649	70	Clogged	0

7.5.5.5 Surface Distress Evaluation

In three field tests, surface distress was evaluated for Site A and Site B. Visual inspection showed that there was no visible change from the 1st field testing to the 2nd at both sites, as shown in Figure 98 and Figure 99. However, during the 3rd field testing, as shown in Figure 100 (7 months after the

construction), insubstantial surface distresses were observed at Site A and Site B, summarized in Table 47 and Table 48, respectively. At Site A and Site B, surface defects like slight loss of coarse aggregate and minor ravelling were observed. In addition, very slight rutting was also found under the wheel paths. Furthermore, very small transverse and longitudinal cracks were observed at both locations. Surface distress evaluations are plotted in Figure 101 and Figure 102 for Site A and Site B, respectively.

Figure 98 Site B right after construction

(a) Site B

(b) Site A

Figure 99 Site A and Site B after two weeks of construction (a) Site A, (b) Site B

(a)

(b)

Figure 100 Site A and Site B after seven months of construction; (a) Site B preparation for testing, (b) Site A preparation for testing

Table 47 Site A distress evaluation

Site	Distress manifestation	Distress type	Severity	Extent	Description
Site A	**Surface defects**	Loss of Coarse Aggregates	2 (Slight)	< 10% area affected (few)	Noticeable loss of pavement material.
		Ravelling	1 (Very slight)	10 to 20% of surface area (Intermittent)	Barely noticeable loss/lack of pavement materials.
	Permanent deformation	Rutting	1 (Very slight)	< 10% area affected (few)	Barely noticeable, less than 6 mm.
	Cracking	Longitudinal crack	1 (Very slight)	< 10% area affected (few)	Single crack width less than 3 mm. Measured length 10 mm.

Table 48 Site B distress evaluation

Site	Distress manifestation	Distress type	Severity	Extent	Description
Site B	Surface defects	Loss of Coarse Aggregates	2 (Slight)	< 10% area affected (few)	Noticeable loss of pavement material.
		Ravelling	1 (Very slight)	10 to 20% of surface area (Intermittent)	Barely noticeable loss/lack of pavement materials.
	Permanent deformation	Rutting	1 (Very slight)	< 10% area affected (few)	Barely noticeable, less than 6 mm.
	Cracking	Longitudinal crack	1 (Very slight)	< 10% area affected (few)	Single crack width less than 3 mm. Measured length 127 mm.
		Transverse crack	1 (Very slight)	< 10% area affected (few)	Single crack width less than 3 mm. Measured length 100 mm.

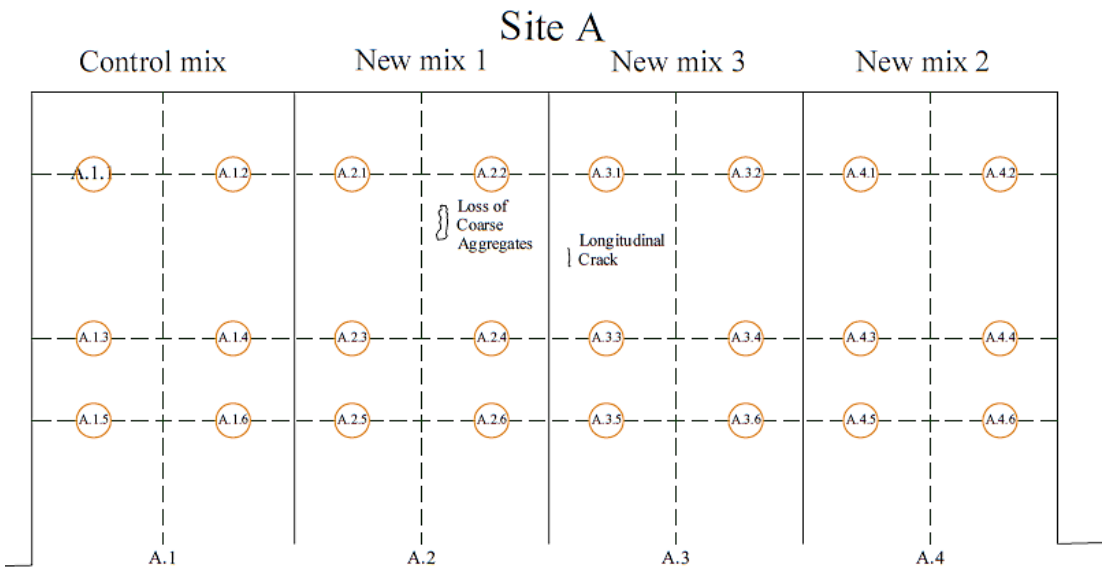

Figure 101 Surface distress evaluation for Site A

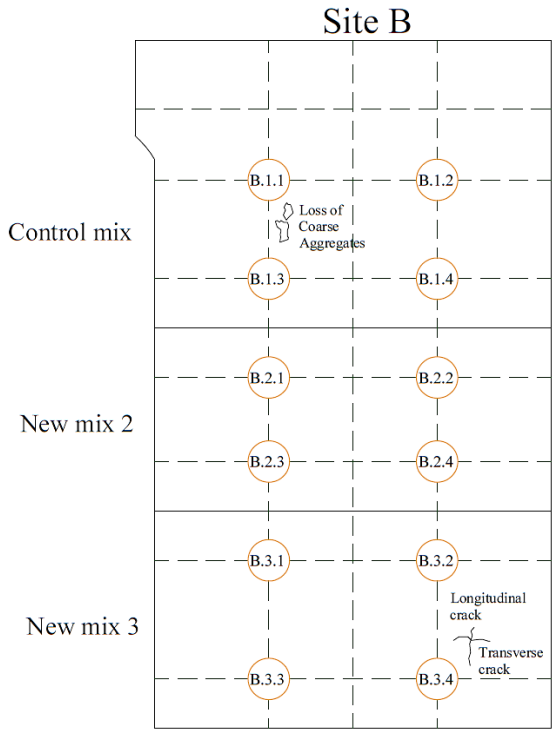

Figure 102 Surface distress evaluation for Site B

7.6 Conclusion

This research aimed to investigate the properties and performance of PRPs from field construction before their large-scale use in the Canadian climate. Two trial sections were constructed using four different mixes. The properties investigated in the laboratory included indirect tensile strength, moisture-induced damage due to freeze-thaw cycles and permanent deformation, while the field investigation covered pavement's stiffness, frictional property, roughness, permeability and surface distress at different times in addition to the subgrade bearing capacity. The results are summarized below:

1. A higher percentage of stone aggregates and binder contents improved the indirect tensile strength of the PRP materials. In contrast, a higher percentage of rubber aggregates and binders improved the moisture-induced damage in the material.
2. All the PRP samples retained more than 68% indirect tensile strength after five freeze-thaw cycles.
3. In terms of permanent deformation, all PRP mixes showed good rutting resistance ranging between 0.81 mm to 0.99 mm.
4. Field evaluation revealed that mixes showed higher stiffness and lower rut depth on the field as soil bearing capacity increased.
5. Frictional values for all the mixes were found to be above the Ministry of Transportation Ontario (MTO) recommended lower threshold value, 30 BPN.
6. All PRP mixes showed excellent permeability, ranging from 28368 mm/h to 45605 mm/h, which is higher than the highest rainfall rate in Canada (298.8 mm/h).

It was observed that material composition, site geometry and existing subgrade conditions mostly influenced the performance of PRP pavements. Though a higher percentage of rubber aggregates improved the moisture-induced damage in the material, those mixes also showed higher stripping-related abrasion and ravelling. The abrasion loss and ravelling were further enhanced when the binder percentages were reduced in the mixes. Thus, the PRP mixes with higher percentages of stone aggregates and binder performed well. Besides the overall procedure of trial section construction, the field and laboratory testing captured much practical know-how about the paving of PRP material and

its performance outside the laboratory. It also provided essential knowledge to gain confidence with the preferred mix designs before widespread application in the Canadian climate.

Chapter 8

Conclusions, Recommendations and Future work

8.1 General Summary

This research aimed to understand the properties of PRP material and improve its performance for the Canadian climate as a pavement material for low-trafficked areas. Therefore, this research can be divided into four major sections, as follows:

- Preliminary evaluation of PRP from the existing sites
- Laboratory evaluation of the current PRP mix
- Development of new PRP mixes and their evaluation under the laboratory facilities
- Construction of trial sections with the selected mixes and monitoring of their field performance

The preliminary study was conducted to better understand the material's behaviour from the existing sites. A commercial parking lot and a residential driveway were tested for the primary investigation; they were five to six years old at the testing time. Hence, the information gathered from the initial field testing created a base for understanding the properties of PRP material. Besides, a few new construction sites were visited to understand the construction process and material behaviour during construction. Subsequently, samples were prepared for lab testing using the current commercial mix to determine their durability and strength as the Control Mix.

Through the experimental design, four new mixes were developed using different proportions of stone aggregates, rubber aggregates and polyurethane binder. Also, using the proportion of the Control Mix, four polyurethane binders were used to make four different mixes to determine the different binder effects in PRPs. Then the newly developed mixes were tested to investigate PRP's strength range, failure criteria, moisture-induced damage and durability.

In the next step, two trial sections were constructed using selected mixes along with the Control Mix. In addition, samples were also prepared from the field mixes to test their properties in the laboratory. Then the field performance of the applied mixes was evaluated at different times. First, they were tested right after construction before fully opening for traffic. Then three weeks after the construction, and after seven months when the sections experienced their first winter. The critical trend of pavement

deterioration and performance changes of different mixes over time was obtained through field evaluations.

Finally, a guideline is developed for using PRPs in different subgrade conditions. A few secondary resources were used for creating these guidelines, which investigated different site conditions, underground water table location, soil condition and rainfall data.

8.2 Major Findings

8.2.1 Finding from Chapter 4 - Preliminary Field Investigation

- The average Modulus of Elasticity of PRP at Location 1 was 37MPa, and at Location 2, 33MPa, with statistically no significant difference between these two locations, even though they had different pavement structures.
- The stiffness of PRP below the wheel path and trafficked areas was found to be lower than in other areas.
- BPN number of PRP ranges between 57 to 74, with frictional values observed to reduce significantly (by 22%) under the wheel path area.
- The T2GO result also shows a lower coefficient of friction (below 0.4) along the wheel path, which indicates the traffic-related abrasion on the surface, with the average coefficient of friction in Location 2 ranging between 0.50 to 0.58.
- Similar trends and magnitude for both T2GO and BPT were observed; however, more variability in results was observed for BPT than for T2GO.
- The IRI value found from SurPRO was between 6.52 m/km to 13.41 m/km, and for Dipstick, this value was between 7.56 m/km to 15.77 m/km. There was statistically no significant difference between the results from the two pieces of equipment. The average IRI value was found to be 10 m/km.
- IRI value was found higher under the wheel path, in heavy traffic areas and in areas where visible surface distresses were observed. Settlement in the base layer and construction method is probably contributing to the high IRI value. Besides, severe ravelling could also have contributed to the higher IRI value.

- The average infiltration rate found for the pavement surface area was 30836 mm/hr, which is significantly higher than the highest rainfall rate in Canada.
- The most visible surface distress for the PRP surface area was ravelling. Moderate to severe ravelling was found all over the study area.
- Lower compaction effort and less adhesion between rubber and stone aggregate were probably contributing to this ravelling or abrasion loss of PRPs.

8.2.2 Findings from Chapter 5 – Investigation of Mechanical Behaviour

- The Compressive strength test results showed that an increase in stone aggregates and binder percentage in PRP mixes increased their compressive strength. In contrast, an increase in rubber aggregates decreased the material's compressive strength. Furthermore, an increase in air voids in PRP samples reduced the material's compressive strength.
- Concerning the types of binder and sources, the obtained results showed no considerable influence of different types of binder in compressive strength test results. However, the lowest compressive was observed when mixing with B2—aromatic binder.
- The material's tensile strength was found to be higher when the stone aggregate and binder percentages in the mixes were greater. Air voids in the sample had a negative impact on the tensile strength. Tensile strength decreased as the air void increased.
- From the perspective of polyurethane binder sources, the outcomes revealed that different polyurethane binder sources influenced the tensile strength of the PRP material.
- PRP samples with varying compositions retained more than 70% of their tensile strength after conditioning with five freeze-thaw cycles. However, due to the variety of binders used, retained tensile strength for PRP samples varied, and some showed retained tensile strength below 70%. Furthermore, all samples had a few aggregate losses and a slight discoloration after freeze-thaw conditioning.

8.2.3 Findings from Chapter 6 – Durability Evaluation

- A relatively high abrasion loss was found for the granite stones that were used for all the sample preparation.
- PRP materials for different compositions showed good rutting resistance, which ranges from 0.3mm to 2.8mm in different mixes. Moisture-induced damage, stripping related abrasion was also found to be very small, ranging from 2.6% to 0.1%.
- The use of different binders from different sources showed that the B2—aliphatic binder could withstand more rutting than other binders. However, among all the aromatic binders, B3—aromatic samples failed after 4000 cycles and deteriorated quickly at a higher temperature. Except for B3—aromatic, moisture-induced damage and stripping-related abrasions are found to be between 0.3% to 0.6%.
- Los Angeles abrasion loss testing gives an indication of the ravelling resistance of the samples. In the conditioned situation, New Mix 2 showed the highest abrasion, which was 25.31%, and the lowest was found in New Mix 3, 6.49%. For unconditioned samples, the highest abrasion loss was reduced in all cases, which was consistent with the mix types. Thus, the highest in New Mix 2(13.23%) and the lowest in New Mix 3 (4.54%).
- Deterioration of samples with different binders occurred differently in the conditioned and unconditioned situations and was inconsistent in the mixes.
- Based on the mix composition, the permeability result was different. New mix 2 showed the highest permeability, which was 168080 mm/h and the lowest permeability was observed in New mix 3. However, permeability does not differ very much for samples with different types and sourced binders. They ranged between 130082 mm/h to 130082mm/h.

8.2.4 Findings from Chapter 7 – Trial Section Construction

- The bearing capacity of subgrade soil for Site B was found to be higher than that of Site A. The calculated CBR for Site A was 18.2, whereas the CBR for Site B was 24.3.
- Indirect tensile strength was found higher in the mixes with a higher percentage of stone aggregates and binder, whereas found to be lower in the mixes with a higher percentage of rubber aggregates. Thus, New Mix 3 showed the highest tensile strength of 682.4 kPa, while

the Control Mix showed the lowest tensile strength of 299.3 kPa. Besides, the tensile strength of the mixes decreased with the increase of air voids in the samples.

- Moisture-induced damage was found to be lower in the mixes with a higher percentage of rubber aggregates and binders. Hence the highest retained tensile strength was found in the Control Mix (80%) and the lowest in the New Mix 2 (68%).
- All the PRP mixes showed good rutting resistance. Therefore, the highest rutting depth was found in the New Mix 2 (0.99 mm), whereas the lowest was found in the Control Mix (0.81 mm). Besides, the highest stripping-related abrasion was found in the Control Mix and the New Mix 1 (3%) and the lowest in the New Mix 2 (0%).
- The LWD results showed that the stiffness modulus differed for the same mixes at Site A and Site B. The possible reason could be the differences in the pavement's sub-grade soil types and their strength. Besides, all the mixes showed higher stiffness in the 2nd field test than the 1st since compaction occurred on the pavement after opening for traffic. However, after experiencing their first winter, a reduction in stiffness was observed for all mixes in the 3rd test.
- The BPT test revealed that a higher frictional value of PRP mixes was associated with a higher percentage of rubber aggregates and a lower percentage of binder in the mixes. Therefore, the Control Mix showed the highest BPN value (73 at Site A and 69 at Site B), whereas smaller values were found for New Mix 2 and New Mix 3. However, a reduction in BPN values was observed in the 2nd test than in the 1st since the sections were further compacted and polished after opening for traffic. However, surface ravelling and transported loose particles affected the frictional values in the 3rd test, increasing the BPN numbers.
- Initial rut depths on Site A for different mixes ranged from -7.0 mm to -8.7 mm, and the range was -5.8 mm to -10.7 mm for Site B. However, after fully opening for traffic, greater rut depths were found on each section due to the additional compaction under the wheel paths. These rut depths ranged from -22.5 mm to -26.0 mm for Site A and from -19.6 mm to -24.4 mm for Site B.
- The permeability of the PRP sections ranged from 28368 mm/h to 45605 mm/h, which is higher than the highest rainfall rate in Canada (298.8 mm/h). However, all the sections showed higher

permeability in the 2nd test except the New Mix 3. However, after the first winter, the permeability of Control Mix and New Mix 1 was found to be further increased at Site A, whereas the permeability of the New Mix 2 and the New Mix 3 was found to be decreased. Moreover, all the sections at Site B showed reduced permeability during the 3rd test.

- In the 1st and 2nd field tests, no visible surface distress was observed at Site A and Site B. However, insubstantial surface distresses were observed after the first winter (seven months after the construction), which included a slight loss of coarse aggregate, minor ravelling, small cracking and rutting.

8.3 Discussion

In today's world, where environmental crises are prevalent, researchers across disciplines are seeking low-impact solutions to tackle sustainability challenges. Pavement research is no exception, as it strives to find ways to reduce the environmental impact, maintain natural hydrological systems, and minimize surface runoff. To address these issues, permeable pavements have emerged as a promising solution. However, researchers are working to identify more efficient and effective permeable pavement options. In this quest, Porous Rubber Pavement has emerged as a viable solution for low-traffic areas in North America. This study aimed to improve the performance of PRP in the Canadian climate as a pavement surface material for a low-trafficked area by achieving the four research objectives.

The first objective of this research was to appraise the performance of existing Permeable Rubber Pavement (PRP) with respect to its design, construction, and field behaviour. To achieve this goal, a preliminary evaluation of two PRP sites situated in Stratford, ON and Kitchener, ON, was conducted. The Stratford site was a residential driveway with a 25 mm PRP layer over a 25 mm durisol block, while the Kitchener site had a commercial driveway with a 50 mm PRP surface layer over a 50 mm crushed stone layer. No hydrological design was considered for either location. Field evaluations were performed on these sites, which were between four and six years old, and yielded significant findings regarding the nature, performance, and concerning issues of PRP material. This assessment revealed that PRP's elastic modulus as a pavement material was significantly low, ranging between 33 MPa to 37 MPa. However, the PRP surface area's average infiltration rate was 30836 mm/h, significantly higher than Canada's highest rainfall rate. Moreover, surface ravelling was identified as the most visible form of distress on the PRP surface, with moderate to severe ravelling found throughout the study area. This preliminary investigation established a benchmark for mechanical properties and durability assessment

in the laboratory. Additionally, it emphasized the need to scrutinize load-bearing capacity and strength despite the material's very low elastic modulus. Furthermore, the evaluation directed attention to the significance of freeze-thaw resistance and durability against ravelling and abrasion, highlighting their importance in evaluating the PRP's long-term performance.

The second objective of this study was to evaluate the mechanical properties and durability of the PRP material using laboratory testing. The third objective was to investigate the performance of various new PRP mixes both in the laboratory and in the field. To achieve the second objective and the first part of the third objective, several laboratory tests were conducted, including indirect tensile, compressive strength, moisture-induced damage, permanent deformation, abrasion resistance, and permeability tests. Two experimental scenarios were investigated: one involved four new different mix compositions and a Control Mix, while the other looked at four mixes with different binders (aliphatic and aromatic).

The laboratory results indicated that the PRP materials exhibited flexible behaviour and low compressive strength, but they can carry more loads within the elastic region. The reason is that the deformation in the elastic region is recovered mostly after removing the load. On the contrary, a deformation that occurs in the plastic region is permanent. An increase in the percentage of stone aggregates and binders enhanced the compressive strength by 71.4% and indirect tensile strength by 70%. Furthermore, a higher percentage of rubber aggregates increased the retained tensile strength after conditioning with freeze-thaw cycles, and all mixes retained more than 73% of their original tensile strength, indicating excellent performance in cold climates with substantial temperature variations. All mixes showed good rutting resistance, less than 2.8 mm, and stripping-related abrasion between 2.6% to 0.1%. An increase in stone aggregates increased the abrasion loss by 51.3%, while an increased binder percentage improved abrasion resistance by 40.4%. The higher porosity and larger interconnected voids found in mixes with more stone aggregates, lower rubber aggregates and binders contributed to 24% higher permeability. Thus, a very high binder percentage must be avoided to prevent clogging of pores and foamification, while maintaining an adequate binder percentage is necessary to mitigate abrasion loss and ravelling.

The permeability of samples did not vary significantly due to the different types of the binder. However, samples with B3-aromatic binder failed after 4000 cycles, whereas B2-aliphatic showed 21.4% better performance withstanding permanent deformation. B3—aromatic binder was found to be

temperature sensitive after further investigation. Thus, it is recommended that the temperature sensitivity of polyurethane binders should be considered in cold regions that experience wide temperature variations to prevent failures at higher temperatures. Freeze-thaw conditioning affected the samples with different binders inconsistently, with the highest abrasion loss found in unconditioned samples with B1-aromatic binder (9.94%), while conditioned samples with B2-aromatic showed a very high abrasion loss of 15.37%.

The second part of the third objective of this study aimed to investigate the performance of various new PRP mixes in the field. This was accomplished by constructing and evaluating two trial sections, a parking lot and a driveway to the loading and unloading dock, located in close proximity to each other on a commercial site. Three newly developed mixes and the Control Mix were utilized in the trial section. The performance of PRP pavements was mostly influenced by material composition, site geometry, and existing subgrade conditions. Field evaluation revealed that mixes exhibited higher stiffness and lower rut depth as soil bearing capacity increased, with the initial elastic modulus of PRPs ranging between 28 MPa and 59 MPa. Although laboratory testing indicated that mixes with a higher percentage of stone aggregate and binder demonstrated higher compressive strength, in the field, mixes with a higher percentage of rubber aggregates and binder were more compacted after opening for traffic, resulting in higher stiffness modulus.

Initial frictional values for all mixes ranged from 58 BPN to 73 BPN, and these values increased during the third test (after seven months of construction) due to surface ravelling and the transport of loose particles. Although mixes with a higher percentage of binder demonstrated good ravelling resistance in the laboratory test, on the site, these mixes exhibited lower initial frictional values. Over time, however, changes in frictional values mostly depended on site conditions and traffic patterns. Rut depth increased by 56.1% to 73% under the wheel paths after opening for traffic, affecting all PRP mixes.

All PRP mixes exhibited excellent initial permeability, ranging from 28368 mm/h to 45605 mm/h, which changed over time depending on material composition and site conditions. Mixes with a higher percentage of binder, clogged pores and exhibited lower permeability in the laboratory testing. In the field, mixes with a higher binder percentage were also more compacted under wheel loading, leading to reduced permeability. Besides composition, site surrounding conditions, site slope, and environmental conditions had a significant impact on permeability changes over time.

The fourth objective of this research aimed to develop guidelines for using PRPs as pavement surface material in the Canadian climate. Detailed recommendations are provided in the recommendation section based on laboratory testing and field evaluation. The primary mechanical performance analysis results indicate that PRP material can be a viable alternative to traditional pavements for low-traffic areas. The use of PRP material in these settings offers significant environmental, safety, and sustainability benefits. Additionally, the PRP material exhibited good resistance to moisture-induced damage in saturated conditions, suggesting its potential for performing well in harsh environmental conditions, including freeze-thaw cycles with substantial temperature fluctuations in cold climates.

8.4 Guidelines and Recommendations

8.4.1 Laboratory Sample Preparation and Site Construction

The mixing time of PRP mixes should be limited to 90 seconds in the laboratory and 180 seconds on the construction site after adding the binder to the dry components. Overmixing of PRP mixes can create fomification of binder and draw moisture. This can also initiate the curing process more quickly than desired, affecting the final properties of the pavement.

Although PRPs have self-compacting properties, external vibration is required to enhance the material bonding and reduce ravelling. Insufficient pavement compaction can result in a weaker bond between the aggregate and binder and loss of material from the pavement's surface. Therefore, external vibration is recommended to improve the pavement material’s bonding and reduce the occurrence of ravelling.

Since the construction process of PRP is still not fully mechanized, the initial roughness of the pavement can be reduced through good workmanship. The pavement quality depends largely on the workers’ skills involved in the construction process. Hence, good workmanship is crucial to minimizing the PRP’s initial roughness.

8.4.2 Material Selection and PRP’s Applicability

In regions with cold climates and significant temperature variations, it is crucial to consider the temperature sensitivity of polyurethane binders. Some binders may fail when exposed to higher temperatures, affecting PRPs’ performance and durability. Therefore, a careful evaluation of the suitability of polyurethane binders in such environments is necessary.

PRP has exhibited remarkable resistance to moisture-induced damage in saturated conditions. This makes it a practical solution for areas where permeable pavement is required and where the risk of saturation can compromise pavement performance. Hence, PRP is a viable option for improving the durability and resilience of pavements in such settings.

8.4.3 Construction Site Evaluation

In order to achieve the expected stiffness and reduce rutting in a PRP surface, it is essential to undertake a site-specific structural design that takes into account the subgrade and loading conditions. This involves a thorough evaluation of the site's soil properties, traffic characteristics, and anticipated environmental stresses, which can affect the surface's mechanical properties and structural integrity.

The site geometry and surrounding conditions ply a crucial role in the performance and longevity of the PRP surface. Therefore, a critical evaluation of the site's topography, drainage patterns, and adjacent land uses is necessary to identify potential sources of surface ravelling by transported particles, permeability and durability issues.

8.4.4 Mixes for Optimum Performance

Based on this study's findings, it is recommended that the material composition, site geometry and existing subgrade conditions should be considered when designing and constructing with Porous Rubber Pavement (PRP). While a higher percentage of rubber aggregates may improve resistance to moisture-induced damage, it should be noted that such mixes also exhibit increased levels of stripping-related abrasion and ravelling. It is also advised to maintain adequate binder percentages in the PRP mix to mitigate the exacerbation of abrasion loss and ravelling. The most effective PRP mix composition is one with a higher percentage of stone aggregates and binders. However, from the new mixes tested in this research, New Mix 3 was found to be the most optimum PRP mix considering the mechanical properties, durability and cost. Thus, this can be recommended for the commercial parking lot.

Table 49 Recommended mix for commercial parking lot

Recommended Mix	A - Stone Aggregate, R - Rubber Aggregate, B – B1—aromatic Polyurethane Binder	Air voids
New Mix 3	A - 55%, R - 33%, B - 12%	Within 24%-38%

8.4.5 Cost Comparison for Different Material

An analysis was conducted to determine the cost of different PRP mixes per square meter. Among all the components in the mixes, stone aggregates were the least expensive, whereas binders were the most costly material. Besides, the price of the aliphatic binder was higher than the aromatic binder. Hence, when the binder percentages increased in the mixes, the price per square meter of PRP mixes was increased. This price was further increased when an aliphatic binder was used instead of an aromatic binder. Cost analysis showed that the most expensive mix was the New Mix 4, and the least expensive one was the Control Mix. A cost comparison is shown in Table 50.

Table 50 Cost comparison of different mixes

Type of mixes (composition)	Weight for 1m^2 (kg)	Stone Aggregate (kg) (A)	Rubber Aggregate (kg) (R)	Binder (kg)(B)	Black rubber and Reg. binder, CAD	Black rubber and Ali. Binder, CAD
Control Mix	48.3	21.9	21.9	4.6	**59.2**	**96.9**
New Mix 1	66.5	36.6	25.0	5.0	69.5	110.5
New Mix 2	77.2	57.9	13.5	5.8	77.1	124.7
New Mix 3	62.5	34.4	20.6	7.5	87.5	149.1
New Mix 4	75.7	56.8	9.8	9.1	**102.5**	**177.1**

8.4.6 Recommended Structural and Hydrological Design for PRP

In current practice, 50 mm (2") of Porous Rubber Pavement is placed over a 100 mm (4") base of 19 mm (3/4") angular crushed clear stone, as shown in Figure 103 below. However, considering the use

and soil types, in some cases, 150 mm (6") of the base is prepared instead of 100 mm directly on top of the subgrade, and a small roller compactor is used to pack the aggregates.

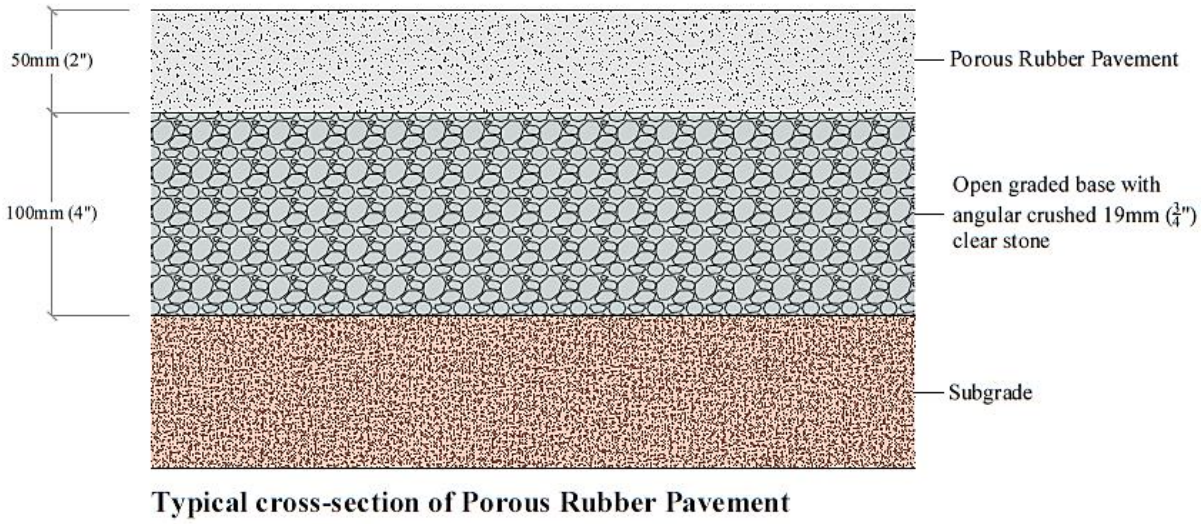

Figure 103 Typical cross-section of PRP

However, with the changes in demand and regulations, sometimes it requires to keep the infiltrated water within the site boundary instead of draining it to the nearest natural water reservoir. In that case, one of the following options needs to be considered for the structural and hydrological design of the Porous Rubber Pavement. The structural design ensures the pavement's load-bearing capacity without failing it, whereas the hydrological design ensures efficient water infiltration and drainage. Therefore, the following drawings (Figure 104 to Figure 107) are adopted and modified from existing works of literature (Drake; Bradford, et al., 2012, EPA, 1999, Hall and Schwartz, 2018, Schaus, 2007, Hansen, 2008, Hein, 2014, Smith, 2006).

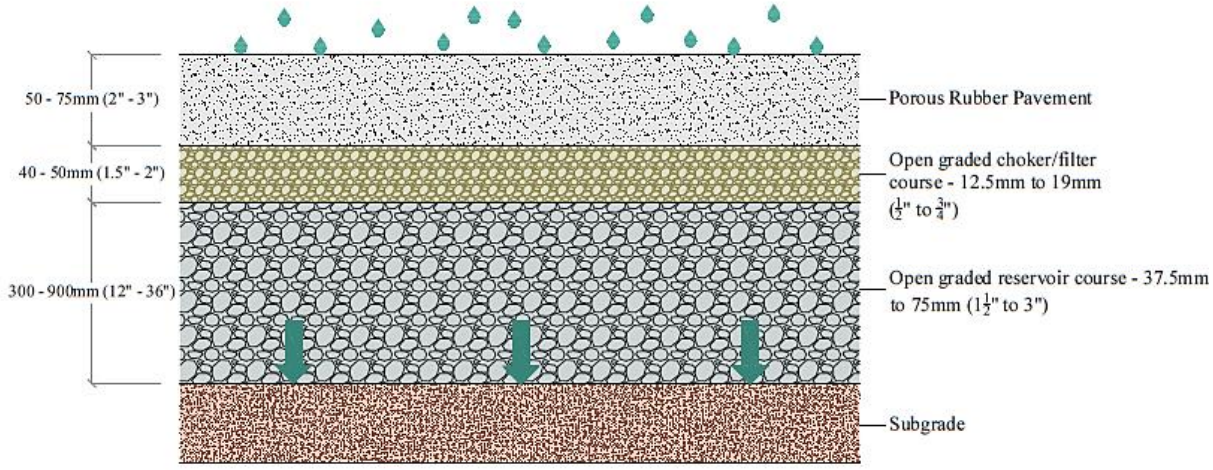

Figure 104 Typical cross-section of PRP with full infiltration to subgrade

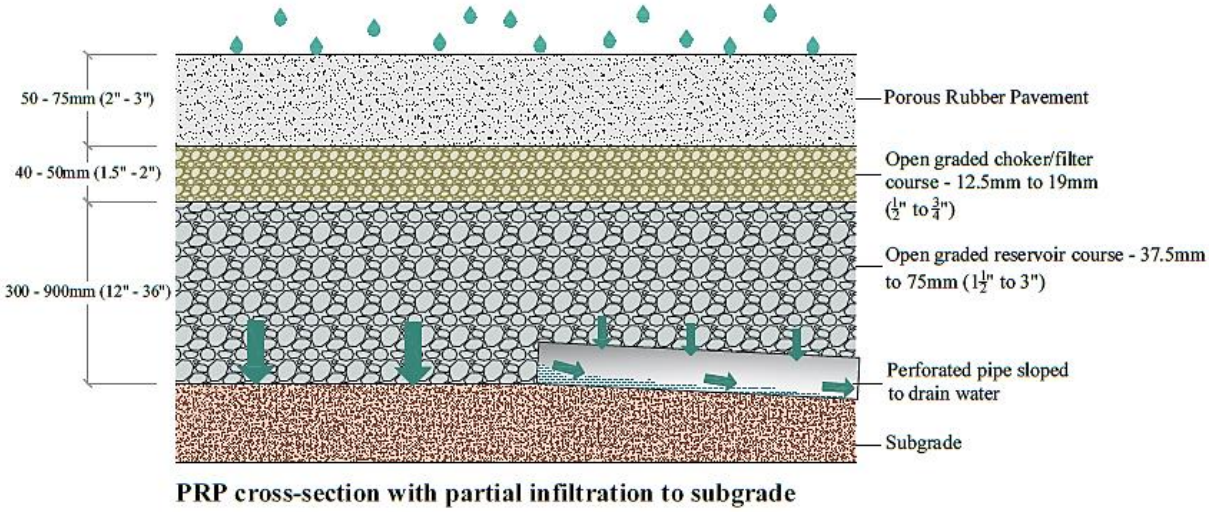

Figure 105 Typical cross-section of PRP with partial infiltration to subgrade

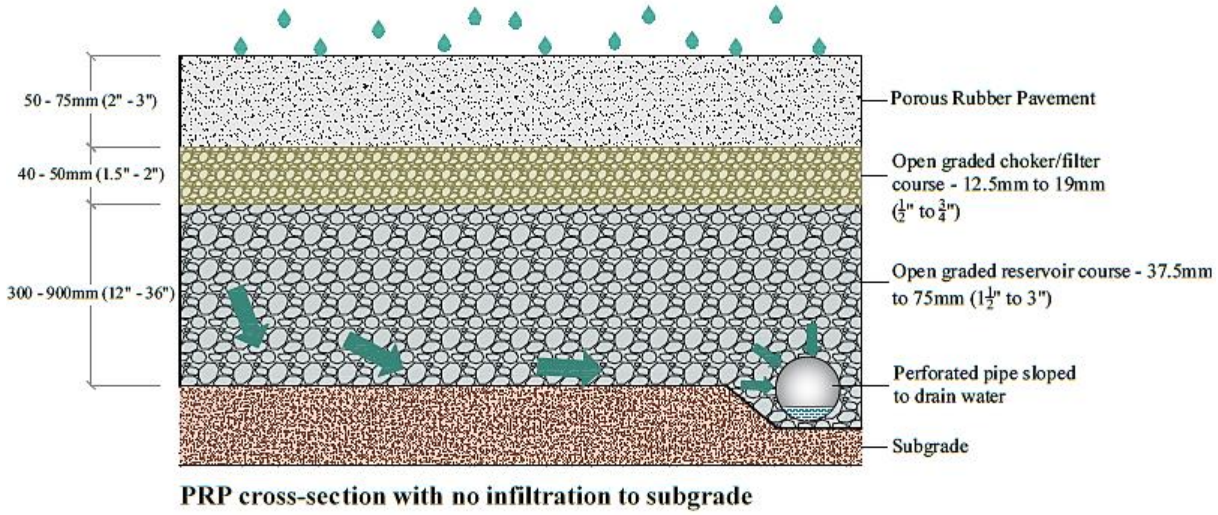

Figure 106 Typical cross-section of PRP with no infiltration to subgrade

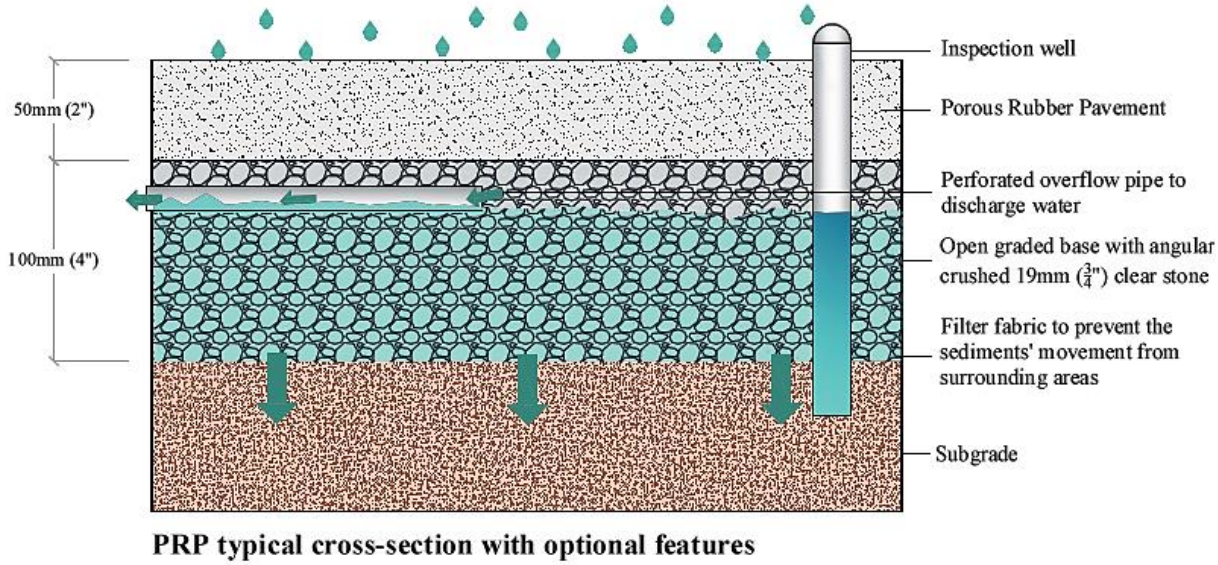

Figure 107 Typical cross-section of PRP with optional features

Permeable pavement should not be placed in those locations where the groundwater table is less than 0.6m (2') from the soil's surface (Smith, 2006, Hein, 2014, Hansen, 2008). Besides, hydrological design can be three types: full infiltration, partial infiltration and no infiltration. It is expected that water stores in the reservoir course will be drained or infiltrated through the subgrade within 12 to 72 hours.

However, the most recommended time is 24 hours (EPA, 1999). Drainage and no infiltration options are usually used in those areas where the soil has lower permeability with higher rainfall incidents.

However, if the soil infiltration rate is a minimum of 12 mm/h (0.5inch/h), a full infiltration design could be chosen for those locations (EPA, 1999, Hein, 2014, Hansen, 2008). Depending on the infiltration and rainfall rate, the reservoir course can be 300 mm to 900 mm (12" to 36") thick and prepared with 37.5 mm to 75 mm (1½" to 3") clear crushed stone. On top of the reservoir course, the choker course could be 40 mm to 50 mm thick and constructed with 12.5 mm to 19 mm (1/2" to ¾") clear crushed stone (EPA, 1999, Schaus, 2007). This layer filters the water before infiltrating into the ground. In the cases of no infiltration and to prevent the sediment's movement from surrounding areas, the impermeable liner of filter fabric can be used to separate the soil from the base and subbase (Hansen, 2008, Hein, 2014, Smith, 2006).

8.5 Significant Contributions

This research investigated PRP as a potential permeable pavement alternative in the Canadian climate. Due to its recent inception in this climate, only limited studies are available on this material. As a consequence, its performance and properties are not fully explored for this region. Besides, no scholarly documents have been identified that work for developing different PRP mixes to investigate its strength range, failure criteria, moisture-induced damage and durability, as well as its feasibility in Canada.

Details of research outcomes are explained in Chapter 4 to Chapter 7. The followings are the major contributions:

1. This research has devised a method for laboratory sample preparation technique, along with an air void calculation methodology, to analyze the PRP materials.
2. The PRP's field response has been quantified by conducting a preliminary field investigation and constructing trial sections.
3. Mechanical properties of the PRPs have been characterized by subjecting the Control and other mixes to testing.
4. The durability of PRPs was evaluated through accelerated permanent deformation and freeze-thaw conditioning.

5. The impacts of varying percentages of different components and binder types in the PRP mixes have been measured and analyzed.
6. The study has identified several new mixes that exhibit superior performance in the Canadian climate.
7. Comprehensive guidelines and recommendations have been formulated for using PRPs in various conditions as an effective alternative to existing permeable pavement systems.
8. Practical knowledge about PRP material paving and its real-world performance has been captured through both field and laboratory testing.

8.6 Future work

Porous Rubber Pavement is a potential permeable pavement material that can contribute to urban stormwater management along with its sustainable material reuse. Its widespread use in Canada should be encouraged as a low-impact material. However, further research on PRP could explore this material's complete performance and properties. Some of the future research could be conducted on:

- Additional tests could be planned to get a clearer idea about the properties of PRPs. For example, dynamic modulus for characterization of its property.
- Appropriate laboratory test protocol should be established for this type of pavement material.
- Life Cycle Assessment could be done to quantify PRPs' contribution toward a sustainable environment.
- A performance prediction model could be developed with more detailed information on its properties.
- A thorough analysis should be conducted for the hydrological behavior of PRP pavements in cold climates.

References

AASHTO T 166, 2013. Bulk Specific Gravity (Gmb) of Compacted Hot Mix Asphalt (HMA) Using Saturated Surface- Dry Specimens. T 166-13), Austin, TX: American Association of State Highway and Transportation Officials.

AASHTO T 209-11, 2011. Standard Method of Test for Theoretical Maximum Specific Gravity (G mm) and Density of Asphalt Mixtures. T 209-11), USA: American Association of State Highway and Transportation Officials.

AASHTO T 27-14, 2018. Standard Method of Test for Sieve Analysis of Fine and Coarse Aggregates. T 27-14), AASHTO.

AASHTO T 283-07, 2011. Resistance of Compacted Hot Mix Asphalt (HMA) to Moisture-Induced Damage. T 283-07), AASHTO.

AASHTO T 322-07, 2016. Standard Method of Test for Determining the Creep Compliance and Strength of Hot Mix Asphalt (HMA) Using the Indirect Tensile Test Device. T 322-07), AASHTO.

AASHTO T 324-17, 2017. Standard Method of Test for Hamburg Wheel-Track Testing of Compacted Asphalt Mixtures. T 324-17), AASHTO.

Akindoyo, J. O., Beg, M. D. H., Ghazali, S., Islam, M. R., et al., 2016. Polyurethane types, synthesis and applications – a review. *RSC Advances, the Royal Society of Chemistry,* 6 pp. 114453-114482 Available at: 10.1039/c6ra14525f .

Almeida Júnior, A. F. D., Battistelle, R. A., Bezerra, B. S. and Castro, R. D. 2012. Use of scrap tire rubber in place of SBS in modified asphalt as an environmentally correct alternative for Brazil. *Journal of Cleaner Production,* 33 pp. 236-238 Available at: 10.1016/j.jclepro.2012.03.039 .

ASTM - D1883, 2016. Standard Test Method for California Bearing Ratio (CBR) of Laboratory-Compacted Soils. ASTM - D1883 − 16), 100 Barr Harbor Drive, PO Box C700, West Conshohocken, PA 19428-2959. United States: ASTM International.

ASTM - D698, 2012. Standard Test Methods for Laboratory Compaction Characteristics of Soil Using Standard Effort (12 400 ft-lbf/ft3 (600 kN-m/m3)). ASTM - D698 - 12), 100 Barr Harbor Drive, PO Box C700, West Conshohocken, PA 19428-2959. United States: ASTM International.

ASTM C127, 2015. Standard Test Method for Relative Density (Specific Gravity) and Absorption of Coarse Aggregate. ASTM C127 - 15), West Conshohocken, PA 19428-2959. United States: ASTM International.

ASTM C1701/C1701M−17a, 2017. Standard Test Method for Infiltration Rate of In Place Pervious Concrete. C1701/C1701M−17a), ASTM.

ASTM C1747/C1747M − 13, 2013. Standard Test Method for Determining Potential Resistance to Degradation of Pervious Concrete by Impact and Abrasion. C1747/C1747M − 13), West Conshohocken, PA 19428-2959. United States: ASTM International.

ASTM D1074 - 17, 2017. Standard Test Method for Compressive Strength of Bituminous Mixtures. D1074 - 17), ASTM.

ASTM D6928−17, 2017. Resistance of Coarse Aggregate to Degradation by Abrasion in the Micro-Deval Apparatus. D6928−17), ASTM.

ASTM D7063/D7063M, 2018. Standard Test Method for Effective Porosity and Effective Air Voids of Compacted Asphalt Mixture Samples. D7063/D7063M − 18), West Conshohocken, PA: ASTM International.

ASTM D7064/D7064M, 2013. Standard Practice for Open-Graded Friction Course (OGFC) Mix Design. D7064/D7064M − 08 (Reapproved 2013)), West Conshohocken, PA 19428-2959. United States: ASTM.

ASTM E303−93, 2018. Standard Test Method for Measuring Surface Frictional Properties Using the British Pendulum Tester. West Conshohocken, PA: ASTM International.

Bindu, C. S., 2012. Influence of additives on the characteristics of stone matrix asphalt. PhD.

Carbone, M., Mancuso, A. and Piro, P., eds., 2014. Porous Pavement Quality Modelling, Anonymous [16th Conference on Water Distribution System Analysis, WDSA 2014]. pp. 758-766.

Chairuddin, F., Tjaronge, M. W., Ramli, M. and Patanduk, J. June 2016. Compressive Strength of Permeable Asphalt Pavement Using Domato Stone (Quarzite Dolomite) and Buton Natural Asphalt (BNA) Blend. *IACSIT International Journal of Engineering and Technology*, 8 (3), pp. 183-186 Available at: DOI: 10.7763/IJET.2016.V8.881 .

Chong, G. J., Phang, W. A. and Wrong, G. A., 2016. Manual for condition rating of flexible pavements - Distress manifestation. SP - 024), ON, Canada: Ministry of Transportation, Highway Standards Branch, Material Engineering and Research Office.

Chu, L., Tang, B. and Fwa, T. F. 2018. Evaluation of functional characteristics of laboratory mix design of porous pavement materials. *Construction and Building Materials*, 191 pp. 281-289 .

Cooley, L. A., Brown, R. E. and Watson, D. E., 2000. Evaluation of OGFC Mixtures Containing Cellulose Fibers. NCAT - 2000-05), Auburn, Alabama: National Center for Asphalt Technology of Auburn University.

Drake, J., Bradford, A., Seters, T. V. and MacMillan, G., 2012. Evaluation of Permeable Pavements in Cold Climates. Final Report), Downsview, Ontario: Toronto and Region Conservation Authority.

Elhakim, A. F., Elbaz, K. and Amer, M. I. 2014. The use of light weight deflectometer for in situ evaluation of sand degree of compaction. *Housing and Building National Research Center,* 10 pp. 298-307 .

Environment Canada, 2019. Engineering Climate Dataset, IDF - Version 1.00. Available at: ftp://client_climate@ftp.tor.ec.gc.ca/Pub/Engineering_Climate_Dataset/IDF/archive/IDF_v1.00/ .

EPA, 1999. Storm Water Technology Fact Sheet - Porous Pavement. EPA 832-F-99-023), Washington, D.C: Office of Water, Environmental Protection Agency.

Google Maps, 2021. 1400 Greenwood Hill Rd, Wellesley, ON N0B 2T0. Available at: https://www.google.com/maps/place/1400+Greenwood+Hill+Rd,+Wellesley,+ON+N0B+2T0/@43.8449203,-81.4463225,9z/data=!4m13!1m7!3m6!1s0x882bfe907aebfedd:0x86c367507c11398!2s1400+Greenwood+Hill+Rd,+Wellesley,+ON+N0B+2T0!3b1!8m2!3d43.4829232!4d-80.75249!3m4!1s0x882bfe907aebfedd:0x86c367507c11398!8m2!3d43.4829232!4d-80.75249 .

Goubert, L. (unpublished) 24th August, 2015. Introduction to PERS(UADE). Seminar Presentation.

Goubert, L. and Sandberg, U., 2016. PERSUADE Final Technical Report. Deliverable D8.7), PERSUADE.

Hagos, E. T., 2008. The Effect of Aging on Binder Properties of Porous Asphalt Concrete. Ph. D.

Hall, K. D. and Schwartz, C. W. 2018. Development of Structural Design Guidelines for Porous Asphalt Pavement. *Transportation Research Record,* 2672 (40), pp. 197-206 Available at: 10.1177/0361198118758335 .

Hansen, K., 2008. Porous Asphalt Pavements for Stormwater Management. 131), Lanham, Maryland: National Asphalt Pavement Association (NAPA).

Hein, D. K., ed., 2014. Permeable Pavement Design and Construction Case Studies in North America, Anonymous [Transportation Association of Canada 2014 Annual Meeting]. Montreal, Quebec, .

Hein, D. K. and Smith, D. R., eds., 2016. How Should You Be Designing Your Permeable Pavements? - New ASCE Standard, Anonymous [StormCon Conference 2016]. Indianspolis, IN, .

Henderson, V., 2012. Evaluation of the Performance of Pervious Concrete Pavement in the Canadian Climate. Doctor of Philosophy.

Huang, B., Wu, H., Shu, X. and Burdette, E. G. 2010. Laboratory evaluation of permeability and strength of polymer-modified pervious concrete. *Construction and Building Materials,* 24 pp. 818-823 Available at: 10.1016/j.conbuildmat.2009.10.025 .

Inglett, P. W., Reddy, K. R. and Corstanje, R. 2005. Anaerobic Soils. *Elsevier,* .

InstroTek, 2011. CoreLok - Asphalt Density Measurement System. v.23), Raleigh, NC: Instrotek, Incorporated.

Ionescu, M., 2016. Chemistry and Technology of Polyols for Polyurethanes. 2nd. Shawbury, Shrewsbury, Shropshire, SY4 4NR, UK: Smithers Rapra Technology Ltd.

Iwanowski, P., Blacha, K. and Wesołowski, M. 2018. Review of modern methods for continuous friction measurement on airfield pavements. *IOP Conference Series: Materials Science and Engineering -Resilient and Safe Road Infrastructure,* 567 (012002), Available at: 10.1088/1757-899X/356/1/012002 .

Kabir, T., Oyeyi, A. G., Al-Bayati, H. and Tighe, S., eds., 2020a. Performance evaluation of Porous Rubber Pavement (PRP) in the Canadian climate, Anonymous [TAC Conference & Exhibition]. Vancouver, Canada, .

Kabir, T., Oyeyi, A. G., Al-Bayati, H. and Tighe, S., eds., 2020b. Performance evaluation of Porous Rubber Pavement (PRP) in the Canadian climate, Anonymous [2020 TAC Conference & Exhibition]. Online, .

Kalman, B. and Biligiri, K., 2013. Laboratory assessment of PERS. WP 2 - Deliverable D2.2), Sweden: Swedish Road and Transport Research Institute (VTI).

Kalman, B., Biligiri, K. P. and Sandberg, U., eds., 2011. Project PERSUADE: Optimization of poroelastic road surfaces in the laboratory, Anonymous [Inter.Noise 2011 - September 4-7]. Osaka, Japan, .

Kalman, B., Leprince, L., Lenart, S., Bańkowski, W., et al., 2015. Revised mix report: PoroElastic Road SUrface: an innovation to Avoid Damages to the Environment. Deliverable D2.6), European Commission - DG Research.

Kandhal, P. S., 2002. Design, Construction, and Maintenance of Open-Graded Asphalt Friction Courses. 115), Lanham, Maryland 20706-4407: National Asphalt Pavement Association.

Karamihas, S. M., 2005. Critical Profiler Accuracy Requirements. UMTRI-2005-24), Michigan: The University of Michigan Transportation Research Institute.

Kayhanian, M., Li, H., Harvey, J. T. and Liang, X. 2019. Application of permeable pavements in highways for stormwater runoff management and pollution prevention: California research experiences. *International Journal of Transportation Science and Technology,* 8 pp. 358-372 Available at: 10.1016/j.ijtst.2019.01.001 .

Krebs, M., Heider, R., Schillings, K. and Gansow, M., 1999. Moisture Curing Polyurethane Hot-melt Adhesive . Henkel Kommanditgesellschaft auf Aktien 524/590; 528/61; 528/65; 528/66; 528/76; 528/83; 156/331.4.

Kritsonis, T., 2018. Re-tired and put back to work. Available at: https://www.theglobeandmail.com/globe-drive/news/industry-news/re-tired-and-put-back-to-work/article18890884/ .

Lian, C. and Zhuge, Y. 2010. Optimum mix design of enhanced permeable concrete – An experimental investigation. *Construction and Building Materials,* 24 pp. 2664-2671 Available at: 10.1016/j.conbuildmat.2010.04.057 .

Lu, G., 2019. Permeable pavements: hydraulic and mechanical investigations. Doctoral Thesis. Germany: Aachener Mitteilungen Straßenwesen, Erd- und Tunnelbau.

Lu, G., Renken, L., Li, T., Wang, D., et al., 2019. Experimental study on the polyurethane-bound pervious mixtures in the application of permeable pavements. *Construction and Building Materials,* 202 pp. 838-850 Available at: 10.1016/j.conbuildmat.2019.01.051 .

Lu, G., Wang, Z., Liu, P., Wang, D., et al., 2020. Investigation of the Hydraulic Properties of Pervious Pavement Mixtures: Characterization of Darcy and Non-Darcy Flow Based on Pore Microstructures. *Journal of Transportation Engineering, Part B: Pavements,* 146 (2) (04020012), .

Mallick, R. B. and El-Korchi, T. eds., 2018. Pavement Engineering - Principles and Practice. Third. Boca Raton, FL: CRC Press, Taylor & Francis Group.

Mbanaso, F. U., Coupe, S. J., Charlesworth, S. M. and Nnadi, E. O. 2013. Laboratory-based experiments to investigate the impact of glyphosate-containing herbicide on pollution attenuation and biodegradation in a model pervious paving system. *Chemosphere,* 90 pp. 737-746 Available at: 10.1016/j.chemosphere.2012.09.058 .

Micor, 2020. Micor Recycling Ltd. Available at: http://www.micorrecycling.com/knowledge.php .

Mo, L., Huurman, M., Wu, S. and Molenaar, A. A. A. 2009. Ravelling investigation of porous asphalt concrete based on fatigue characteristics of bitumen–stone adhesion and mortar. *Materials and Design,* 30 pp. 170-179 Available at: 10.1016/j.matdes.2008.04.031 .

Mohammadinia, A., Disfani, M. M., Narsilio, G. A. and Aye, L. 2018. Mechanical behaviour and load bearing mechanism of high porosity permeable pavements utilizing recycled tire aggregates. *Construction and Building Materials,* 168 pp. 794-804 Available at: 10.1016/j.conbuildmat.2018.02.179 .

Montes, F., Valavala, S. and Haselbach, L. M., 2009. Test Method for Porosity Measurements of Portland Cement Pervious Concrete . T-040R), Mississauga, ON, Canada: Concrete Ontario (Ready Mixed Concrete Association of Ontario).

Mugdha, P., How to Design Bituminous Mixes: Steps and Methods . Available at: https://www.engineeringenotes.com/transportation-engineering/highway-materials/how-to-design-bituminous-mixes-steps-and-methods-with-mix-formula-highway-materials/48578 [Accessed 2022].

Multipurpose Surface Profiler Operating Manual, 2014. SurPRO 3500. Revision 8), Cherry Systems Research.

Nazef, A., Mraz, A., Scott, S. and Whitaker, J., 2008. Evaluation of Surpro as a Reference Device For High-Speed Inertial Profilers. FL/DOT/SMO/08-512), FL: Florida Department of Transportation (FDOT).

Novalynx Corporation, 2009. Instructional Manual for Model 260-2501-A & 260-2501M-A Tipping Bucket Rain Guage. Grass Valley, CA: Novalynx Corporation. Available at: www.novalynx.com [Accessed March 29, 2023].

NRMCA, 2004. Freeze Thaw Resistance of Pervious Concrete . Silver Spring, MD: National Ready Mixed Concrete Association.

Pavement Tools Consortium, 2019. Pavement Interactive - Reference Desk. Available at: https://www.pavementinteractive.org/reference-desk .

Persuade, 2015. PoroElastic Road SUrface: an innovation to Avoid Damages to the Environmen. Available at: http://persuade.fehrl.org/ .

Pervious Pavement, Engineering Properties. Available at: https://www.perviouspavement.org/engineering.html#:~:text=In%20the%20laboratory%2C%20pervious%20concrete,2500%20psi%20(17%20MPa) .

Pickel, D. J., 2018. Precast Concrete Inlay Panels: Rehabilitation Strategy for High-Volume Highways in Ontario. Doctor of Philosophy in Civil Engineering.

Pierard, N., Kalman, B., Biligiri, K., Cesbron, J., et al., 2013. Accelerated loading tests of PERS. Deliverable D2.3), PERSUADE.

Porous Pave Inc, 2019. Porous Pave.

Porous Pave Inc., 2017. Porous Pave. Grant, MI: Porous Pave Inc.

Rubberway, 2020. Flexible, porous rubber pavements. Available at: https://www.rubberway.com/ .

Safety Direct America, 2019. COF vs. Pendulum Test Value. Available at: https://safetydirectamerica.com/coefficient-friction-vs-pendulum-test-value/ .

Saito, K. and et al 1996. Development of Portable Tester for Measuring Skid Resistance and Its Speed Dependency on Pavement Surfaces. *Transportation Research Record: Journal of the Transportation Research Board,* 1536 pp. 45-51 .

Sandberg, U. (unpublished) August 24, 2015. PERS – A Historical Review . Seminar Presentation.

Sandberg, U. and Ejsmont, J. A., 2002. Tyre/Road Noise Reference Book. Kisa, Sweden: Informex.

Sandberg, U., Goubert, L., Biligiri, K. P. and Kalman, B., 2010. State-of-the-Art regarding poroelastic road surfaces. Deliverable D8.1), PoroElastic Road SUrface: an innovation to Avoid Damages to the Environment.

Sarsys-ASFT, 2019. T2GO Friction Tester. Available at: https://www.sarsys-asft.com/t2go .

Sayers, M. W. and Karamihas, S. M., 1998. The Little Book of Profiling - The Basic Information about measuring and Interpreting Road Profiles. Michigan: University of Michigan.

Schaus, L. K., 2007. Porous Asphalt Pavement Designs: Proactive Design for Cold Climate Use. MSc. Waterloo, ON, Canada: Waterloo University.

Scholz, M. and Grabowiecki, P. 2007. Review of permeable pavement systems. *Building and Environment,* 42 pp. 3830-3836 .

Schwartz, C., 2020. Porous Pavement Design with PAVEXpress. Available at: https://www.pavexpressdesign.com/ .

Singh, S., Nimmo, W., Gibbs, B. M. and Williams, P. T. 2009. Waste tyre rubber as a secondary fuel for power plants. *Fuel*, 88 pp. 2473-2480 Available at: 10.1016/j.fuel.2009.02.026 .

Smith, D. R., 2006. Permeable Interlocking Concrete Pavements - Selection, Design, Construction, Maintenance. 3rd. Washington, DC: Interlocking Concrete Pavement Institute (ICPI).

Soft-Surfaces, 2020. Moisture Cure Polyurethane Binder. Available at: https://www.softsurfaces.co.uk/blog/moisture-cure-polyurethane-binders/ .

Stempihar, J. J., Pourshams-Manzouri, T., Kaloush, K. E. and Rodezno, M. C. 2012. Porous Asphalt Pavement Temperature Effects for Urban Heat Island Analysis . *Transportation Research Record: Journal of the Transportation Research Board*, 2293 pp. 123-130 Available at: 10.3141/2293-15 .

Sun, W., Lu, G., Ye, C., Chen, S., et al., 2018. The State of the Art: Application of Green Technology in Sustainable Pavement . *Advances in Materials Science and Engineering,* 2018 Available at: 10.1155/2018/9760464 .

Szycher, M., 2013. Szycher'S handbook of PolyurethaneS. 2nd Edition. Boca Raton, FL: CRC Press, Taylor & Francis Group.

Thelen, E. and Howe, L. F., 1978. Porous Pavement. Philadelphia, Pennsylvania: The Franklin Institute Press.

Törzs, T., Lu, G., Monteiro, A. O., Wang, D., et al., 2019. Hydraulic properties of polyurethane-bound permeable pavement materials considering unsaturated flow. *Construction and Building Materials,* 212 pp. 422-430 Available at: 10.1016/j.conbuildmat.2019.03.201 .

USDA - NRCS, 2012. Part 631 - National Engineering Handbook - Chapter 3 - Engineering Classification of Earth Materials . Part 631 - National Engineering Handbook - Chapter 3 - Engineering Classification of Earth Materials . 2012. National Engineering Handbook. United States Department of Agriculture, Natural Resources Conservation Service. pp. 3-1-3-20.

Valeo, C. and Gupta, R. 2018. Determining Surface Infiltration Rate of Permeable Pavements with Digital Imaging. *Water,* 10 (133), Available at: 10.3390/w10020133 .

Wakefield, A., 2020. Four tips for controlling asphalt mix designs in the lab and field. *Asphalt - the Magazine of the Asphalt Institute,* 35 pp. 22-27 .

Wang, D., Liu, P., Leng, Z., Leng, C., et al., 2017. Suitability of PoroElastic Road Surface (PERS) for urban roads in cold regions: Mechanical and functional performance assessment. *Journal of Cleaner Production,* 165 pp. 1340-1350 .

Wang, D., Schacht, A., Leng, Z., Leng, C., et al., 2017. Effects of material composition on mechanical and acoustic performance of poroelastic road surface (PERS). *Construction and Building Materials,* 135 pp. 352-360 .

Xu, H., Guo, W. and Tan, Y. 2015a. Internal structure evolution of asphalt mixtures during freeze–thaw cycles. *Materials and Design,* 86 pp. 436-446 Available at: 10.1016/j.matdes.2015.07.073 .

Xu, H., Guo, W. and Tan, Y. 2015b. Permeability of asphalt mixtures exposed to freeze–thaw cycles. *Cold Regions Science and Technology,* 123 pp. 99-106 Available at: 10.1016/j.coldregions.2015.12.001 .

Appendix A

Regression Statistics for Compressive Strength Vs Air Voids

SUMMARY OUTPUT FOR COMPRESSIVE STRENGTH VS AIR VOID OF PRP MIXES

Regression Statistics	
Multiple R	0.955471863
R Square	0.91292648
Adjusted R Square	0.883901974
Standard Error	0.476393734
Observations	5

ANOVA

	df	*SS*	*MS*	*F*	*Significance F*
Regression	1	7.138435502	7.138435502	31.4536434	0.011203751
Residual	3	0.680852969	0.22695099		
Total	4	7.819288471			

	Coefficients	*Standard Error*	*t Stat*	*P-value*	*Lower 95%*	*Upper 95%*	*Lower 95.0%*	*Upper 95.0%*
Intercept	7.780616847	0.896673617	8.677200594	0.003220678	4.927001206	10.63423249	4.927001206	10.63423249
X Variable 1	-0.169612933	0.030242904	-5.608354786	0.011203751	-0.26585935	-0.073366516	-0.26585935	-0.073366516

PROBABILITY OUTPUT

Percentile	*Y*
10	1.176385706
30	1.636278754
50	3.438502674
70	4.027798998
90	4.1998557

Appendix B

Regression Statistics for Indirect Tensile Strength Vs Air Voids

SUMMARY OUTPUT FOR ITS VS AIR VOIDS								
Regression Statistics								
Multiple R	0.985249236							
R Square	0.970716057							
Adjusted R Square	0.960954742							
Standard Error	39.09655186							
Observations	5							
ANOVA								
	df	*SS*	*MS*	*F*	*Significance F*			
Regression	1	152006.0332	152006.0332	99.44522006	0.002145815			
Residual	3	4585.621103	1528.540368					
Total	4	156591.6543						
	Coefficients	*Standard Error*	*t Stat*	*P-value*	*Lower 95%*	*Upper 95%*	*Lower 95.0%*	*Upper 95.0%*
Intercept	1205.934869	82.3711201	14.64026309	0.000691158	943.7932024	1468.076536	943.7932024	1468.076536
Air voids	-25.7784241	2.585022977	-9.972222423	0.002145815	-34.00512092	-17.55172727	-34.00512092	-17.55172727
PROBABILITY OUTPUT								
Percentile	*Indirect Tensile Test (kPa)*							
10	169.6708303							
30	205.1508617							
50	528.0483495							
70	547.7742555							
90	565.5068048							

Appendix C

Single Factor ANOVA analysis for Moisture Induced Damage in mixes with different binders

Anova: Single Factor anylysis for Moisture Induced Damage in mixes with different binders

SUMMARY

Groups	*Count*	*Sum*	*Average*	*Variance*
Stockmeier binder - Control	3	2.496556826	0.832185609	0.000813
Polyval Aromatic binder	3	1.977725599	0.659241866	0.005519
Polyval Aliphatic binder	3	2.114100035	0.704700012	0.004681
Lesson Bound binder	3	1.724264995	0.574754998	0.004148

ANOVA

Source of Variation	*SS*	*df*	*MS*	*F*	*P-value*	*F crit*
Between Groups	0.103892111	3	0.034630704	9.136942	0.005801	4.066181
Within Groups	0.030321484	8	0.003790185			
Total	0.134213595	11				

Appendix D

Regression Statistics for Indirect Tensile Strength Vs Air Voids (Trial Section)

SUMMARY OUTPUT for ITS VS AIR VOID (TRIAL SECTION)

Regression Statistics	
Multiple R	0.89
R Square	0.79
Adjusted R Square	0.69
Standard Error	103.24
Observations	4

ANOVA

	df	*SS*	*MS*	*F*	*Significance F*
Regression	1	80829.71229	80829.71229	7.58299781	0.110451215
Residual	2	21318.66956	10659.33478		
Total	3	102148.3819			

	Coefficients	*Standard Error*	*t Stat*	*P-value*	*Lower 95%*	*Upper 95%*	*Lower 95.0%*	*Upper 95.0%*
Intercept	1114.458664	246.1856071	4.52690422	0.045493372	55.20748935	2173.709838	55.20748935	2173.709838
X Variable 1	-22.78411733	8.27392811	-2.753724353	0.110451215	-58.3839567	12.81572204	-58.3839567	12.81572204

Appendix E

ANOVA analysis for Light Weight Deflectometer test on trial-section

Site A						
Anova: Single Factor analysis for Control Mix in different times						
SUMMARY						
Groups	*Count*	*Sum*	*Average*	*Variance*		
Right after construction	6	217.6222	36.27037	132.7685		
After 2 weeks	6	269.1	44.85	227.9544		
After 6 months	6	231.1453	38.52422	128.2662		
						Not significant
ANOVA						
Source of Variation	*SS*	*df*	*MS*	*F*	*P-value*	*F crit*
Between Groups	237.4107	2	118.7054	0.72827	0.499052	3.682320344
Within Groups	2444.946	15	162.9964			
Total	2682.357	17				

Site A						
Anova: Single Factor analysis for Improved Mix 1 in different times						
SUMMARY						
Groups	*Count*	*Sum*	*Average*	*Variance*		
Right after construction	6	190.1833	31.69722	36.10505		
After 2 weeks	6	227.75	37.95833	99.81042		
After 6 months	6	169	28.16667	9.544444		
						Not significant
ANOVA						
Source of Variation	*SS*	*df*	*MS*	*F*	*P-value*	*F crit*
Between Groups	295.0861	2	147.5431	3.042964	0.077757	3.682320344
Within Groups	727.2995	15	48.48664			
Total	1022.386	17				

Site A						
Anova: Single Factor analysis for Improved Mix 3 in different times						
SUMMARY						
Groups	*Count*	*Sum*	*Average*	*Variance*		
Right after constructic	6	203.4694	33.91156	100.5427		
After 2 weeks	6	202.6	33.76667	56.46967		
After 6 months	6	168.8907	28.14844	5.717631		
						Not significant
ANOVA						
Source of Variation	*SS*	*df*	*MS*	*F*	*P-value*	*F crit*
Between Groups	129.5979	2	64.79896	1.194598	0.330057	3.682320344
Within Groups	813.65	15	54.24334			
Total	943.2479	17				

Site A						
Anova: Single Factor analysis for Improved Mix 2 in different times						
SUMMARY						
Groups	*Count*	*Sum*	*Average*	*Variance*		
Right after constructi	6	165.6571	27.60952	8.425116		
After 2 weeks	6	172	28.66667	10.65567		
After 6 months	6	136.444	22.74067	22.27953		
						Significant
ANOVA						
Source of Variation	*SS*	*df*	*MS*	*F*	*P-value*	*F crit*
Between Groups	119.8816	2	59.94078	4.347702	0.032412	3.682320344
Within Groups	206.8016	15	13.78677			
Total	326.6832	17				

Site B						
Anova: Single Factor analysis for Control mix in different times						
SUMMARY						
Groups	*Count*	*Sum*	*Average*	*Variance*		
Right after construction	4	169.8667	42.46667	110.0378		
After 2 weeks	4	152.0333	38.00833	56.00028		
After 6 months	4	145.5833	36.39583	104.386		
						Not significant
ANOVA						
Source of Variation	*SS*	*df*	*MS*	*F*	*P-value*	*F crit*
Between Groups	79.10921	2	39.55461	0.438806	0.657896	4.256494729
Within Groups	811.2722	9	90.14135			
Total	890.3814	11				

Site B						
Anova: Single Factor analysis for Improved Mix 2 in different times						
SUMMARY						
Groups	*Count*	*Sum*	*Average*	*Variance*		
Right after construction	4	234.9143	58.72857	213.2601361		
After 2 weeks	4	290.2	72.55	78.95166667		
After 6 months	4	254.4667	63.61667	73.32851852		
						Not significant
ANOVA						
Source of Variation	*SS*	*df*	*MS*	*F*	*P-value*	*F crit*
Between Groups	392.9731	2	196.4865	1.612570708	0.252028	4.256494729
Within Groups	1096.621	9	121.8468			
Total	1489.594	11				

Site B						
Anova: Single Factor analysis for Improved Mix 3 in different times						
SUMMARY						
Groups	*Count*	*Sum*	*Average*	*Variance*		
Right after construction	4	164.75	41.1875	9.890625		
After 2 weeks	4	271.0833	67.77083	33.59896		
After 6 months	4	220.9833	55.24583	50.98063		
						Significant
ANOVA						
Source of Variation	*SS*	*df*	*MS*	*F*	*P-value*	*F crit*
Between Groups	1414.915	2	707.4573	22.46604	0.000317	4.256495
Within Groups	283.4106	9	31.49007			
Total	1698.325	11				

Site A and Site B						
Anova: Two-Factor Without Replication for Control mix in two different sites and times						
SUMMARY	*Count*	*Sum*	*Average*	*Variance*		
Control	3	163.8	54.6	108.36		
	3	141.4722222	47.15740741	106.2503		
	3	105.2	35.06666667	233.4578		
	3	112.3791887	37.45972957	275.2171		
	3	95.16666667	31.72222222	3.953704		
	3	99.84947479	33.28315826	0.840667		
Control	3	114.45	38.15	6.3175		
	3	86.86666667	28.95555556	7.005926		
	3	149	49.66666667	65.33333		
	3	117.1666667	39.05555556	43.4537		
Test 01	10	387.4888889	38.74888889	120.678		
Test 02	10	421.1333333	42.11333333	157.7904		
Test 03	10	376.7286635	37.67286635	107.2624		
						Not significant
ANOVA						
Source of Variation	*SS*	*df*	*MS*	*F*	*P-value*	*F crit*
Rows	1878.513201	9	208.723689	2.358366	0.057972	2.456281149
Columns	107.3168598	2	53.65842992	0.606286	0.556139	3.554557146
Error	1593.063064	18	88.50350356			
Total	3578.893125	29				

Site A and Site B						
Anova: Two-Factor Without Replication for Improved Mix 2 in two different sites and times						
SUMMARY	*Count*	*Sum*	*Average*	*Variance*		
Improved 2	3	75	25	42.75		
	3	88.9	29.63333333	33.30333		
	3	83.69400353	27.89800118	9.571225		
	3	77.75	25.91666667	28.14583		
	3	78.95714286	26.31904762	11.0768		
	3	69.8	23.26666667	1.453333		
Improved 2	3	216.1833333	72.06111111	210.5445		
	3	178.5238095	59.50793651	82.82162		
	3	183.2738095	61.09126984	193.6678		
	3	201.6	67.2	107.56		
Test 01	10	400.5714286	40.05714286	334.006		
Test 02	10	462.2	46.22	545.7696		
Test 03	10	390.9106702	39.09106702	482.3796		
						Significant
ANOVA						
Source of Variation	*SS*	*df*	*MS*	*F*	*P-value*	*F crit*
Rows	11116.72736	9	1235.191929	19.45746	1.58E-07	2.456281149
Columns	299.1193204	2	149.5596602	2.355951	0.123359	3.554557146
Error	1142.669739	18	63.48165214			
Total	12558.51642	29				

Site A and Site B						
Anova: Two-Factor Without Replication for Improved Mix 3 in two different sites and times						
SUMMARY	*Count*	*Sum*	*Average*	*Variance*		
Improved 3	3	128.7641026	42.92136752	100.2032		
	3	82.87619048	27.62539683	4.754316		
	3	88.80128205	29.60042735	20.29949		
	3	77.97398589	25.99132863	8.22818		
	3	94.27777778	31.42592593	29.69239		
	3	102.2666667	34.08888889	31.0237		
Improved 3	3	162.5	54.16666667	117.8958		
	3	167.0833333	55.69444444	262.6134		
	3	164.8333333	54.94444444	353.6759		
	3	162.4	54.13333333	112.5033		
Test 01	10	368.2193529	36.82193529	73.27109		
Test 02	10	473.6833333	47.36833333	350.9139		
Test 03	10	389.8739859	38.98739859	215.975		
						Significant
ANOVA						
Source of Variation	*SS*	*df*	*MS*	*F*	*P-value*	*F crit*
Rows	4300.179595	9	477.7977328	5.885577	0.000713	2.456281149
Columns	620.5193675	2	310.2596838	3.821821	0.041365	3.554557146
Error	1461.260147	18	81.18111925			
Total	6381.959109	29				

Appendix F

ANOVA analysis for British Pendulum test on trial-section

Site A - BPT						
Anova: Single Factor analysis for Control Mix in different times						
SUMMARY						
Groups	*Count*	*Sum*	*Average*	*Variance*		
Right after construction	6	440.3333	73.38889	102.1741		
After 2 weeks	6	360.9333	60.15556	14.19366		
After 6 months	6	381.75	63.625	771.9938		
						Not significant
ANOVA						
Source of Variation	*SS*	*df*	*MS*	*F*	*P-value*	*F crit*
Between Groups	564.9834	2	282.4917	0.953975	0.407382	3.682320344
Within Groups	4441.807	15	296.1205			
Total	5006.791	17				

Site A - BPT						
Anova: Single Factor analysis for Improved Mix 1 in different times						
SUMMARY						
Groups	*Count*	*Sum*	*Average*	*Variance*		
Right after construction	6	413.5238	68.92063	57.6856		
After 2 weeks	6	331.7976	55.2996	20.75739		
After 6 months	6	431	71.83333	81.35556		
						Significant
ANOVA						
Source of Variation	*SS*	*df*	*MS*	*F*	*P-value*	*F crit*
Between Groups	934.7611	2	467.3806	8.774433	0.002997	3.682320344
Within Groups	798.9928	15	53.26618			
Total	1733.754	17				

Site A - BPT						
Anova: Single Factor analysis for Improved Mix 3 in different times						
SUMMARY						
Groups	*Count*	*Sum*	*Average*	*Variance*		
Right after construction	6	347.6984	57.94974	39.4426		
After 2 weeks	6	289.8869	48.31448	16.72427		
After 6 months	6	271.4167	45.23611	237.0567		
						Not significant
ANOVA						
Source of Variation	*SS*	*df*	*MS*	*F*	*P-value*	*F crit*
Between Groups	527.9014	2	263.9507	2.700506	0.099609	3.682320344
Within Groups	1466.118	15	97.74119			
Total	1994.019	17				

Site A - BPT						
Anova: Single Factor analysis for Improved Mix 2 in different times						
SUMMARY						
Groups	*Count*	*Sum*	*Average*	*Variance*		
Right after construction	6	361	60.16667	32.21111		
After 2 weeks	6	301.375	50.22917	6.447049		
After 6 months	6	329.6667	54.94444	477.1741		
						Not significant
ANOVA						
Source of Variation	*SS*	*df*	*MS*	*F*	*P-value*	*F crit*
Between Groups	296.5187	2	148.2594	0.862253	0.442114	3.682320344
Within Groups	2579.161	15	171.9441			
Total	2875.68	17				

Site B - BPT						
Anova: Single Factor analysis for Control Mix in different time						
SUMMARY						
Groups	*Count*	*Sum*	*Average*	*Variance*		
Right after construction	4	277.3333	69.33333	38.93259		
After 2 weeks	4	256.8619	64.21548	6.181276		
After 6 months	4	268	67	89.77778		
						Not significant
ANOVA						
Source of Variation	*SS*	*df*	*MS*	*F*	*P-value*	*F crit*
Between Groups	52.52064	2	26.26032	0.584031	0.577457	4.256494729
Within Groups	404.6749	9	44.96388			
Total	457.1956	11				

Site B - BPT						
Anova: Single Factor analysis for Improved Mix 2						
SUMMARY						
Groups	*Count*	*Sum*	*Average*	*Variance*		
Right after construction	4	235.4	58.85	59.23667		
After 2 weeks	4	269.994	67.49851	38.17886		
After 6 months	4	333.6667	83.41667	38.5463		
						Significant
ANOVA						
Source of Variation	*SS*	*df*	*MS*	*F*	*P-value*	*F crit*
Between Groups	1242.274	2	621.137	13.7054	0.001856	4.256494729
Within Groups	407.8855	9	45.32061			
Total	1650.16	11				

Site A and B						
Anova: Two-Factor Without Replication for Control Mix in different sites in different time						
SUMMARY	*Count*	*Sum*	*Average*	*Variance*		
Control	3	173.1	57.7	60.87		
	3	206.7916667	68.93055556	119.6811343		
	3	178.3333333	59.44444444	175.3981481		
	3	169.375	56.45833333	439.3177083		
	3	192.1666667	64.05555556	110.0092593		
	3	263.25	87.75	566.2986111		
Control	3	195.9666667	65.32222222	24.27814815		
	3	184.0666667	61.35555556	30.03259259		
	3	203.2619048	67.75396825	18.14191232		
	3	218.9	72.96666667	50.01444444		
Test 01	10	717.6666667	71.76666667	74.12691358		
Test 02	10	617.7952381	61.77952381	14.34124521		
Test 03	10	649.75	64.975	461.8488426		
						Not significant
						Not significant
ANOVA						
Source of Variation	*SS*	*df*	*MS*	*F*	*P-value*	*F crit*
Rows	2285.038517	9	253.8931686	1.713041534	0.158220845	2.456281149
Columns	520.2694221	2	260.1347111	1.755153819	0.201202305	3.554557146
Error	2667.814495	18	148.2119164			
Total	5473.122435	29				

Site B - BPT						
Anova: Single Factor analysis for Improved Mix 3						
SUMMARY						
Groups	*Count*	*Sum*	*Average*	*Variance*		
Right after construction	4	249.0667	62.26667	174.0978		
After 2 weeks	4	241.1667	60.29167	8.636574		
After 6 months	4	335.5	83.875	46.46991		
						Significant
ANOVA						
Source of Variation	*SS*	*df*	*MS*	*F*	*P-value*	*F crit*
Between Groups	1369.326	2	684.6629	8.961389	0.00722	4.256494729
Within Groups	687.6128	9	76.40142			
Total	2056.939	11				

Site A and B						
Anova: Two-Factor Without Replication for Improved Mix 2 in different sites in different times						
SUMMARY	*Count*	*Sum*	*Average*	*Variance*		
Improved 2	3	159.9583333	53.31944444	13.20197		
	3	143.0833333	47.69444444	217.794		
	3	150.5	50.16666667	216.1944		
	3	200	66.66666667	563.6944		
	3	173.8333333	57.94444444	68.62037		
	3	164.6666667	54.88888889	21.92593		
Improved 2	3	209.8095238	69.93650794	367.9645		
	3	201.1428571	67.04761905	128.2925		
	3	212.2666667	70.75555556	289.3348		
	3	215.8416667	71.94722222	19.90002		
Test 01	10	596.4	59.64	38.10291		
Test 02	10	571.3690476	57.13690476	95.83606		
Test 03	10	663.3333333	66.33333333	494.1235		
						Not significant
						Not significant
ANOVA						
Source of Variation	*SS*	*df*	*MS*	*F*	*P-value*	*F crit*
Rows	2290.850908	9	254.5389898	1.362908	0.274612	2.456281149
Columns	452.1349845	2	226.0674923	1.210459	0.3212	3.554557146
Error	3361.710943	18	186.7617191			
Total	6104.696836	29				

Site A and B						
Anova: Two-Factor Without Replication for Improved Mix 3 in different sites in different times						
SUMMARY	*Count*	*Sum*	*Average*	*Variance*		
Improved 3	3	131	43.66666667	262.9864		
	3	174.2857143	58.0952381	30.75737		
	3	144.0357143	48.01190476	11.52594		
	3	173.375	57.79166667	90.22049		
	3	142.8055556	47.60185185	286.4478		
	3	143.5	47.83333333	46.19444		
Improved 3	3	211.1666667	70.38888889	366.787		
	3	203.8	67.93333333	224.1911		
	3	185.1	61.7	157.17		
	3	225.6666667	75.22222222	137.9259		
Test 01	10	596.7650794	59.67650794	84.91472		
Test 02	10	531.0535714	53.10535714	50.42423		
Test 03	10	606.9166667	60.69166667	545.3118		
						Not significant
						Not significant
ANOVA						
Source of Variation	*SS*	*df*	*MS*	*F*	*P-value*	*F crit*
Rows	3236.652636	9	359.6280706	2.240515	0.069397	2.456281149
Columns	339.208874	2	169.604437	1.056651	0.368216	3.554557146
Error	2889.204111	18	160.5113395			
Total	6465.06562	29				

Appendix G

ANOVA analysis for Dipstick test on trial-section

Site A						
Anova: Single Factor analysis for Control Mix in different times						
SUMMARY						
Groups	*Count*	*Sum*	*Average*	*Variance*		
Depth of Rut (mm) - 1st test	2	-15.4051	-7.70255	0.243951125		
Depth of Rut (mm) - 2nd test	2	-44.9072	-22.4536	1.161288		
						Significant
ANOVA						
Source of Variation	*SS*	*df*	*MS*	*F*	*P-value*	*F crit*
Between Groups	217.5934761	1	217.5934761	309.6888953	0.003213491	18.51282051
Within Groups	1.405239125	2	0.702619563			
Total	218.9987152	3				

Site A						
Anova: Single Factor analysis for Improved Mix 1 in different times						
SUMMARY						
Groups	*Count*	*Sum*	*Average*	*Variance*		
Column 1	2	-15.8496	-7.9248	0.77451458		
Column 2	2	-47.2694	-23.6347	2.11644738		
						Significant
ANOVA						
Source of Variation	*SS*	*df*	*MS*	*F*	*P-value*	*F crit*
Between Groups	246.800958	1	246.800958	170.7396786	0.005805912	18.51282051
Within Groups	2.89096196	2	1.44548098			
Total	249.69192	3				

Site A						
Anova: Single Factor analysis for Improved Mix 3 in different times						
SUMMARY						
Groups	*Count*	*Sum*	*Average*	*Variance*		
Column 1	2	-13.9954	-6.9977	1.12290098		
Column 2	2	-45.2374	-22.6187	9.21320738		
						Significant
ANOVA						
Source of Variation	*SS*	*df*	*MS*	*F*	*P-value*	*F crit*
Between Groups	244.015641	1	244.015641	47.2161538	0.020529257	18.51282051
Within Groups	10.33610836	2	5.16805418			
Total	254.3517494	3				

Site A						
Anova: Single Factor analysis for Improved Mix 2 in different times						
SUMMARY						
Groups	*Count*	*Sum*	*Average*	*Variance*		
Column 1	2	-17.4752	-8.7376	5.36805378		
Column 2	2	-51.943	-25.9715	0.54225698		
						Significant
ANOVA						
Source of Variation	*SS*	*df*	*MS*	*F*	*P-value*	*F crit*
Between Groups	297.0073092	1	297.0073092	100.504803	0.009803697	18.51282051
Within Groups	5.91031076	2	2.95515538			
Total	302.91762	3				

Site B

Anova: Single Factor analysis for Control Mix in different times

SUMMARY

Groups	*Count*	*Sum*	*Average*	*Variance*
Depth of Rut (mm) - 1st test	2	-21.336	-10.668	66.48889928
Depth of Rut (mm) - 2nd test	2	-48.7172	-24.3586	0.80645

Not Significant

ANOVA

Source of Variation	*SS*	*df*	*MS*	*F*	*P-value*	*F crit*
Between Groups	187.4325284	1	187.4325284	5.57044522	0.142203553	18.51282051
Within Groups	67.29534928	2	33.64767464			
Total	254.7278776	3				

Site B

Anova: Single Factor analysis for Improved Mix 2 in different times

SUMMARY

Groups	*Count*	*Sum*	*Average*	*Variance*
Column 1	2	-13.2842	-6.6421	10.33578578
Column 2	2	-39.2176	-19.6088	6.322568

Not Significant

ANOVA

Source of Variation	*SS*	*df*	*MS*	*F*	*P-value*	*F crit*
Between Groups	168.1353089	1	168.1353089	20.18630545	0.046137168	18.51282051
Within Groups	16.65835378	2	8.32917689			
Total	184.7936627	3				

Site B

Anova: Single Factor analysis for Improved Mix 3 in different times

SUMMARY

Groups	*Count*	*Sum*	*Average*	*Variance*
Column 1	2	-11.6332	-5.8166	43.21152648
Column 2	2	-43.0022	-21.5011	114.9704152

Not Significant

ANOVA

Source of Variation	*SS*	*df*	*MS*	*F*	*P-value*	*F crit*
Between Groups	246.0035403	1	246.0035403	3.110387161	0.219846029	18.51282051
Within Groups	158.1819417	2	79.09097085			
Total	404.185482	3				

Site A and Site B

Anova: Two-Factor Without Replication for Control mix in two different sites and times

SUMMARY	*Count*	*Sum*	*Average*	*Variance*		
Control Mix	2	-31.2674	-15.6337	114.9704152		
	2	-29.0449	-14.52245	102.7934234		
Control Mix	2	-28.6258	-14.3129	177.122549		
	2	-41.4274	-20.7137	36.63508802		
Depth of Rut (mm) -	4	-36.7411	-9.185275	25.17558137		
Depth of Rut (mm) -	4	-93.6244	-23.4061	1.865587667		

Not Significant

Significant

ANOVA

Source of Variation	*SS*	*df*	*MS*	*F*	*P-value*	*F crit*
Rows (Site)	54.0657588	3	18.0219196	1.998161791	0.292037	9.276628153
Columns (Time)	404.4637274	1	404.4637274	44.84449957	0.006794	10.12796449
Error	27.0577483	3	9.019249435			
Total	485.5872345	7				

Site A and Site B

Anova: Two-Factor Without Replication for Improved Mix 2 in two different sites and times

SUMMARY	*Count*	*Sum*	*Average*	*Variance*		
Improved mix 2	2	-32.5501	-16.27505	168.3888		
	2	-36.8681	-18.43405	129.8676		
Improved Mix 2	2	-30.3022	-15.1511	77.76791		
	2	-22.1996	-11.0998	90.61272		
Depth of Rut (mm) - 1st test	4	-30.7594	-7.68985	6.69832		
Depth of Rut (mm) - 2nd test	4	-91.1606	-22.79015	15.78293		
						Not Significant
						Significant

ANOVA

Source of Variation	*SS*	*df*	*MS*	*F*	*P-value*	*F crit*
Rows (Site)	56.84488631	3	18.94829544	5.363307	0.100625	9.276628
Columns (Time)	456.0381202	1	456.0381202	129.0814	0.001463	10.12796
Error	10.59884977	3	3.532949923			
Total	523.4818563	7				

Site A and Site B

Anova: Two-Factor Without Replication for Improved Mix 3 in two different sites and times

SUMMARY	*Count*	*Sum*	*Average*	*Variance*		
Improved mix 3	2	-28.2194	-14.1097	80.9679		
	2	-31.0134	-15.5067	171.4322		
Improved Mix 3	2	-39.5478	-19.7739	173.3187		
	2	-15.0876	-7.5438	81.29145		
Depth of Rut (mm) -	4	-25.6286	-6.40715	15.24314		
Depth of Rut (mm) -	4	-88.2396	-22.0599	41.81088		
						Not Significant
						Significant

ANOVA

Source of Variation	*SS*	*df*	*MS*	*F*	*P-value*	*F crit*
Rows (Sites)	154.1689659	3	51.38965529	9.072439	0.051495	9.276628
Columns (Time)	490.0171651	1	490.0171651	86.50867	0.002631	10.12796
Error	16.99311118	3	5.664370392			
Total	661.1792422	7				

Appendix H

ANOVA analysis for permeability test on trial-section

Site A and Site B						
Anova: Two-Factor Without Replication for Control mix in different sites in different time						
SUMMARY	*Count*	*Sum*	*Average*	*Variance*		
Control mix	3	132072.663	44024.22098	1.35E+08		
	3	174357.9262	58119.30874	65485675		
	3	148810.595	49603.53167	26168801		
Control mix	3	95886.08332	31962.02777	2.94E+08		
	3	131081.6714	43693.89046	43661334		
Test 01	5	216176.8865	43235.37729	36310210		
Test 02	5	241951.8464	48390.36929	63646516		
Test 03	5	224080.206	44816.0412	4.38E+08		
						Not significant
						Not significant
ANOVA						
Source of Variation	*SS*	*df*	*MS*	*F*	*P-value*	*F crit*
Rows	1094402070	4	273600517.6	2.068585	0.177142	3.837853355
Columns	69747103.53	2	34873551.76	0.263665	0.774654	4.458970108
Error	1058116370	8	132264546.3			
Total	2222265544	14				

Site A and Site B						
Anova: Two-Factor Without Replication for Improved Mix 2 in different sites in different times						
SUMMARY	*Count*	*Sum*	*Average*	*Variance*		
Improved mix 2	3	89330.94489	29776.98163	2.62E+08		
	3	131938.7857	43979.59522	35714632		
	3	154717.597	51572.53232	39059002		
Improved mix 2	3	94755.95939	31585.3198	5.99E+08		
	3	104694.5492	34898.18308	2.64E+08		
Test 01	5	194222.1511	38844.43022	19905926		
Test 02	5	238424.3204	47684.86408	21682478		
Test 03	5	142791.3646	28558.27293	5.82E+08		
						Not significant
						Not significant
ANOVA						
Source of Variation	*SS*	*df*	*MS*	*F*	*P-value*	*F crit*
Rows	1013098505	4	253274626.2	1.366229	0.326903	3.837853355
Columns	916307986.8	2	458153993.4	2.471402	0.145964	4.458970108
Error	1483057699	8	185382212.4			
Total	3412464191	14				

Site A and Site B						
Anova: Two-Factor Without Replication for Improved Mix 3 in different locations in different times						
SUMMARY	*Count*	*Sum*	*Average*	*Variance*		
Improved mix 3	3	94795.56619	31598.52206	3099520		
	3	72509.44592	24169.81531	37765409		
	3	59858.03988	19952.67996	7979799		
Improved mix 3	3	52253.76168	17417.92056	2.48E+08		
	3	51983.35778	17327.78593	2.44E+08		
Test 01	5	146041.7383	29208.34765	14776434		
Test 02	5	117383.8037	23476.76073	31324912		
Test 03	5	67974.62951	13594.9259	1.76E+08		
						Not significant
						Significant
ANOVA						
Source of Variation	*SS*	*df*	*MS*	*F*	*P-value*	*F crit*
Rows	431438141.1	4	107859535.3	1.88733	0.20614	3.837853355
Columns	623801145	2	311900572.5	5.457646	0.031997	4.458970108
Error	457194272.9	8	57149284.11			
Total	1512433559	14				